Fetal cardiovascular simulations to assess the feasibility of intrauterine ECMO

Esther Wachter

Technische Universiteit Delft

TU Delft

Fetal cardiovascular simulations to assess the feasibility of intrauterine ECMO

by

E.A.M. Wachter

to obtain the degree of Master of Science
at the Delft University of Technology,
to be defended publicly on Tuesday August 27, 2019 at 2.00 pm.

Student number:	4064429	
Project duration:	September 17, 2018 – August 27, 2019	
Thesis committee:	Prof. dr. J. Dankelman,	TU Delft, supervisor
	Ir. T. G. Goos,	Erasmus MC, Sophia Children's Hospital
	Dr. M. Kok,	TU Delft, DCSC

An electronic version of this thesis is available at http://repository.tudelft.nl/.

TU Delft

Erasmus MC
Universitair Medisch Centrum Rotterdam

Abstract

The placenta is very important during the start of life, providing the fetus with oxygen and nutrients from the maternal blood. Impaired growth of the placenta and additional placental ischaemia endangers the exchange of gasses, exchange of nutrients, and optimal growth of the fetus. This thesis investigates the feasibility of intrauterine ECMO to improve oxygen levels in fetal blood during placental ischaemia. Fetal blood would be retrieved from the umbilical artery, oxygenated in the ECMO system and fed back into the umbilical artery. The objective of this thesis is to design a cardiovascular model to simulate the cardiovascular response to an ECMO support system. A lumped parameter model is created to approximate the fetal cardiovascular system. By performing a parameter search, haemodynamic parameters were gathered for the fetal model. Data from 30 week fetuses was used as initial input, because of parameter accessibility. Parameters for the gestational age of 20 to 29 weeks were obtained by extrapolating the parameters from the fetus of 30 weeks with scaling factors. A sensitivity analysis was performed to analyse the flow and pressure distribution through the fetal cardiovascular system and the cardiovascular response to different parameters. Implementation of a cannula into one of the umbilical arteries increases the resistance of that artery. Simulating the cardiovascular response to the addition of the cannula showed promising results for the feasibility of intrauterine ECMO. The fetal heart is able to maintain blood flow through the cannula despite the fact that the resistance of the artery is increased. The placental resistance increases during placental ischaemia. Because of this higher resistance, blood flow through the placenta will decrease. However, even at a lower flow rate, oxygenation of blood flow via the umbilical artery is mostly sufficient. The reason is the high percentage of fetal cardiac output flowing through the placental circulation. The designed model is able to simulate the fetal cardiovascular system and provides a simulation tool to further develop an intrauterine ECMO support system.

Preface

A quick choice made between liver or placental research, resulted in me ending up in the Sophia Children's Hospital in Rotterdam for an internship. Here, I acquired knowledge about care for premature newborns, pregnancy, and childbirth. I learned about the importance and complexity of the placenta. On the one hand, its praised for its complexity and seen as "the chronicle of intrauterine life", but on the other, it is also called "a parasite upon the mother" [18]. These different views of the placenta fascinated me and were the reason that I also chose to do my thesis project into this subject. This versatility and complexity of the placenta made my thesis project very challenging. However, it was also fulfilling to contribute to research into improving the health of newborns. It was wonderful to see how much care is provided to support premature newborns in the neonatal intensive care unit, but these children will obtain so much advantage if they are born stronger and healthier.

First of all, I want to thank Jenny Dankelman for the opportunity of a very interesting and unique internship. Also, thank you for your time, critical questions and knowledge which you provided during my thesis project. I also want to thank my daily supervisor Tom Goos. Tom, thank you for your time and patience during the many brainstorm sessions to translate the complexity of this problem into a model. I admire your endless enthusiasm for your research and the assistance of students.

I also want to thank my parents for their support over the years. You're always proud of me and giving me confidence and therefore I am very grateful.

I want to thank my brother, Erik, for the many coffees, dinners and running sessions to keep me healthy an happy. Also credits to Erik for the beautiful picture on the cover of this thesis report.

Then I want to thank Vera and Maurice. It was really nice to kick start my thesis project with you.

Lastly, I want to thank Tim, my boyfriend. Thank you for your patience, humour, numerous pep-talks, and hugs to cheer me up. I want to end with a quote from you.

"Studeren is passie"

Esther Wachter
Delft, August 2019

Contents

List of Figures

List of Tables

Abbreviations

aorta	AO
cardiac output	CO
combined ventricular output	CVO
ductus arteriosus	DA
ductus venosus	DV
extra corporeal life support	ECLS
extra corporeal membrane oxygenation	ECMO
end diastolic volume	EDV
end systolic volume	ESV
fetal growth restriction	FGR
gestational age	GA
haemoglobin	Hb
haemoglobin fetus	HbF
hepatic system	HE
Haemolysis, Elevated Liver enzymes and Low Platelets	HELLP
Human Placenta Project	HPP
heart rate	HR
intrauterine growth restriction	IUGR
intervillous space	IVS
left atrial pressure	LAP
lower body	LB
mean arterial pressure	MAP
neonatal intensive care unit	NICU
pulmonary artery	PA
pre-eclampsia	PE
placenta	PLA
pulmonary vascular resistance (lungs)	PVR
right atrial pressure	RAP
small for gestational age	SGA
stroke volume	SV
systemic vascular resistance	SVR
umbilical artery 1	UA1
umbilical artery 2	UA2
upper body	UB
umbilical vein	UV

1 | Introduction

The placenta is very important during pregnancy for the fetus [6]. When the child is born, the placenta, birthed after the child, is quickly forgotten. However, more and more research is being done, to solve the mystery of the exact functioning of the placenta during pregnancy and the start of life. There are initiatives started into placental research, such as the Human Placenta Project (HPP) launched by the National Institute of Child Health and Human Development[1]. The goal of the Human Placenta Project is to develop abilities to monitor the human placenta real-time. Next, to the HPP, research is executed into medicine and cures for symptoms of placental failure. Lastly, research is carried out into possibilities for an artificial womb with the use of extracorporeal support systems. In 2017, Partridge et al. [43] managed to support a lamb inside an extra-uterine device for 4 weeks under stable conditions. However, if the child would need to grow further outside the womb, a caesarian section is needed. Also, parents can not be with their child, because it is placed inside the artificial womb. These circumstances could be a drawback for parents. That is why it would be useful to look into the possibilities to enhance conditions for the child inside the womb with the use of extracorporeal support systems. The following chapter contains a summary of the anatomy and physiology of the placenta. Secondly, the options for extracorporeal support are introduced.

1.1. The placenta

The placenta is a disk with one side attached to the uterine wall and on the other side joined to the child via the umbilical cord. During pregnancy, the placenta provides gas and nutrients exchange between mother and child. It functions as a substitute for major organs of the child, such as the lungs, kidneys, and liver. The placenta establishes its final form at the end of the first trimester [6]. A placenta grows during pregnancy towards an average diameter of 22 cm with a thickness in vivo of 5 cm and an average weight of 470 g [60]. The fetal heart is pumping blood through the fetal body after three weeks of gestation and the embryo is then called a fetus [57]. Mother and fetus cohabit symbiotically and any malfunction of the placenta can be harmful to both. It can be harmful during pregnancy, but can also have an impact on their health later in life [22].

Growth of the placenta, called placentation, starts when a fertilised oocyte implants in the inner wall of the uterus. The body of the uterus consists of three layers. The outside is called the perimetrium, followed by the myometrium and the endometrium is the most inner layer. The myometrium is built up out of intertwined smooth muscle bundles. In here lay arcuate vessels, which are an anastomosis of arteries and veins originating from the uterine and ovarian arteries and veins. The endometrium consists of two layers, the stratum basalis and stratum functionalis layer. The basalis is a thin layer and forms the functionalis layer during every menstruation cycle [33]. Blood flows from the arcuate arteries via radial arteries towards the endometrium, where they end in straight arteries in the basalis layer and spiral arteries in the functionalis layer.
The endometrium layer forming the maternal part of the placenta is called the decidua. The cell mass implanting in this layer is called a blastocyst. A blastocyst is a fluid-filled sphere with trophoblast cells on the outside and a cell mass inside which will become the fetus. Trophoblast cells are forming the fetal part of the placenta, called the chorionic plate. Trophoblasts are also responsible for the secretion of digestive enzymes, displaying of immunosuppressive factors to protect the embryo, and forming the chorion [33]. The chorion is the outer membrane surrounding the embryo, which is shown in Figure 1.1. The trophoblast cells form a layer of cytotrophoblasts on the inside and syncytiotrophoblasts at the outside. Syncytiotrophoblasts lose their plasma membranes and invade the endometrium to digest uterine cells and anchor the blastocyst to the uterine wall [3]. Extravillous trophoblast cells, differentiated from the cytotrophoblast cells, migrate one-third deep into the myometrium of the uterus. Extravillous trophoblast cells remodel the spiral arteries into large conduits and remove smooth muscle cells to prevent vasoconstriction of the arteries [5]. The remodeled spiral arteries lower the velocity

[1] https://www.nichd.nih.gov/research/supported/HPP/default - Accessed November 2, 2018

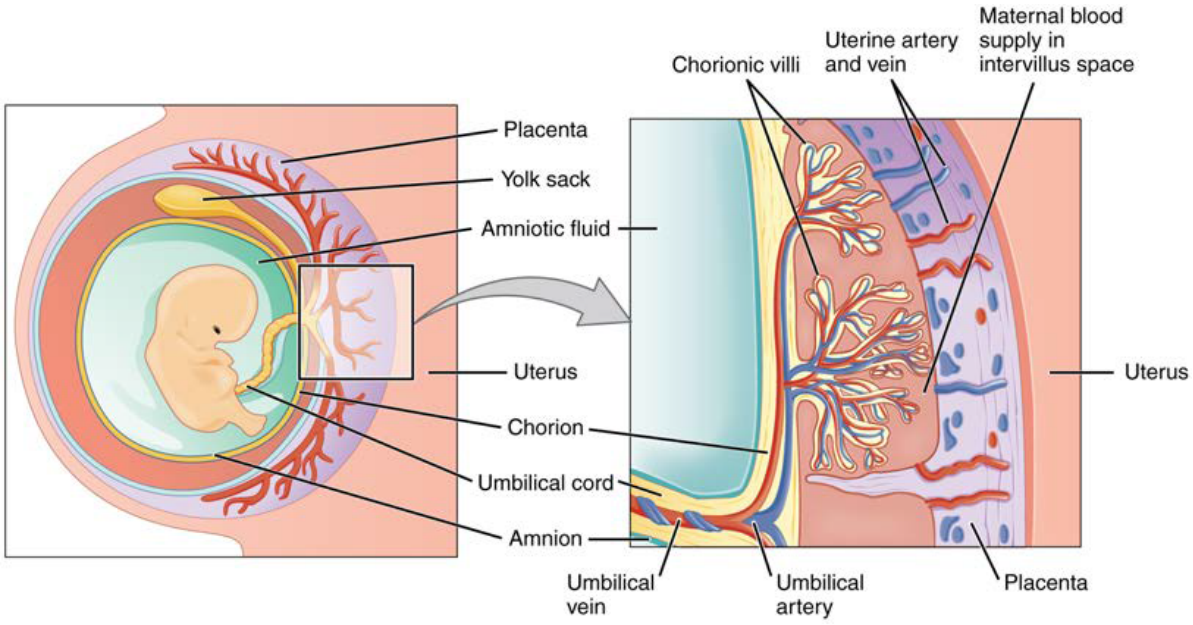

Figure 1.1: In the figure, the fetus is shown inside the womb. Via the umbilical cord, the fetus is attached to the placenta. At the right side the fetal chorionic villi are shown, submerged in maternal blood inside the intervillous space [3, pg.1333].

of blood flow towards the placenta. As a consequence of the dilation of spiral arteries and proximal arteries leading towards the uterus, changes in maternal blood pressure are proportional to changes in placental blood pressure [19].

The enlarged spiral arteries deliver blood from the mother into the intervillous space (IVS). The intervillous space is the space between the basal plate, the maternal side of the placenta, and the chorionic plate. Blood of the mother travels via 100 to 150 spiral arteries into the IVS and leaves via decidual veins [16]. Every minute around 20% of the maternal blood flow travels through the placenta [54]. Exchange of oxygen and nutrients between maternal and fetal blood happens via the chorionic villi that are submerged in the IVS, as can be seen in Figure 1.1. Human placentas are called haemomonochorial placentas because of the separated blood flows [46]. Chorionic villi grow from the chorionic plate towards the basal plate. Arteries and veins invade the villi to carry blood from and to the fetus via the umbilical cord. The villous trees structure is built up out of four major types of villi. Stem villi give rise to immature intermediate villi, mature intermediate villi and finally terminal villi. Exchange happens mostly in the terminal villi, because of a small layer of the villous membrane between maternal blood and the fetal arteries [60]. In hemispheric parts, called cotyledons, the villi trees grow towards the basal plate. These hemispheric parts are separated from each other by placental septa. Blood flow from the spiral arteries enters the IVS as a jet stream and creates central cavities inside the villi trees. Central cavities are protecting the villous tissue from high stresses and damage, and have a optimal size to keep exchange between mother and fetus as efficient as possible [9]. If the spiral arteries are not dilated enough, then blood flow will not be slowed down and flows turbulently into the central cavities. This could damage the villi trees and creates lesions on its surface, making exchange complicated.

1.1.1. Placental pathology

Optimal growth of the fetus is endangered when the maternal arteries are not dilated properly and the placenta is malfunctioning. Incorrect development of the placenta complicates oxygen uptake and increases fetal workload. This obstruction of blood flow is called placental ischaemia [53]. Related to placental ischaemia are several other placental diseases, which are organised in Figure 1.2 and further explained in Appendix A. The main effects of placental ischaemia are oxidative and endoplasmic reticulum stress leading eventually to pre-eclampsia (PE).

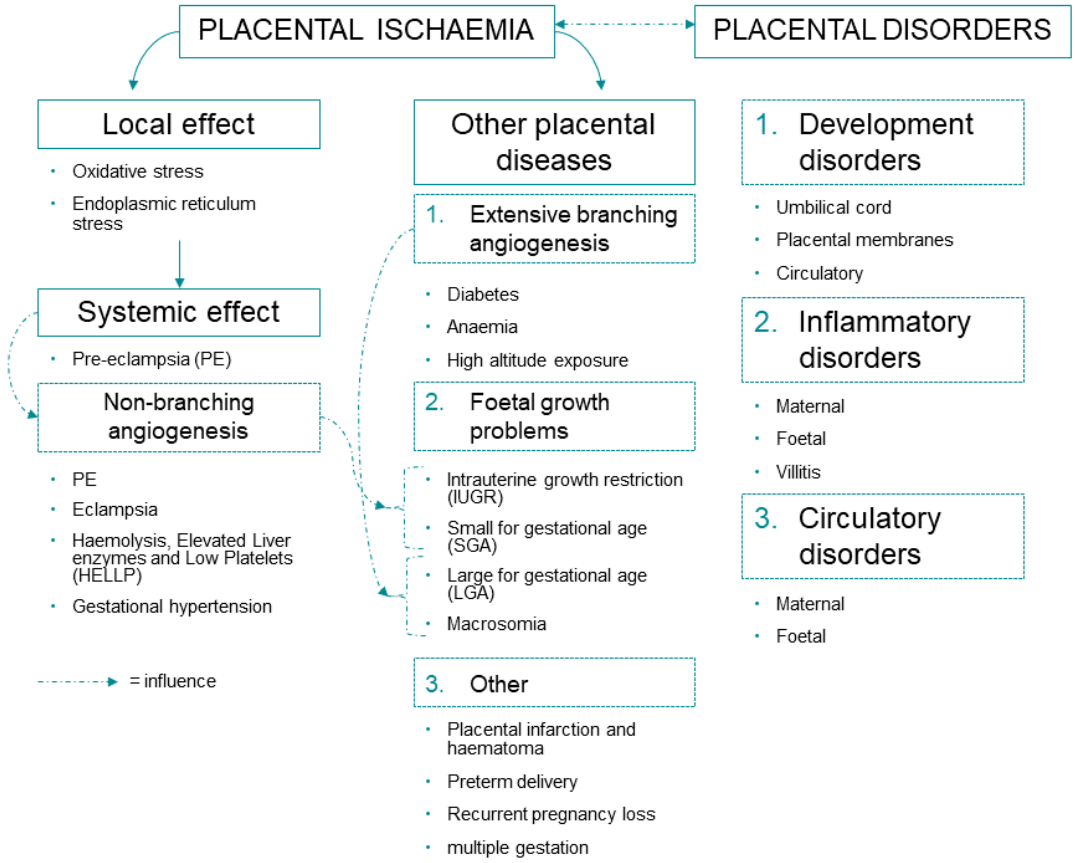

Figure 1.2: A schematic overview of placental ischaemia and placental diseases inspired on the articles of Roberts [53], Silver [62] and Gill et al. [16]. ©Esther Wachter

Oxidative and endoplasmic reticulum stress are local effects of placental ischaemia [53]. Oxidative stress is due to less available antioxidants and a higher generation of reactive oxygen species. Reactive oxygen species harm proteins, lipids and nuclei acids [66]. Shortage of gas and nutrients disturb the protein synthesis. Shortage of proteins lets endoplasmic reticulum stress activate the unfolded protein response, which can induce cellular apoptosis, also known as programmed cell death. Inflammation and oxidative stress are also present in normal pregnancy. However, during placental ischaemia, oxidative stress is not halted because of lower levels of antioxidants and protection against reactive oxygen species fails. Local effects of oxidative and endoplasmic reticulum stress can lead to systemic impact with PE as a systemic effect [53].

PE has an incidence of 2 to 10% among the pregnant population [36]. Symptoms occurring to the mother in the clinical stage of PE are hypertension, oedema, and proteinuria. Hypertension, high blood pressure, is harmful to the kidneys and liver of the mother and increases the chance of haematoma. A haematoma between the placenta and uterine wall can cause the placenta to come loose and risk the child's life. PE can occur halfway in gestation or in the last weeks of gestation. The clinical symptoms say something about the severity of PE and if it is early or late onset PE. It is assumed that these two are two different diseases on placental level [38].

The pre-clinical stage of early onset PE is characterised by poor placentation and angiogenic imbalance. In the first-trimester trophoblast invasion is failing, with the consequence of a view or many spiral arteries not remodelled [50]. Angiogenesis is the formation of new blood vessels from existing ones. Pre-eclamptic angiogenic imbalance is a form of non-branching angiogenesis, where only longer cap-

illaries are formed [16]. As mentioned in Section 1.1 blood flows turbulently into the intervillous space and damages the chorionic villi, because of the higher speed caused by non-dilated arteries. As a consequence oxygenated and non-oxygenated blood are mixed and travel through the intervillous in just one second, resulting in poor oxygen exchange [5]. Early onset PE occurs between 20 and 34 weeks of gestation and is found by measuring placental function. Early onset PE still happens to 1% of the pregnant population [38]. Related to PE are eclampsia, gestational hypertension and HELLP-syndrome (Haemolysis, Elevated Liver enzymes, and Low Platelets), which are also non-branching angiogenesis disorders and mentioned in Figure 1.2. Lastly, PE could lead to other placental pathologies like intrauterine growth restriction (IUGR) and children that are small for gestational age (SGA). Other pathologies originating from placental ischaemia do not have a systemic impact or are experiencing different levels of oxidative and endoplasmic reticulum stress. The systemic impact and high incidence among pregnant women is the reason to focus on early onset pre-eclampsia and to leave the other placental diseases for now.

1.2. Extracorporeal support systems

Extracorporeal support systems in the form of mechanical assist devices could be an option to support in nutrient and gas exchange during placental ischaemia. Technical solutions from other medical fields could be used as an example to design an assist device to improve gas transport towards the fetus. During the preceding literature study, some options were considered.
Firstly, there is the option of a ventricle assist device. Ventricle assist devices are used for people who are experiencing heart failure. It is seen as a bridge to recovery, bridge to transplant, bridge to decision or as destination therapy instead of a heart transplant [4]. A ventricle assist device supports the heart with pumping blood around the body. This is done with axial or centrifugal pumps. When looking at placental ischaemia, an assist device could be placed on the uterine artery to raise blood flow towards the placenta. However, concerns are the possibilities of compression of the fetal capillaries or creating haematoma between basal and chorionic plates as a result of higher blood pressure [26]. In the case of placental ischaemia, blood flow is already turbulent inside the IVS and increasing blood flow towards the IVS could maybe result in even more lesions on the chorionic villi trees. Also, the uterine artery changes in size during gestation which asks for variability. Lastly, there are concerns about how to place the device and when it needs to be removed.

Next, there is the option of extracorporeal life support (ECLS), also called extracorporeal membrane oxygenation (ECMO). ECMO filters venous blood from carbon-dioxide and adds oxygen, to support people with cardiac or pulmonary failure. There are two options of collecting and returning blood, namely venoarterial and venovenous ECMO [12]. With both, blood is collected via cannulae, passed through an artificial lung and then returned to the body. Proximal to the placenta, on the maternal side, ECMO would have the function of a pump. Blood values of the mother will already be sufficient and the level of oxygen is relatively hard to increase. Distal to the placenta, on the fetal side, ECMO will probably be more effective as to increase oxygen levels. Due to partial oxygen pressures being lower in comparison to adult blood.
There are already some points of concern:

- Would the system be compatible with fetal blood and haemoglobin, because it differs from adult blood. The differences between fetal and adult haemoglobin will be explained in Section 2.1.
- Would it change the placental oxygen gradient? If so, could this provoke a reaction of maternal blood supply?
- The placement of the device could be inside one of the umbilical vessels and near the placenta or near the fetal abdomen.
- Would the elevated vascular resistance be too high for the fetal heart to pump the blood around.
- A fetus moves in the womb, which could detach the cannula.
- The amniotic sac needs to stay attached to the uterine wall without rupturing.

The two options could be simplified to two basic ideas, namely placing a pump to increase the supply of blood flow. Or extracting blood with the use of cannulae and oxygenating it ex vivo, whereupon it

is returned into the blood circulation. Important questions are where inside the womb these options could be implemented and if they provide enough improvement to offset the additional risk to mother and child.

1.3. Objective

1.3.1. Research scope

The scope of this research concerns the distal side of the placenta and the fetal cardiovascular system during pregnancy. During placental ischaemia blood flow towards the placenta is impaired. The placenta is approached on the proximal side by the maternal blood circulation and on the distal side by the fetal blood circulation. After evaluating the structure of blood vessels proximal and distal to the placenta, it seems more promising to support the fetus on the distal side of the placenta. Proximal to the placenta maternal vessels are not dilated enough and increasing blood flow on that side could create potentially even more damage. Distal to the placenta fetal blood can be influenced directly. The umbilical cord could be used to access the fetal bloodstream. The umbilical cord contains two umbilical arteries, so by accessing one of the two, blood flow in the other vessels will stay untouched.
The gestation period looked at is from 20 to 28 weeks of gestation. Usually, at 20 weeks ultrasound is performed and the first signs of malfunctioning of the placenta would be discovered. In the Netherlands, abortion is allowed until the 24^{th} week of gestation or later in case of health-threatening circumstances. Most doctors work with 22 weeks because the pregnancy duration is estimated with two weeks margin [51]. When the child would not be in severe danger and abortion will not be performed, support could be useful when optimal blood circulation is impaired and the child is not ready to live on its own. At 28 weeks, the child would be delivered and taken care of at the neonatal intensive care unit (NICU). At this age, the development of the child is sufficient enough to survive outside the womb with less chance of serious health issues. The focus of this research is to find out if attaching cannulae inside the umbilical cord is possible and if it would be save. The exchange of oxygen and nutrients would be the next step, but will not be examined in this thesis.

1.3.2. Research objective

Support devices could be an opportunity to provide oxygen and nutrients to the fetus in case of placental ischaemia. These devices should not obstruct blood flow or be too demanding for the fetal heart. It needs to be examined if devices could be implemented on umbilical arteries and if blood flow can remain sufficient. To know if it is possible to intervene during gestation inside the mother's body, more information is needed about the blood circulation distal to the placenta and parameters to describe blood flow. The goal of this research is to find an option to support the fetus during placental ischaemia during the period of 20 to 28 weeks of gestation. Ultimately, this leads to the following research question:

Is it possible to place an assist device on blood vessels distal to the placenta to improve conditions for the fetus during placental ischaemia?

1.4. Content of this thesis

First, a study was done into the mechanics of blood to identify how blood flow can correctly be simulated and what assumptions are allowed to be made. Next, research was performed into existing cardiovascular models. Also, a search was performed to find the sizes of the fetal cardiovascular system during the period of 20 to 28 weeks of gestation. This information was used to examine the placenta and fetus in a Simulink model. With this model, the blood pressure and blood flow of the placenta and cardiac output of the fetus were calculated for different conditions. It was evaluated if intervention is possible on the umbilical vessels. Finally, an evaluation followed if and how an assist device could be placed on the umbilical vessels.

2 | Theory

This chapter elaborates on blood flow, blood circulation, and blood flow dynamics. In the previous chapter, information was given about the growth of the child inside the womb. Also, possible placental pathologies were illustrated and potential support systems as a remedy were introduced. An option to evaluate the potential of support systems is to use fetal cardiovascular model. To be able to establish the basic building structure of a fetal cardiovascular model, information is needed about blood flow and how it circulates in the fetal body. As well as basic fluid dynamics to describe the blood flow.

2.1. Blood

Blood is composed of approximately 55% blood plasma, 45% erythrocytes and less than 1% are leukocytes and platelets. The erythrocytes, leukocytes, and platelets are submerged in the blood plasma, as are plasma proteins, electrolytes, hormones, and nutrients. The human adult body contains around 4.5 to 6 litres blood [68]. Blood is a unique type of fluid because of all the formed elements in it. Erythrocytes are commonly known as red blood cells and the volume of erythrocytes is called haematocrit. Oxygen is transported by erythrocytes and a small percentage of oxygen is transported in blood plasma. Leukocytes are known as white blood cells, which lack haemoglobin and assist with immunity and inflammation. Erythrocytes do contain haemoglobin (Hb) and this protein helps with the transport of oxygen. A haemoglobin molecule is built up out of four haem groups within each centre an iron atom (Fe^{2+}). In fetal blood two haem groups are of a different structure, giving fetal haemoglobin (HbF) a higher affinity for oxygen [3]. This greater affinity helps fetal blood to collect oxygen from maternal blood.

2.1.1. Blood circulation

The functions of blood circulation are to transport substances, protection against blood loss and infections, regulation of temperature, body fluids volume and normal pH in tissues [3]. The total blood circulation is divided into the pulmonary and systemic circuit. In adults blood travels from the right side of the heart into the pulmonary circuit, to receive oxygen and get rid of carbon dioxide. After passing through the pulmonary circuit blood travels back across the left side of the heart into the systemic circuit. The systemic circuit provides the body with blood.

Blood flow is controlled by the heart and heart function is influenced by age, gender, exercise and body temperature. The heart contains two atria receiving blood from the pulmonary veins and vena cava and two ventricles two pump blood into the pulmonary and systemic circuits. The volume pumped per minute by each ventricle is called the cardiac output (CO). For adults, resting CO is around 5 L/min and during maximal effort increases 4 to 5 times [3]. The difference between these two cardiac outputs is called the cardiac reserve. The cardiac output itself can be influenced by heart rate (HR), the loading conditions of the heart called preload and afterload, and contractility of the heart muscle.
The cardiovascular circulation is dictated by vasoconstriction and vasodilation of blood vessels. During vasoconstriction the smooth muscle cells in the vessel wall constrict, narrowing the diameter of the vessels. Especially larger arteries and arterioles are controlled in this way. Vasoconstriction of vessels decreases blood flow and increases resistance and blood pressure. The cardiovascular and vasomotor centres control these diameter changes of the blood vessels. In rest via parasympathetic stimulation and during action via sympathetic stimulation. Blood is provided where it is needed by extrinsic control via hormones and the nerves system. Intrinsic control provides enough blood to individual organs and the surrounding tissue. With autoregulation, organs can keep their blood flow constant under changing perfusion pressure or during higher metabolic needs. Lastly, the body uses homeostatic mechanisms or receptors as baroreceptors and volumereceptors to keep blood flow and pressure constant [3].

The cardiac cycle involves the diastole and systole. During diastole, the ventricles fill with blood because of the relaxation of the heart. Systole follows, which is the contraction of the ventricles to pump

the blood into the blood circuits. The cardiac cycle can be described with a pressure-volume relationship as visualised in Figure 2.1. First, there is the filling phase of the ventricles until the end diastolic volume (EDV) is reached. This is the volume of blood in the ventricles before systole. Secondly, comes an isovolumetric contraction phase until the aortic and pulmonary valves open. Thirdly, is the ejection phase until the end systolic volume (ESV) point, which is the volume of blood in the ventricles after contraction. Lastly, comes a period of isovolumetric relaxation [68]. The difference between EDV and ESV is called stroke volume (SV). By multiplying HR with SV, the CO can be calculated. ESV and EDV are influenced by preload and afterload.

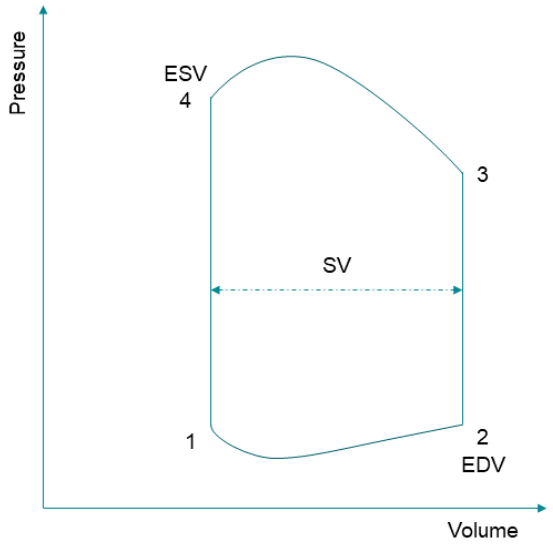

Figure 2.1: A pressure-volume loop visualising the cardiac cycle. The filling phase of the heart is from point 1 to 2 and point 2 resembles the end diastolic volume. From point 2 to 3 is the isovolumetric contraction phase and point 3 to 4 is the ejection phase. Point 4 resembles the end systolic volume and from point 4 to 1 is the phase of isovolumetric relaxation. [68, pg.58]

Preload is a measure for wall tension build-up and increased sarcomere length in the ventricles during diastole. Increase in EDV means an increase in preload and results in higher contractile forces, which is known as the Frank-Starling law. This law states that for a higher venous return, there will be an increased force of contraction [68]. In this way, the heart keeps the ventricle output the same for the left and right ventricle and compensates for higher venous blood pressure.

Afterload is a measure of wall tension during the ejection phase. It is often defined as the pressure the heart needs to overcome to discharge blood from the ventricles. Afterload increases by an increase of pulmonary or aorta pressure and when the heart is more dilated. CO decreases by an increase of afterload. Lastly, an increase in ESV means an increase in afterload.

CO can be calculated with the use of blood pressure and peripheral resistance, which will be elaborated in Section 2.2. Besides the CO, there is the option to calculate the mean arterial pressure (MAP), which is calculated with the diastolic pressure, the lowest pressure between two heartbeats, and the systolic pressure, the maximal aorta pressure. The mean arterial pressure is maintained stable by extrinsic control and correlates with the afterload.

$$\text{MAP} = \frac{(2 \cdot \text{diastolic pressure}) + \text{systolic pressure}}{3}$$

Blood pressure drops gradually while flowing across the systemic circuit. The pressure drop is little in the bigger elastic arteries, then drops with 70% in the small arteries and arteriole and with another 20% in the capillaries [68]. There is a lower pressure drop over the capillaries because it is a network

of many parallel vessels. The arteries are seen as the supply vessels, the capillaries are for exchange and the veins have a reservoir function.

2.1.2. Fetal circulation

The composition of the placenta has been explained in Section 1.1. In short, it is a disk attached to the uterus wall and on the chorionic side attached to the fetus via the umbilical cord. After the exchange of oxygen, carbon dioxide and nutrients in the placenta, fetal blood will flow from the chorionic villi via the umbilical vein towards the fetal body. The fetal blood circulation differs from the adult circulation. It contains three shunts to protect and bypass the immature liver and lungs. In Figure 2.2 can be seen that blood travels via the umbilical vein into the inferior vena cava. The flow partly bypasses the liver via the ductus venosus shunt. Reaching the heart, blood shunts via the foramen ovale shunt from

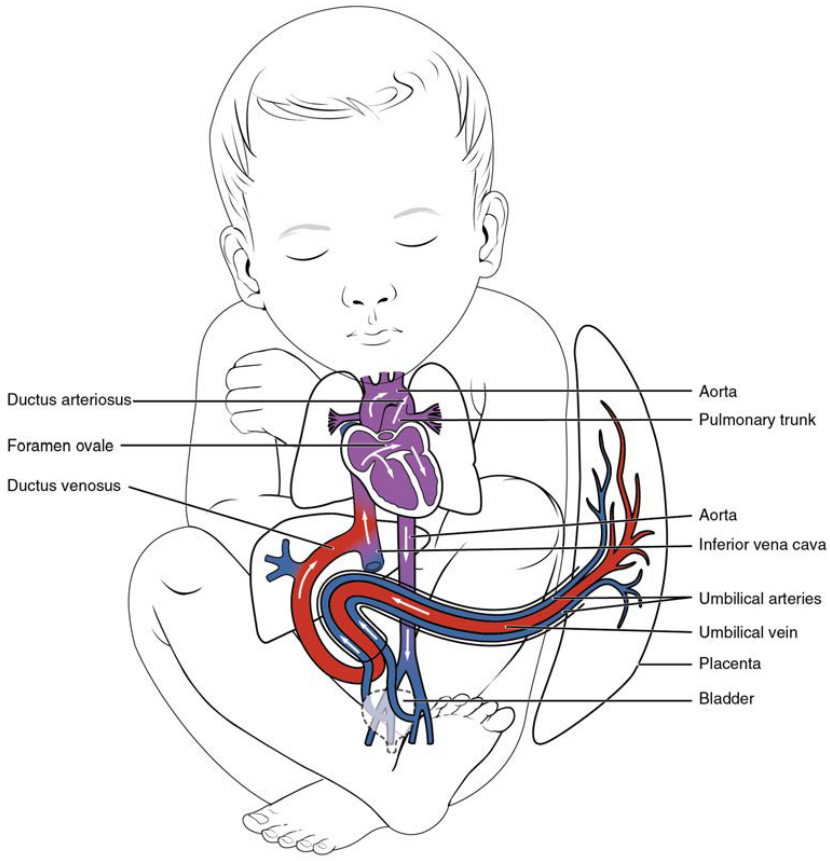

Figure 2.2: Blood circulation of the fetus and the placenta. Visible are the ductus arteriosus shunt, foramen ovale shunt and ductus venosus shunt [3, pg.960].

the right to the left atrium, to bypass the lungs. Lastly, the third shunt is the ductus arteriosus shunt, placed between the pulmonary artery and the aorta. In this way, only a small fraction of blood travels through the lungs. Because of the three shunts, deoxygenated and oxygenated blood are mixed and via the aorta travelling through the fetal body. Via the internal iliac arteries blood is pumped towards the placenta via two umbilical arteries. After birth, the three shunts will eventually close and the umbilical vessels collapse after being clamped and detached from the placenta. With the first breath, the lungs will inflate and the child can absorb oxygen for itself.

The fetal circulatory system differs from the adult system because of the three shunts, the lungs with low gas exchange and low blood flow, and the connection to the placenta. The ventricles of the fetal heart work in parallel due to the foramen ovale and the output of this parallel system is referred to as combined ventricular output (CVO). Opposite to adults, the pulmonary resistance in the fetal body is higher than the systemic resistance, to stimulate shunting past the pulmonary circuit [8]. The lungs of

the fetus are still collapsed and providing higher vascular resistance. The systemic resistance is low because of the low resistance of the placenta, almost 50% of the combined ventricular output goes towards the placenta [63].

2.2. Blood flow dynamics

To create a cardiovascular model of the fetus and placenta some fluid dynamics needs to be explained. Modelling blood flow is very complex. So, to create an acceptable model for this study some assumptions and simplifications were used. This paragraph will enumerate the basic fluid dynamics that were used to create the cardiovascular model of the fetus.

2.2.1. Hagen-Poiseuille's law

The Hagen-Poiseuille law gives the opportunity to model blood flow in blood vessels. The Hagen-Poiseuille law, in short Poiseuille's law, is derived from the Navier-Stokes equations, differential equations of motion for incompressible Newtonian fluids [68]. Poiseuille's law computes the volumetric flow rate, Q (L s^{-1}) for a cylindrical pipe based on the resistance, R (Pa s L^{-1}) delivered to the fluid and the pressure drop, ΔP (Pa). The resistance is over total the pipe length, L_v (m), with a radius r (m), for a fluid with viscosity η (kg m^{-1} s^{-1} or Pa s).

$$Q = \frac{\Delta P}{R} = \frac{\pi r^4 \Delta P}{8 \eta L_v} \tag{2.1}$$

Poiseuille's law is valid under the following conditions:

- no-slip condition
- a homogeneous Newtonian fluid
- laminar flow
- steady flow
- fully developed flow without entrance or exit effects
- incompressible flow
- a straight circular pipe with a constant radius

The definition for a fluid is that a fluid, in comparison to a solid, will deform when shear stress is applied on it [70]. Shear stress causes shear deformation of a fluid and is biggest at the wall alongside which a fluid flows. Alongside this wall, the velocity of the fluid is zero relative to the wall, because a fluid adheres to the surface. This is called the no-slip condition and this condition is applicable for viscous fluid flows, so also for blood. The resistance of a fluid to shear deformation is defined by the viscosity of the fluid. It is denoted with μ or η and called dynamic viscosity.

For Newtonian fluids as water, the shear stress and viscosity are proportional. However, for a non-Newtonian fluid, this is not the case. Some increase in resistance with higher shear stress, others decrease in resistance. This last group, the shear-thinning group is also applicable for blood, that decreases in viscosity at higher shear rates. Also, blood contains formed elements as erythrocytes that influence its viscosity. The viscosity of human blood is approximately 3 to 6 mPa s and its density is 1060 kg m^{-3} [33]. In very small vessels viscosity fluctuates, because of blood behaving non-Newtonian. For vessels bigger than 1 mm in diameter blood is considered to behave Newtonian as well as at shear rates above 100 s^{-1} [68]. So for the model, blood will be assumed to behave Newtonian. However, when the shear stress becomes too high, red blood cells could be destroyed. Viscosity is slightly affected by pressure but strongly affected by the temperature. Viscosity decreases with temperature. Human bodies are maintained at a constant temperature of 37 °C, so viscosity is hardly affected by temperature in the human body. Lastly, viscosity is also changing for different haematocrit levels and vessel diameters. For higher haematocrit levels, the viscosity increases slowly.

The third condition is laminar flow. The dimensionless Reynolds number can tell if the fluid flow is

laminar or turbulent. It is computed with the density, ρ (kg m^{-3}), viscosity, velocity, v (m s^{-1}), of the fluid and the vessel diameter, D (m):

$$Re = \frac{\rho v D}{\mu} \tag{2.2}$$

Laminar flow is slow and has a Reynolds number below 2300. Turbulent flow is fluctuating and occurs at a Reynolds number above 4000. Between these two is a transition region. Normally, in humans the Reynolds number stays below 2000, so blood flow is considered laminar. However, branching of vessels and other fluid-wall interactions can result in local turbulence [68]. In micro-vessels, which are vessels smaller than 0.3 mm, the flow is dominated by viscous forces, because of the interaction of blood cells with blood vessel walls. This is called the Fahraeuss-Lindqvist effect. The viscosity decreases because of a cell-free layer on the vessel walls [13]. This means that with standard calculations the resistance is overestimated and in reality a little bit smaller.

The fourth point is a steady flow, which is a flow that is independent of time. Obviously, blood flow is pulsating and the velocity of the flow would change over time, as will the pressure across the length of the vessels. So using Poiseuille's law will mean a simplification of the fluid flow. It is considered that blood flow is pulsating in large arteries, becomes less pulsatile when flowing towards the peripheral blood vessels and it flows steady into the capillaries. It starts pulsating again when flowing back to the heart via the larger veins [68].

Within a pipe, the viscous effect of laminar or turbulent flow will spread throughout the entire flow. Except at the entrance of the pipe. Viscous boundary layers start growing at the entrance until they merge and the entire flow becomes viscous. After this entrance length, the velocity profile and wall shear stress will be constant. The velocity profile changes from a flat profile into a parabolic profile, as can be seen in Figure 2.3. Also, in the fully developed region, the pressure drop along the length of the pipe will be linear.

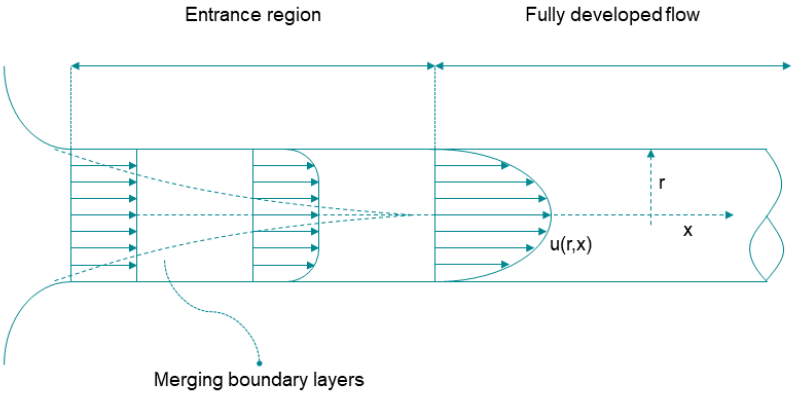

Figure 2.3: At the entrance region of a pipe, the viscous boundary layers will merge eventually, after which the flow is considered fully developed. The velocity profile, $u(r, x)$, changes from flat to parabolic during this transition. Inspired on White [70, pg.363].

Incompressible flow means that within an infinite small fluid parcel, which moves at flow velocity, the density is constant ($\rho_{in} = \rho_{out}$) [68]. This is also useful for the principle of conservation of mass, as shown in (2.3) with A (m^2) being the area of the cross-section of the vessel. This law states that mass flowing in over time also leaves the system with the same mass flow over the same time.

$$\rho_{in} A_{in} v_{in} = \rho_{out} A_{out} v_{out} = \text{constant} \tag{2.3}$$

For incompressible flow with a constant density, (2.3) can be simplified to $A_{in} v_{in} = A_{out} v_{out}$, which is the flow rate going in and out. The volumetric flow rate can be used to calculate the average velocity

in m s^{-1} inside the vessel. This is done by dividing the flow rate by the area of the cross section of the pipe:

$$v_{avg} = \frac{Q}{A} \tag{2.4}$$

Poiseuille's law requires a pipe with a constant radius. Blood vessels are considered to be of fairly constant radius and decreasing in radius at bifurcation points. In (2.1) the radius is to the fourth power, which means that changing the radius highly affects the volume flow rate. Reducing the blood vessel diameter with 2 increases the resistance 16 times. The resistance to blood flow is regulated by changing the radius of blood vessels, the earlier explained vasodilation and vasoconstriction.

2.2.2. Additional equations

In the medical world, the stiffness of structures is described with elastance, E (Pa m^{-3}). Elastance describes the ability of hollow organs to return to their original volume when outside forces are removed [68]. The symbol for volume is V and its units are L or m^3.

$$E = \frac{\Delta P}{\Delta V} = \frac{1}{C} \tag{2.5}$$

Elastance is inversely related to compliance, C (m^3 Pa^{-1}). Compliance is a measure for how much an organ yields to outside forces. Veins are more compliant than arteries and are therefore seen as the capacitors of the vascular system [3]. So higher compliance and constant volume result in a lower the pressure difference.

2.3. Chapter conclusion

Information in this chapter was used to simulate the dynamics of the model correctly. For the physical constraints, it is important to know that the blood circulation of the fetus differs from the adult circulation because of three vascular shunts, non-inflated lungs, and the placental vasculature. As regards the blood circulation through the body, the compensatory mechanisms of the heart and vasoactivity of the vessels in the body are especially important for later evaluation of the cardiovascular model. The objective of this study is to intervene with the vessels in the umbilical cord and so making changes to the systemic vascular resistance and venous return to the heart. Poiseuille's law is convenient to use for the cardiovascular model because of its simplicity. It gives an opportunity to evaluate changes in the cardiovascular system without making the model too elaborate. However, some assumptions are needed to use Poiseuille's law.

The velocity of blood flow is zero alongside the wall because of the no-slip condition for viscous fluids. Blood is a non-Newtonian fluid because it contains formed elements. However, it is assumed to behave Newtonian in vessels bigger than 1 mm in diameter. Also, the body temperature inside the womb is considered very constant, so the viscosity does not change much. In the majority of the vessels, blood flow is laminar, so this is assumed to be the case for the whole model. Steady flow means a flow which does not change over time, so a flow without a pulse. Blood flow is especially pulsatile in the bigger arteries close to the heart but more steady in the peripheral vessels. In the model, blood flow will be modelled steady in all parts. The flow is considered to be fully developed without entrance or exit effects. The density of the flow is assumed to be constant, so the flow would be incompressible. Lastly, the blood vessels are assumed to be straight circular pipes with a constant radius. With the combination of Poiseuille's law and compliance, a basic model can be made for blood flow in the fetal body.

3 | Design

The basic anatomy of the fetal body and blood flow dynamics were discussed. The goal of this chapter is to categorise the most important parts of the fetal cardiovascular system and to make a design for the layout that needs to be implemented into a fetal cardiovascular model.

3.1. Cardiovascular models in literature

An search was performed in online databases as Pubmed[1], Google Scholar[2] and Scopus[3] to identify existing cardiovascular models and in particular of models of the fetal and placental vascular system. In Appendix B a summary is given of the exact steps taken to find cardiovascular models. These models should preferably be made in Simulink. Simulink is a simulation tool and used to make block-diagrams of dynamic systems and is integrated into MATLAB 2018a (The MathWorks, Inc., Natick, Massachussetts, Unites States).

3.1.1. Cardiovascular models

Sheffer et al. [61] designed a toolbox to model the cardiovascular system and this toolbox was updated over the next years by other researchers [2, 40, 41]. They created separate subsystems to be combined together by the users own preferences. Unfortunately, this toolbox is no longer available or compatible with the available versions of MATLAB and Simulink. However, it is still a useful example to see how to separate and model the different components of the vascular system.

The study of Sheffer et al. [61] focuses on the cardiovascular system and the heart is modelled extensively. The heart chambers and valves are available in the toolbox and with use of pressure-volume relationships, they are able to calculate the varying pressure in the heart due to filling and emptying of the heart chambers. The mathematical models used to model the blood vessel segments in the cardiovascular toolbox are based on reduced Navier-Stokes equations. Lastly, oxygen and carbon dioxide distribution are implemented in the cardiovascular simulation toolbox, but this will not be implemented in the model of this thesis project.

In the described search of Appendix B, more studies were found that use the same elements to describe pressure-flow relations. There is the study of Garcia-Canadilla et al. [14], who also made a fetal cardiovascular model in Simulink. However, they focused on the major arteries and outflow from these arteries. Also, the placenta and lower body are integrated into one segment, which makes analysing placental flow more difficult. More complex models were also found, like the model of Van der Hout-van der Jagt et al. [65]. They included the maternal circulation and uterine pressure to observe hemodynamic and oxygenation changes during umbilical cord compression. The increase in uterine pressure and compression of the umbilical cord in this study are due to contractions. The focus of this thesis project is not during the time of contractions and uterine pressure variations are less present, so uterine pressure could be assumed more constant. The models of Garcia-Canadilla et al. [14] and Van der Hout-van der Jagt et al. [65] are still useful to evaluate the fetal cardiovascular model.

3.1.2. Lumped parameter model and Windkessel model

In the studies of cardiovascular systems as from Sheffer et al. [61], they make use of lumped parameter models. The lumped parameter model is an approximation of a complex system that is divided into a finite amount of discrete segments to study its behaviour. The use of lumped segments is comparable to using rigid bodies in mechanical calculations, where the rigid body functions as one entity. For instance, all the aorta segments can be lumped together into one lumped segment representing the aorta. The segments in a lumped parameter model are connected by wires that work instantaneously

[1] www.ncbi.nlm.nih.gov/pubmed
[2] scholar.google.nl
[3] www.scopus.com

and are joined in nodes. The wires represent the blood flow between segments [52]. At the nodes, information can be calculated about the segments [68].

The pressure-flow relation in a segment can be described with the use of Ohm's law:

$$I = \Delta V / R \tag{3.1}$$

Ohm's law states that the current through a conductor, measured in amperes (A), is proportional to the voltage difference across the conductor, measured in volts (V). The resistance of the conductor is measured in units of Ohm (Ω). The hemodynamic relation analogue to Ohm's law is $Q = \Delta P / R$. Here the current is the blood flow, Q, the pressure gradient across the segment is related to the voltage difference and the resistance is the resistance of the segment to the blood flow.

In a lumped parameter model, flow and pressure work according to Kirchhoff's Voltage and Current Laws [68]. Kirchhoff's Current Law states that the sum of currents flowing into a node is the same as currents flowing out. So, segments in series have the same volume of flow flowing through. Kirchhoff's Voltage Law states that the sum of voltages around any closed loop is zero.

It is also possible to include the compliance of blood vessels or organs into the model in the form of a capacitor or inertia to blood flow in the form of an inductor. Compliance is primarily present in the aorta and other major vessels as the pulmonary artery. Compliance of the major vessels compensates for fluctuations in blood flow between diastole and systole. To describe this mechanism the windkessel model can be used, which is a lumped element model. The windkessel model was first described by Otto Frank in 1899 [13]. It represents a pumped fire engine. Water is pumped periodically into a high-pressure air chamber, resembling the heart pumping blood in the aorta. Whereupon water is drained from the chamber in a steady flow, because of the high mean pressure of the chamber, which resembles the interaction between the aorta and peripheral blood vessels. During systole, the vessel wall of the aorta enlarges and stores blood, which is released during diastole to make the pulsatile flow more continuous. The windkessel model is represented with 2, 3 or 4 elements in the form of resistors, capacitors, and inductors. In Figure 3.1 a two element model is shown with a resistor and capacitor. Compliance does not only compensate for blood flow fluctuations but is also influences blood pressure. In vessels, vasodilation and vasoconstriction influence the vascular tone. When vessels constrict, their compliance is lowered and also the blood volume. The blood pressure will then increase. The blood pressure in the system is influenced by the pressure-volume relationship of vessels, so by compliance.

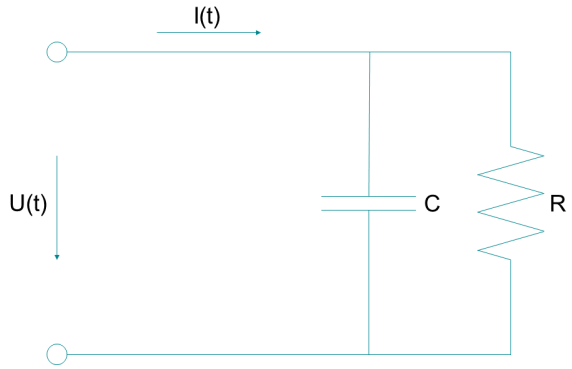

Figure 3.1: Example of a two element windkessel model which could represent a blood vessel with peripheral resistance and compliance.

3.2. Pressure and flow rate equations

The lumped parameter model and windkessel model are considered to be appropriate methods to obtain information about the cardiovascular system [41]. They are a useful tool to perform pressure calculations based on cardiac output. The theory of Chapter 2 will be applied to the segments in the

models described in this chapter.

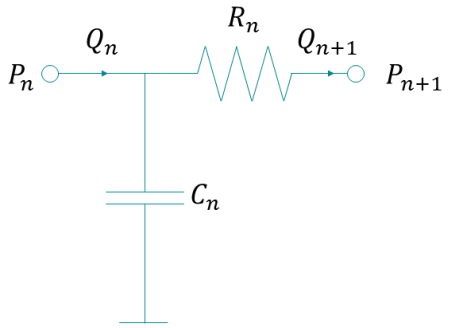

Figure 3.2: The layout of a separate segment, with one capacitor and one resistor.

In Figure 3.2 the structure of a single segment is represented. This layout will be used for all the segments in the fetal cardiovascular model. Poiseuille's law described in (2.1) is used to calculate the pressure change between nodes. After rewriting (2.1), the pressure drop over a segment is calculated with:

$$\Delta P(t) = RQ(t) \tag{3.2}$$

Inertia, I (mmHg s^2 mL^{-1}), is left out of this equation, to keep the model simple, because this would mean yet another variable that needs to be estimated. When an inductor would be added to the system, (3.2) would become $\Delta P = RQ + I(dQ/dt)$ [2]. The cardiac output will be modelled as a constant input into the system, so there will be no velocity changes of the flow over time besides from the start-up time of the model.
The intervention in the umbilical artery will locally increase the resistance to blood flow. Important is then to see how this changes blood flow and pressure in the rest of the systemic system to estimate the feasibility of the intrauterine support system. A constant cardiac output is chosen because information about the mean arterial pressure inside the cardiovascular system is sufficient enough to give information about blood flow and pressure distribution through the peripheral system. However, this has as a consequence that the flow is primarily influenced by the peripheral resistance of the cardiovascular system.

If the pressure drop over the n^{th} segment is known, then it can be used to calculate the outward flow towards the $n^{\text{th}} + 1$ segment by using (3.2):

$$Q_{n+1}(t) = \frac{P_n(t) - P_{n+1}(t)}{R_n} \tag{3.3}$$

The resistance, R_n, can be calculated as described in (2.1):

$$R = \frac{8\eta L_v}{\pi r^4} \tag{3.4}$$

The second element in Figure 3.2 is the capacitor. The capacitor resembles compliance. It depends on the volume in the n^{th} segment and the pressure, as was shown in (2.5). According to the law of conservation of mass, in a closed system mass can not be added or destroyed. So the change of the volume in the segment over time depends on the mass inflow and outflow.

$$\frac{dV_n(t)}{dt} = Q_n(t) - Q_{n+1}(t) \tag{3.5}$$

Rewriting (3.5) into (2.5) gives a formula to describe the pressure difference inside a segment [45].

$$\frac{dP_n(t)}{dt} = \frac{Q_n(t) - Q_{n+1}(t)}{C_n} \tag{3.6}$$

With (3.3) and (3.6) the resistance that blood flow experiences over the length of a segment is described and the volume change inside a segment because of compliance.

3.3. Layout of the segments of the fetal cardiovascular model

The organs and important vessels will be modelled as lumped elements. Important is to decide which parts will be lumped together and which ones not.
In Section 1.1 and Section 2.1.1 the fetal cardiovascular system was described and the three points in which it differs from an adult cardiovascular system. These are the three shunts, the not expanded lungs and the connection with the placenta, as visible in Figure 2.2. Together with the information about the fetal anatomy, examples from other studies are useful to form a design for the fetal cardiovascular model. This needs to be sufficient in representing the fetal cardiovascular system without being too complicated for the available information and needs to answer the research question.

The cardiovascular system is divided into the systemic and pulmonary system. The pulmonary system contains the non-expanded lungs. Van Vonderen et al. [67] divide the systemic system into the upper body and lower body. The upper body is a combined unit resembling the brain and upper extremities. The lower body resembles the lower regions of the fetal body and organs beneath the heart. The stream towards the lower extremities is also partly led towards the placenta via the umbilical cord. However, in the model of Van Vonderen et al. [67] the blood vessels and shunts are not represented as separate blocks. Yet, this is needed for the fetal cardiovascular model, because it needs to be visualised how flow redistributes among the different segments in the fetal body. Also, the umbilical artery needs to be accessible for experiments. The model of Van Vonderen et al. [67] was used as the starting point for the model because of its simplicity.

A model which does describe also the arteries is the model of Luria et al. [31]. In their study, they based their calculations on the study of Barnea [2], who designed the cardiovascular simulation toolbox mentioned in Section 3.1.1. Luria et al. [31] split up the upper body unit in two streams, one with the carotid arteries and brain and in the other the remaining parts of the upper body. Both streams end into the superior vena cava. This is because the focus of their study lays on fetal growth restriction (FGR). The fetal body keeps the flow of oxygen to the brains as optimal as possible during FGR despite a shortage of oxygen in the blood, which is called the brain-sparing effect. However, the focus of this thesis study is on the umbilical blood flow and possible redistribution of flow to other parts in the cardiovascular system. This bypass of blood flow to other parts of the system could be created by increased resistance in the umbilical cord. A general picture of redistribution of blood flow is sufficient enough, so the brain does not have to be modelled as a separate lumped unit. What does need to be modelled separate are the umbilical arteries, placenta, and umbilical vein. Luria et al. [31] do model these separate with the umbilical vein leading into the ductus venosus and hepatic system. The hepatic system directs blood flow from the gastrointestinal tract towards the liver.

It is now possible to summarise all the segments for the design of the fetal cardiovascular model and this is visualised in Figure 3.3. First, the pump of the system is important. This is the fetal heart providing combined ventricular output, because of the foramen ovale. Secondly, the pulmonary system containing the pulmonary artery and the lungs. Also, the ductus arteriosus will get a block, to simulate blood shunting from the pulmonary artery towards the aorta. Then, the systemic system with the aorta, which directs blood towards the upper body and lower body. And last, the umbilical arteries, placenta, umbilical vein, ductus venosus, and hepatic system.

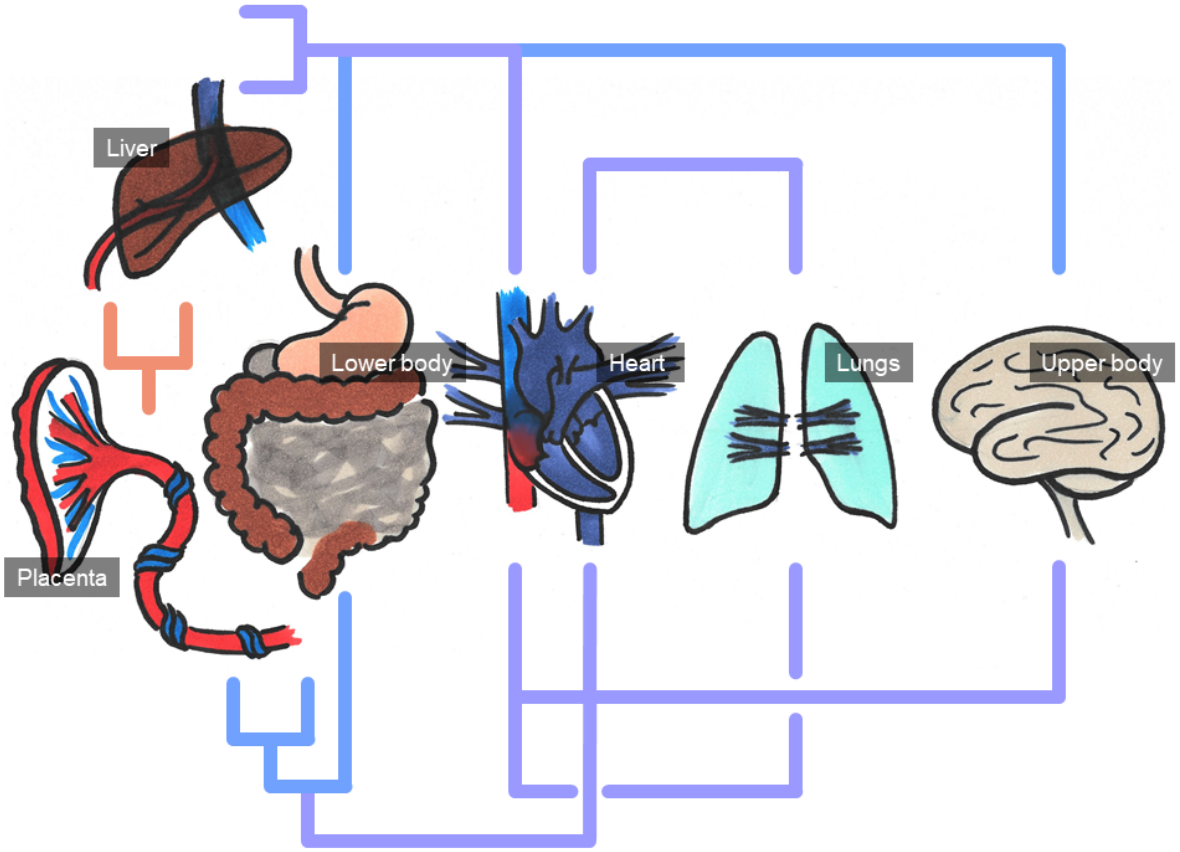

Figure 3.3: An overview of the segments that will be included in the fetal cardiovascular model. From left to right the placenta, including the umbilical cord with two umbilical arteries and the umbilical vein, the liver, representing the ductus venosus and hepatic system, the lower body, the heart, including the pulmonary artery, aorta and ductus arteriosus, the lungs and the upper body. Flow is oxygenated in the placenta and mixed with non-oxygenated blood in the body. ©Esther Wachter

3.4. Chapter conclusion

With the information gathered in Chapters 1 to 3, it is now evident what the important elements are to implement in the fetal cardiovascular model. Literature provided the lumped parameter model, which simplifies the cardiovascular system into relevant pieces. Blood vessels, organs, and body parts will be lumped together to visualise the primary flows through the fetal body and the placenta.
Blood flow and pressure will be simulated with a model resembling an electrical circuit. The reason is that an analogy can be drawn from Ohm's law for electric circuits and a flow circuits. This circuit will include resistors and capacitors, resembling resistance and compliance to calculate blood flow and pressure in the fetal body. The next step is to design the fetal cardiovascular model in Simulink and find the appropriate values for the resistance, compliance, blood flow, and blood pressure.

4 | Method

The chapter will explain how the fetal cardiovascular model was designed in Simulink and how the connections between the segments were built. The second part of this chapter will explain the parameters that were used in the model and how they were found or determined.

4.1. Design of the fetal cardiovascular model

In Chapter 3 the various segments for the fetal cardiovascular model were determined. In Figure 4.1, the segments are neatly ordered and this is the way how they were implemented in Simulink. First, there is the heart. Officially, it consists of the left and right atria and ventricles and the foramen ovale shunt between the two atria. In the fetal cardiovascular model, these 5 elements will not be modelled and the heart will be modelled as a pump with a constant outflow of blood and the pressure in the heart atria is set to a constant value. More information about this choice can be found in Section 4.1.2. The two outflows from the heart are the pulmonary artery (PA) and the aorta (AO). The connection between the two is formed by the ductus arteriosus shunt (DA). Flow from the pulmonary artery leads to the lungs, represented by the pulmonary vascular resistance (PVR). The systemic vascular resistance (SVR) is divided into the upper body (UB) and lower body (LB). Lastly, there is the path via the placenta (PLA), with the two umbilical arteries (UA1 and UA2), the umbilical vein (UV), the ductus venosus shunt (DV) and the hepatic system (HE). Normally, blood flowing through the upper body is collected in the superior vena cava and flow from the lower body in the inferior vena cava. Both veins enter the heart in the left atrium but are not included as separate segments. The pulmonary veins enter the heart in the right atrium. In this model, however, there will be no clear difference between the two atria.

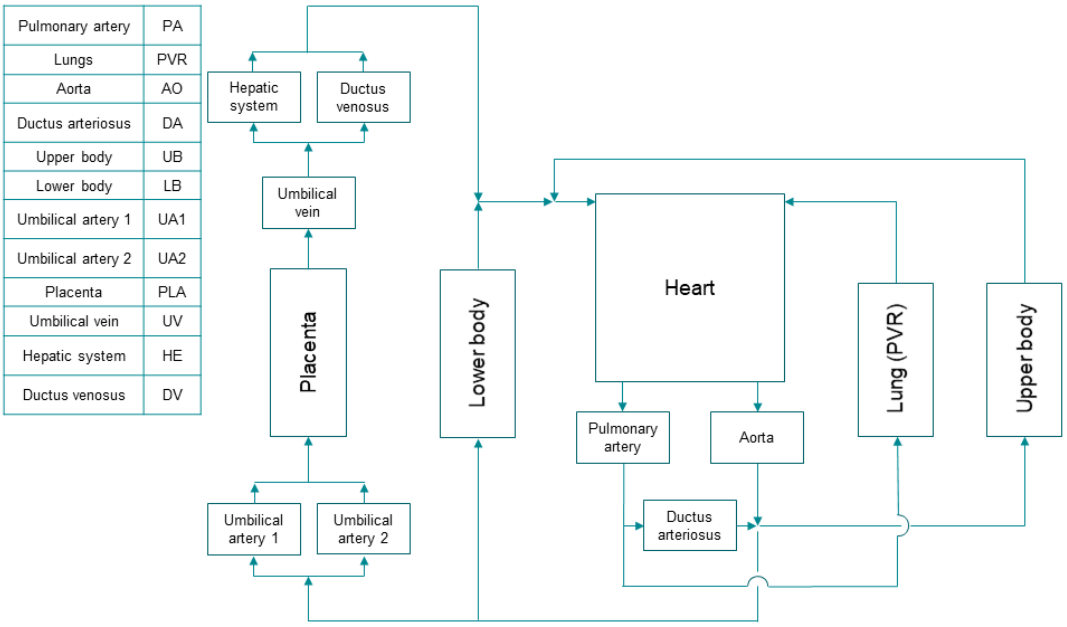

Figure 4.1: The simplified version of Figure 3.3 and the layout for the fetal cardiovascular model. Based on Van Vonderen et al. [67] and Luria et al. [31].

4.1.1. Series and parallel system blocks

Most of the vessels and organs are connected in series, as can be seen in Figure 4.1. Only the two uterine arteries and the ductus venosus and hepatic system are running parallel. This applies when looking at the elements separately. When zooming out it is also clear that for instance, the lower body

runs parallel to the stream of the placenta and hepatic system. However, the connections between all the segments will be explained in the next paragraph.

First, an explanation about the layout of a single series element. Every element block will have its own resistance and compliance, except for the heart. The heart provides the blood flow, Q, and will be discussed later. For convenience, (3.3) and (3.6) will be repeated here to make explaining the layout of the Simulink blocks easier.

$$Q_{n+1}(t) = \frac{P_n(t) - P_{n+1}(t)}{R_n} \tag{4.1}$$

$$\frac{dP_n(t)}{dt} = \frac{Q_n(t) - Q_{n+1}(t)}{C_n} \tag{4.2}$$

When looking at (4.2), known input variables of a series block are the compliance and the blood inflow. The blood outflow and time-varying pressure are unknown. The resistance is the only known input in (4.1). Simulink can be a very useful tool to find the unknown variables. By integrating dP/dt, the pressure at the node in front of a block can be calculated. The integrator needs an initial value for the pressure in the element. If the pressure after the block is known, the outflow of Q_{n+1} could be calculated. Whereupon the Q_{n+1} can be fed back into (4.2) to calculate dP/dt. These steps can be seen in the block diagram in Figure 4.2. First (4.2) was implemented, followed by (4.1) to be fed back into the first step. P_{n+1} needs to be given as input into the block, to be able to solve the equations.

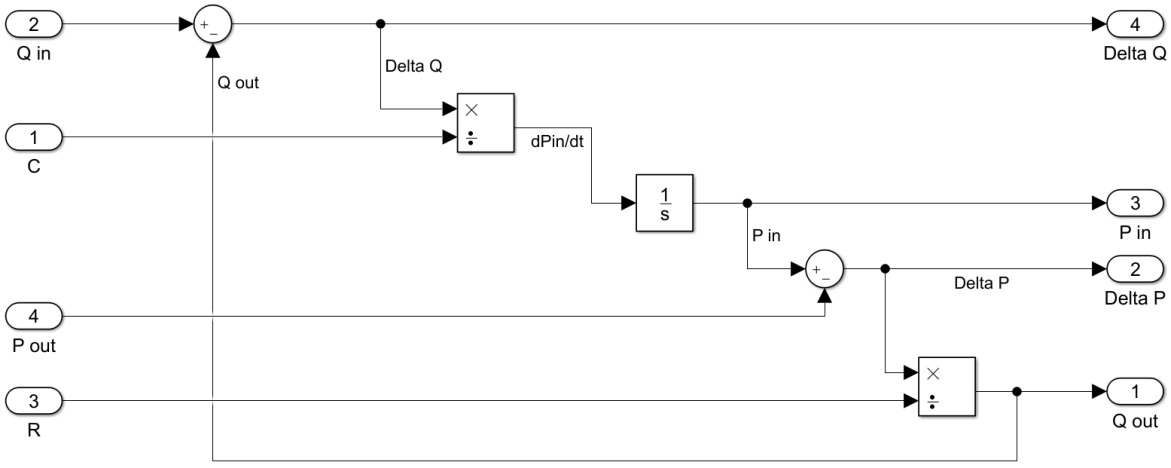

Figure 4.2: Series block as implemented in Simulink. On the left the input ports for C, Q_{in}, P_{out} and R and on the right the output ports for ΔQ, P_{in}, ΔP and Q_{out}.

As explained in Chapter 3, elements in parallel do have the same pressure drop across them. If the two elements have different resistances, then with (4.1) the distribution of blood flow across both vessels can be calculated. In a parallel system, capacitors have the same pressure drop across them. Both store a volume of blood to release later at the same node. The total compliance is therefor added up, opposite to resistors in parallel. So, the differences with the series block are the two resistors to calculate the separate outflows of blood and the two capacitors that are add up to calculate the total compliance of both blocks together. The layout of a parallel block diagram can be seen in Figure 4.3.

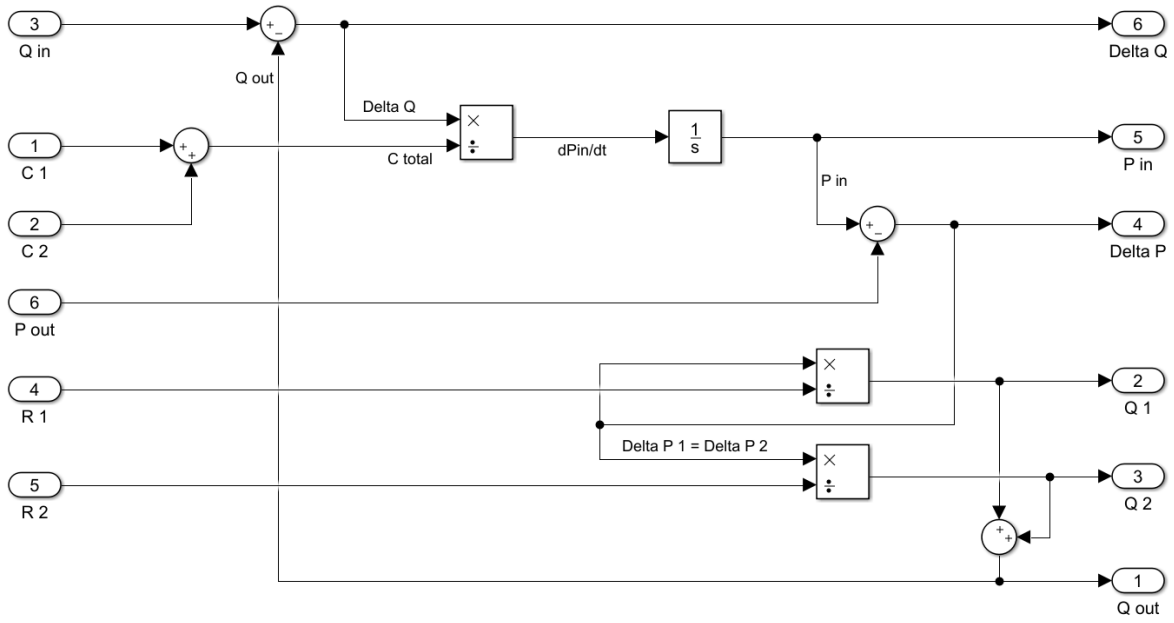

Figure 4.3: Parallel block as implemented in Simulink. On the left the input ports for $C1$, $C2$, Q_{in}, P_{out} $R1$ and $R2$ and on the right the output ports for ΔQ, P_{in}, ΔP, $Q1$, $Q2$, and Q_{out}.

4.1.2. The modelled heart

The heart is modelled as a pump supplying constant blood flow to the vascular system. Adding all the different compartments of the heart and making the model closed loop would complicate the model hugely. The model created is an open-loop model and its output variables are the blood flow entering the heart atria. Two other outputs of the heart will be the pressure at the pulmonary artery and aorta. Next to flow as input, also the pressure of the left and right atria (LAP and RAP) needs to be given as input. It was established with (4.1) and (4.2) that the output pressure was needed to calculate all the missing variables. The residual pressure of the two heart atria was given a constant value. The blood flow, Q, travels through the system until it reaches the heart again. The pressure of LAP and RAP is known. So the output pressure of HE, DV, LB, PVR and UB, which all end in the heart, are also known. Now, the input pressure of these segments can be calculated and in their turn can be fed back to the segments in front of them. This means that the output pressure of PA is the input pressure of DA and PVR. The output pressure of DA and AO are the same and are the input pressure of UB, LB, UA1, and UA2.

The pressure in the atria was set to zero to easily calculate the overall pressure drop over the total system. This is not very contrasting to the real-life situation, because the pressure in the atria is around 2 to 3 mmHg [42]. It is very useful to calculate the total pressure drop over the system to make sure that it is not too high for the fetal heart to overcome. However, with constant values for blood flow from the heart and output pressures at the atria, there is no compensation from the heart to applied changes to the system. For instance, higher pressures in the aorta and pulmonary artery would in real life mean an increase in afterload and a decrease in stroke volume and cardiac output, as discussed in Section 2.1.1. Still, the open-loop model can show the changes in blood distribution.

4.1.3. Connections between the segments

When zooming out from the separate segments to the whole fetal cardiovascular system, more series and parallel paths can be identified. As mentioned before, the lower body is parallel to the path with the umbilical arteries, placenta, umbilical vein, ductus venosus, and hepatic system. The upper body is in its turn parallel to those two paths of the lower body and placenta. Then there is the complex part, which is the ductus arteriosus. The path of PVR is in a way parallel to the path of the ductus arteriosus and SVR. However, the aorta also provides input of blood flow into SVR. Without the ductus, SVR and

PVR would be two separate loops only connected by the heart.

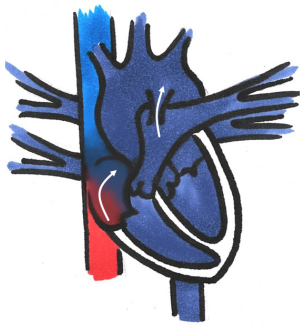

Figure 4.4: Close-up of a heart with the ductus arteriosus and foramen ovale. The ductus arteriosus is indicated with the right arrow that starts in the pulmonary artery and points towards the aorta. The left arrow in the right atrium indicates how flow travels towards the left atrium via the foramen ovale, which is hidden behind the pulmonary trunk and aorta.

In Figure 4.4, it is visible that the ductus arteriosus is connected to the aorta at the end of the aortic arch. From the aortic arch the carotid and subclavian arteries sprout. This anatomy structure implies that a part of the upper body receives more blood directly from the left ventricle and that flow of the ductus arteriosus is probably directed more towards the lower body. This distribution of blood flow was not implemented into the model, because then the aorta needed to be split up into different resistance parts as well. Also, the ductus arteriosus is a very small segment in comparison to the aorta and to predict how blood flow from the ductus arteriosus and left ventricle are distributed in the aortic arch is to complex for this study. In the fetal cardiovascular model, the ductus arteriosus and aortic blood flow are first connected with a node, after which the flow is divided over the upper and lower body streams.

The flow between segments needs to be distributed by the model correctly. The output and input pressures will be connected and for segments in series also the output and input flow rate will be connected. However, there are four points where the distribution of flow rate is more complex.

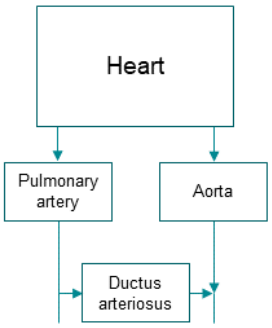

Figure 4.5: The loop including the heart, the pulmonary artery, ductus arteriosus, and aorta.

The first point is the part of the heart, pulmonary artery, ductus arteriosus, and aorta, as shown in Figure 4.5. The combined ventricular output needs to be distributed over the pulmonary artery and the aorta. Kirchhoff's Voltage law will be used for this part of the system. This law states that the sum of voltages around a closed loop is zero. The heart, PA, DA, and AO can be seen as a closed-loop. In the model, the heart was modelled as a pump with no information about the ventricles. The ventricles work in parallel and can be seen as a current source for the pulmonary artery and aorta. The sum of

the voltages in the closed-loop is the pressure drops over PA, DA, and AO and they need to be zero together. In the Simulink model, the pressure difference over the pulmonary artery was calculated by subtracting the pressure difference of the ductus arteriosus from the aorta. Subsequently, with the resistance of PA, the flow rate through PA was calculated. This flow rate was subtracted from the CVO constant to give the flow rate for AO.

$$\Delta P_{AO} - \Delta P_{DA} = \Delta P_{PA} \tag{4.3}$$

$$\frac{\Delta P_{PA}}{R_{PA}} = Q_{inPA} \tag{4.4}$$

$$CVO - Q_{inPA} = Q_{inAO} \tag{4.5}$$

The consequence is that eventually the pressure into the pulmonary artery and the aorta become equal. This difference is in real-life also small because of shunting of blood through the heart, resulting in CVO [8, 42]. The pressure difference across the pulmonary artery and aorta is still differing. If the heart is modelled in total, differences in pressure could be applied between the atria and ventricles.

The next complex part is the flow distribution across the lower body and placenta, which is shown in Figure 4.6. The total path of the placenta contains the uterine arteries, placenta, umbilical vein, hepatic system, and ductus venosus and is abbreviated as PLAT. The total pressure difference over PLAT is the sum of the pressure differences over an umbilical artery, the placenta, the umbilical vein, and the ductus venosus or hepatic system. The mean between the pressure differences of LB and PLAT can be calculated with $(\Delta P_{PLAT} + \Delta P_{LB})/2$. Next, the same is done as for the heart. With the resistance of the lower body, a new flow rate for the lower body is calculated. This flow rate of the lower body is subtracted from the flow rate flowing towards the placenta and lower body to calculate the flow rate going into PLAT.

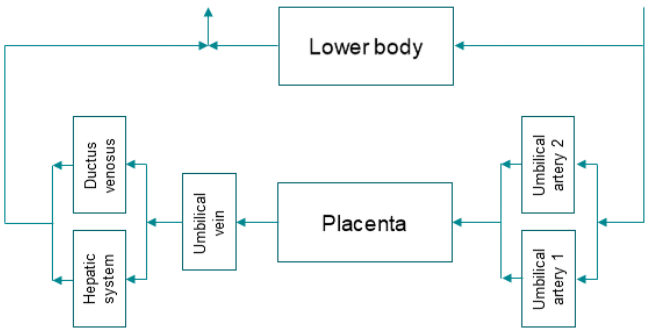

Figure 4.6: The two parallel streams of the lower body and placenta.

Thirdly, the flow distribution between the upper body, lower body and PLAT is summarised in Figure 4.7. The pressure difference across LB and PLAT is the same. That part is in its place parallel to the upper body. So, the mean pressure difference between the lower and upper body can be calculated. Then, the resistance of the upper body is used to calculate the flow rate for the upper body and it is subtracted from the flow coming from the aorta and the ductus arteriosus to calculate the flow rate towards LB and PLAT. Again according to the steps described with (4.3), (4.4), and (4.5).

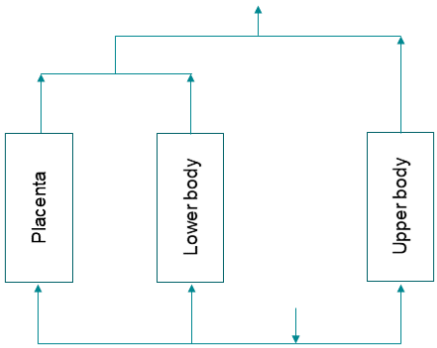

Figure 4.7: The three parallel streams of the upper body, lower body and placenta.

Lastly, the flow distribution across the pulmonary artery, ductus arteriosus, and lungs, shown in Figure 4.8. This part differs from the two previous distributions because the ductus arteriosus and lungs are not parallel. The pressure difference across the ductus arteriosus is calculated with the output pressure of PA and the output pressure of DA. Subsequently, the resistance of DA is used to calculate the flow rate through DA and by subtracting it from the flow rate out of PA the flow rate that remains for PVR is calculated.

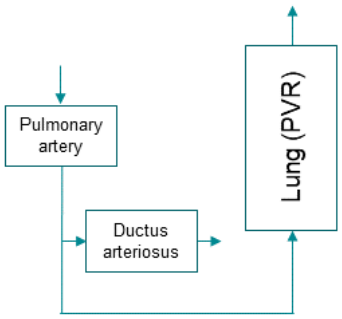

Figure 4.8: The connection between the pulmonary artery, the ductus arteriosus, and lungs.

With (4.1) and (4.2) and the prescribed distribution of flow, the model is able to calculate an equilibrium state for which the CVO is correctly distributed over all the resistance elements. The total fetal cardiovascular model is shown in Figure 4.9. The only input variables for the model now become the combined ventricle output, the pressure of LAP and RAP, and R and C for all the separate elements. Lastly, the integrator functions in Simulink demand initial conditions. These initial conditions for the integration of dP/dt are the values of the pressure at the start of each element. If the pressure of an element is known, this could be set as the initial condition. However, a random number would also suffice, but it would take more time steps for the simulation to reach the correct value for the pressure of that element.

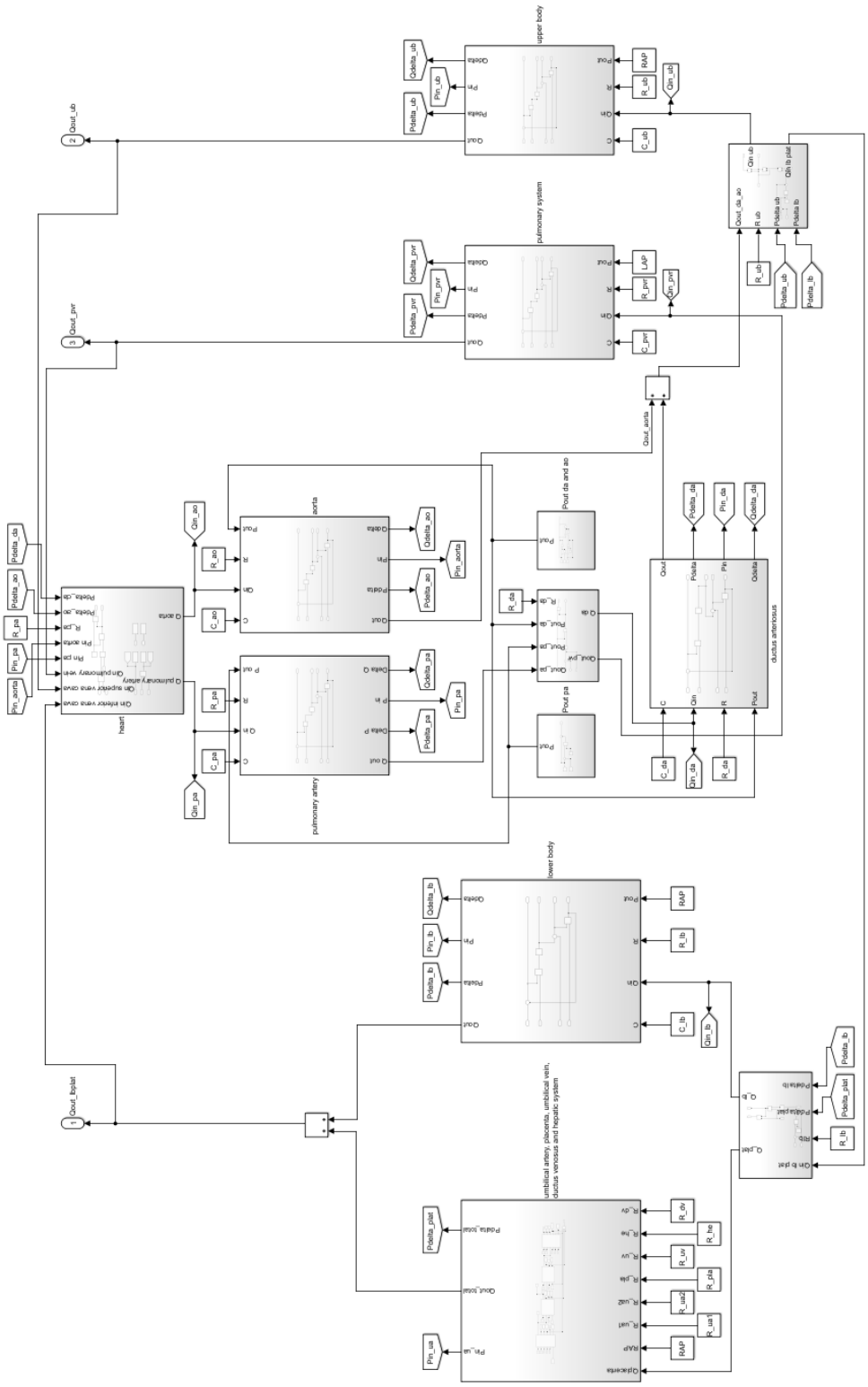

Figure 4.9: The total fetal cardiovascular model in Simulink.

4.2. Parameter research for the fetal cardiovascular model

It is difficult to obtain data from the fetus in utero. Haemodynamic parameters of the fetus are difficult to measure because the fetus is inside the safe environment of the womb and blood flow and blood pressure can not be measured as easily as when the child is born. This is why data is obtained by simulations or with imaging techniques like obstetric ultrasound or MRI. For the model, data is needed about cardiac output and for the lumped segments a resistance and compliance needs to be determined. Other useful data for analysing the model is information about the distribution of flow through the body and across the placenta as well as information about pressure differences of the lumped segments.

In Section 2.2 SI units were used to express the quantities. However, in the medical world, it is more common to measure blood pressure in millimetre of mercury (mmHg). One millimetre of mercury is equal to 133.322 Pascal. Further, there is made use of millilitres instead of litres, because of the small volumes. So flow rate is given in mL s^{-1}, resistance in mmHg s mL^{-1}, pressure in mmHg and compliance in mL $mmHg^{-1}$.

4.2.1. Scaling data to cover multiple weeks of gestation

The goal of this study was to look at a period of 20 to 28 weeks of gestation. A scaling factor is an option to cover a gestational period in the model when data is limited available. Scaling factors are used by more studies, like the studies of Luria et al. [31] and Garcia-Canadilla et al. [14]. The scaling method of Luria et al. [31] is specifically for their study, while the method used by Garcia-Canadilla et al. [14] is more general. This method comes from the study of Pennati and Fumero [44]. They describe that a variable, Y, in the body is related to the body size, W, by an allometric equation. Often the cube root of the body volume is used as a scaling factor. When a reference weight and variable are used, then the equation is expressed as:

$$Y_i = Y_0 \frac{W_i}{W_0}^{b} \tag{4.6}$$

To make it even easier to calculate the growth of variables in the fetal body, Pennati and Fumero [44] give an equation that can be used to estimate the fetal weight, W (g), based on its gestational age, GA (weeks).

$$Log_{10}(W) = 0.2508 + 0.1458GA - 0.0016GA^2 \tag{4.7}$$

The two parameters that will be used can also be scaled. The resistance decreases when the fetal body and its vessels grow. The radius of the vessels also grows and as can be seen in (3.4), this decreases the resistance. Compliance increases during growth [44].

$$R_i = R_0 \frac{W_i}{W_0}^{-1} \tag{4.8}$$

$$C_i = C_0 \frac{W_i}{W_0}^{1.33} \tag{4.9}$$

Not all segments in the fetal body grow with the same scaling factor. Pennati and Fumero [44] give these scaling factors that differ for some parameters and in Table 4.1 the values applicable for the fetal cardiovascular model can be found.

Table 4.1: The scaling factors for the segments and separate ones for the ductus venosus, lungs and upper body. These scaling factors are used in (4.8) and (4.9).

Parameter	Scaling Factor	Ductus venosus	Lungs	Upper body
R (mmHg s mL^{-1})	-1	-0.55	-1.2	-1.1
C (mL $mmHg^{-1}$)	1.33	1.33	1.6	1.47

4.2.2. Generic information about the fetus

Fetal weight can be calculated with (4.7). The results seem very comparable to literature. According to (4.7), the weight of a fetus of 30 weeks is around 1530 g. This is comparable with the weight of the fetus of 1500 g and 30 weeks in the model of Luria et al. [31]. Pennati et al. [45] use a weight of 3000 g at term, which is also an average birth weight found in other studies where the birth weight fluctuates between 2.5 and 3.5 kilograms [11, 17, 35, 47, 48, 63]. The weight for 40 weeks of gestation would be 3333 g when calculated with (4.7). Capper et al. [7] also give an equation to calculate the weight of the fetus based on gestational age in weeks. This equation gives comparable outcomes to (4.7), but the scaling factors of Pennati and Fumero [44] are also used and the choice is made to use the same source to calculate the weight.

The change in cardiac output during this period of 20 to 30 weeks is based on the information given by Pennati and Fumero [44]. The combined ventricular output per weight is calculated with (4.10) and in combination with the weight of the fetus the CVO is estimated. The cardiac output grows steadily with the volume growth of the child, so the change of the cardiac output per weight is minimal [31].

$$CVO(mL/s/kg) = -0.3GA(weeks) + 18 \tag{4.10}$$

Table 4.2: The weight of the fetus and combined ventricular output of the heart for 20 to 30 weeks of gestation.

GA (weeks)	Weight (g)	CVO (mL/s)
20	336	4.04
21	405	4.73
22	483	5.51
23	573	6.35
24	674	7.27
25	787	8.26
26	912	9.30
27	1050	10.39
28	1199	11.51
29	1360	12.64
30	1530	13.77

As mentioned in Section 2.1.1, heart rate and cardiac output can be used to calculate the stroke volume of the heart. This can give extra information about the heart function in the model. Fetal heart rate fluctuates between 140 and 160 beats per minute [33]. Struijk [63, pg.101] gives an equation to estimate the heart rate of a fetus in beats per minute for a certain gestational age in weeks during the second half of the pregnancy.

$$FHR = -0.268GA + 162 \tag{4.11}$$

The blood volume of the fetus is 150 mL at 30 weeks according to Luria et al. [31] and increases to 369 mL at term [11, pg.94].

Using a form of ECMO on the umbilical artery requires information about the size of the umbilical artery. The resistance of the umbilical artery has to be recalculated during the experiments because when a cannula is inserted into the artery, this will change the resistance. To calculate R with (3.4), the radius and length of the umbilical artery are needed. To measure the size of the uterine artery, researchers make use of Doppler flow examination via ultrasound. Lees et al. [29] measured the umbilical artery area at 23 and 33 weeks of gestation. The area can be translated to radius by assuming the area of arteries to be a circle, which means that the area is calculated with πr^2. This results in an average radius of 1.26±0.6 mm at 23 weeks and 1.78±0.6 mm at 33 weeks. Saw et al. [55] found a radius of 1.5 mm at 30 weeks of gestation. Capper et al. [7] gives the formula to calculate the umbilical artery diameter, UAD (mm), for different weeks of gestation. The values calculated with (4.12) are comparable to Lees

et al. [29] and Saw et al. [55].

$$UAD = -0.0003GA^2 + 0.094GA + 0.7714 \tag{4.12}$$

The outer diameter of a French cannula is $D_{out} = Fr/3$, and the wall thickness of a cannula is assumed to be 0.25 mm. With this information an estimation can be made for the umbilical artery diameters for 20 to 30 weeks of gestation and the french cannula sizes that would fit in the artery.

Table 4.3: The radius and diameter of the uterine artery for 20 to 30 weeks of gestation and the French cannula sizes that are compatible.

GA (weeks)	r_{UA} (mm)	D_{UA} (mm)	Fr	D_{Fr-out} (mm)	D_{Fr-in} (mm)
20	1.27	2.53	7	2.3	1.8
21	1.31	2.61	7	2.3	1.8
22	1.35	2.69	7	2.3	1.8
23	1.39	2.77	8	2.7	2.2
24	1.43	2.85	8	2.7	2.2
25	1.47	2.93	8	2.7	2.2
26	1.51	3.01	8	2.7	2.2
27	1.55	3.09	9	3	2.5
28	1.58	3.17	9	3	2.5
29	1.62	3.25	9	3	2.5
30	1.66	3.32	10	3.3	2.8

4.2.3. Flow rate

To verify the model, information about the distribution of flow rate through the body can be used. In the study of Kiserud and Acharya [27] a very complete overview is given for 20, 30 and 38 weeks of gestation. The distribution corresponds with other sources like Cavaliere [8], Guettouche et al. [20], Ménigault et al. [35], Nowak et al. [39], van der Hout-van der Jagt et al. [64] and Couto [11]. However, the distribution of blood leaving the left and right ventricles is different from Van Vonderen et al. [67]. Initially, Van Vonderen et al. [67] would be used as verification, but the majority of sources are in disagreement with them. In Table 4.4 the distribution of flow rate as the percentage of CVO is given. The values for PA, PVR, AO, DA, PVR, and PLA are all from the study of Kiserud and Acharya [27]. Information about flow towards the upper body is found in the articles of Garcia-Canadilla et al. [14], Ménigault et al. [35] and Capper et al. [7]. An average of these values is taken for the upper body. The flow to the lower body is calculated from what remains of the flow towards the placenta and the upper body. Lastly, the flow ratio between the hepatic system and the ductus venosus is 50/50 according to MacDonald and Seshia [32, Ch.16]. An overview of the found variables can be found in Appendix C. Figure 4.10 visualises the flow distribution per segment for 20, 30 and 40 weeks of gestation. In this way, it is clear which parts receive more flow over the weeks and which less.

Table 4.4: The distribution of flow (%CVO) across the different segments at 20, 30 and 40 weeks of gestation.

GA (weeks)	Pulmonary artery	Lung	Aorta	Ductus arteriosus	Upper body	Lower body
20	53	13	47	40	20	17
30	57	21	43	36	20	17
40	60	25	40	35	23	19
GA (weeks)	Umbilical artery 1	Umbilical artery 2	Placenta	Umbilical vein	Hepatic system	Ductus venosus
20	25	25	50	50	25	25
30	21	21	42	42	21	21
40	16.5	16.5	33	33	16.5	16.5

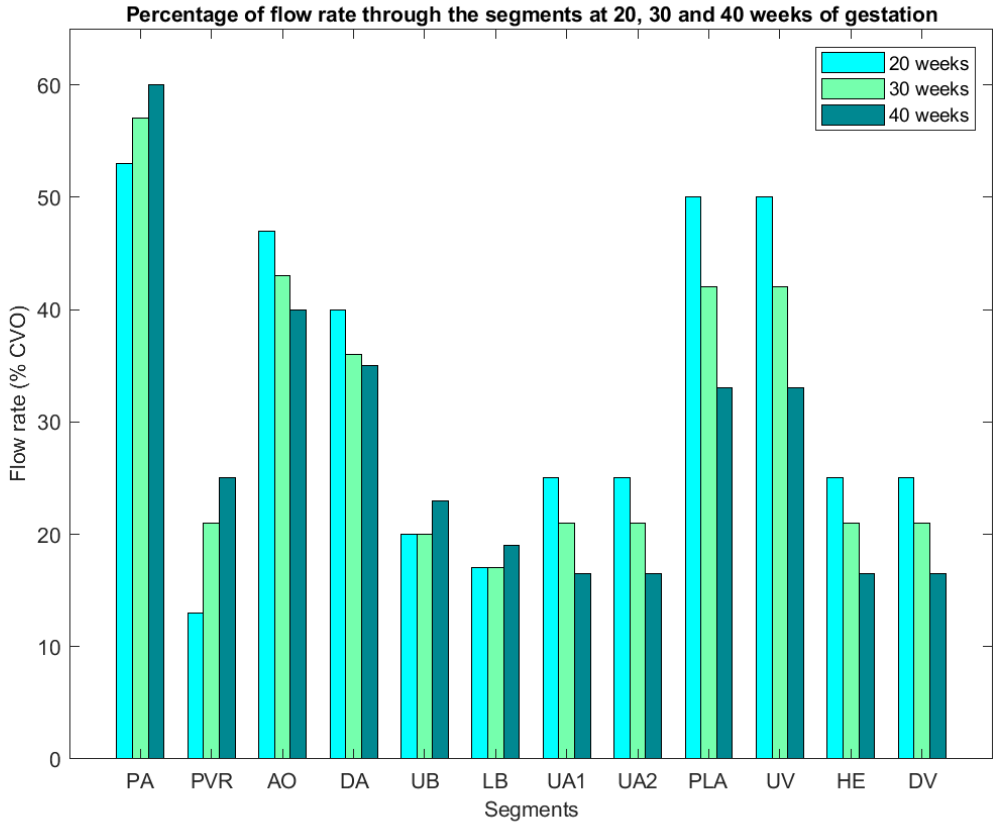

Figure 4.10: Distribution of the combined ventricular output at 20,30 and 40 weeks of gestation.

4.2.4. Pressure

To establish an overview of the pressure across the system, the same plan was used like for the flow rate. For this part applies the same as for the other parts, which is that many sources are needed to find all the values because many researchers focused on a small part of the cardiovascular system. The found variables are summarised in Appendix D. Table 4.5 gives an overview of the found values for pressure in the fetal system. Most of the information is found in the studies of Guettouche et al. [20] and Couto [11]. In the study from Struijk [63] a relation is given to calculate the mean arterial pressure:

$$P_{MAP}(mmHg) = 0.87GA(weeks) + 10.33 \tag{4.13}$$

Table 4.5: Pressure in mmHg in the different segments at 20, 30 and 40 weeks of gestation.

GA (weeks)	MAP	LAP	RAP	Pulmonary artery	Lungs
20	27.73			53.88 [20]	
30	36.43				
40	45.13	2 to 5 [11, 42]	3 to 6 [11, 42]		47 [11]
GA (weeks)	Aorta	Ductus arteriosus	Upper body	Lower body	Umbilical artery 1
20					
30	53.90 [20]	53.72 [20]			35.36 to 52.67 [7, 20]
40	41 [35]		46 [11]	46 [11]	50 [10, 69]
GA (weeks)	Umbilical artery 2	Placenta	Umbilical vein	Hepatic system	Ductus venosus
20			4.5 [27]		
30	35.36 to 52.67 [7, 20]		5.5 [27]		
40	50 [10, 69]	30 [69]	6 to 20 [10, 27, 69]	1 to 14 [64]	1 to 14 [64]

4.2.5. Resistance and compliance

A study earlier mentioned is the study of Luria et al. [31], who made a cardiovascular model of the fetus. Their model does differ on some points with the model of this thesis, but they published a very complete list of the used resistance and compliance values. With some adjustments, it could be used in the Simulink model. Pennati et al. [45] also made an elaborate model. It is clear that Luria et al. [31] used their study as inspiration, although the model of Pennati et al. [45] is for a fetus of 3 kg, so two times as big as the fetus of Luria et al. [31]. The model of Pennati et al. [45] is more elaborate than this thesis model. However, their data is more comparable than other data found in the literature. For instance, the values used by Garcia-Canadilla et al. [14] differ greatly. Their model is built up differently, it focuses on the pulmonary artery and aorta and their outflow vessels, and they did not include the venous system. Still, the resistance that they use for the brain, upper body and lungs are around ten times as high and the compliance around 100 times as small. Differences as this between studies made it difficult to use many sources for the data that was used in the thesis model.

To show the differences between studies, three sources were compared. These are the models of Luria et al. [31], Pennati et al. [45] and Couto [11]. These studies all provide data for the two important variables R and C for a fetal cardiovascular model. The models are designed with different purposes, so some adjustments were needed to fit the models and their variables into the fetal cardiovascular model. The next three figures will explain which segments were lumped together or were separated to become comparable.

Comparison between Luria et al. [31] and the fetal cardiovascular model.

Adjustments to make the model compatible with the fetal cardiovascular model:

- Heart: It is modelled as a pump in the fetal cardiovascular model and all the parts available in the model of Luria et al. [31], including the foramen ovale, tricuspid valve, and mitral valve, were ignored.
- Pulmonary artery: Luria et al. [31] did not model a pulmonary artery, so values for R and C are assumed to be the same as for the aorta.
- Lungs and DA: Luria et al. [31] modelled the lungs as a separate stream, not connected to the stream flowing towards the ductus arteriosus.
- Aorta: It was placed after the node where the ductus arteriosus stream is added, but in the fetal cardiovascular model the aorta is placed in front of this node.

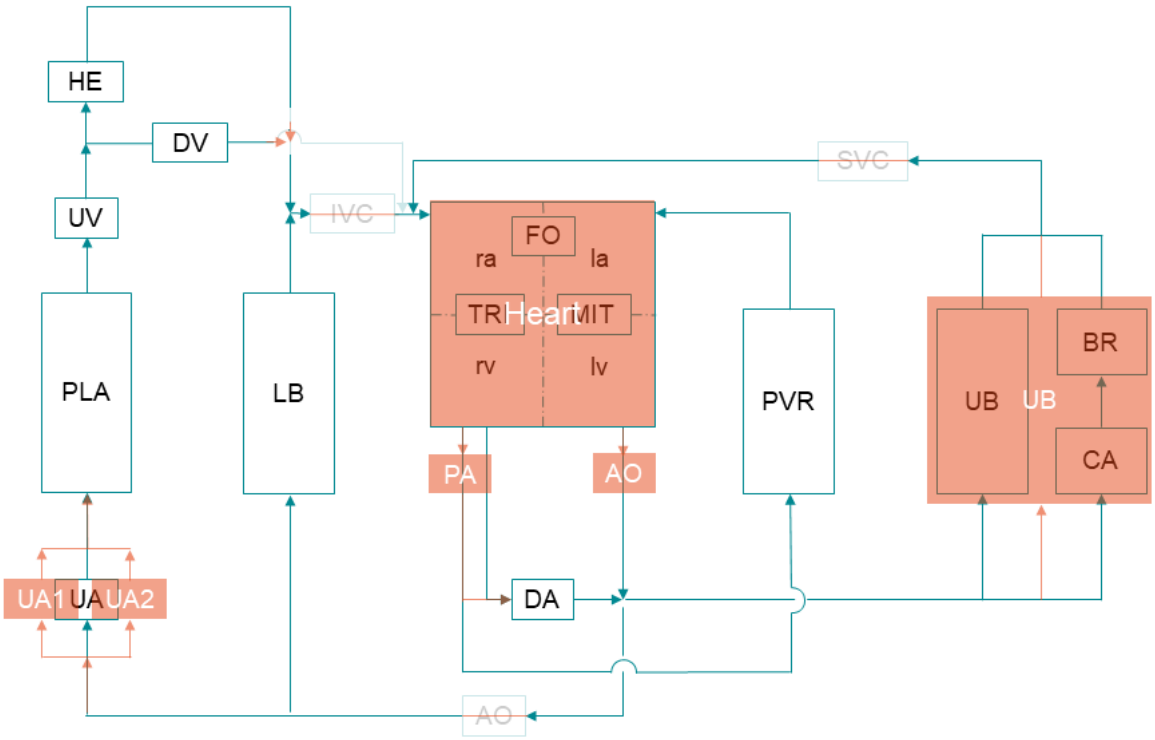

Figure 4.11: In green the segments available in the model of Luria et al. [31] and in orange the adjustments that were made to fit the model to the fetal cardiovascular model. The biggest differences are the heart, in which all parts are ignored. The pulmonary artery is added and the aorta placed proximal to the heart. The upper body, cerebral arteries, and brain are lumped together into one upper body segment. The umbilical artery is split into two segments and the inferior and superior vena cava are ignored.

- Upper body: a combination of three segments in the model of Luria et al. [31], namely the upper body, cerebral arteries, and brain. An equivalent resistance and compliance were calculated for the fetal cardiovascular model.
- The inferior and superior vena cava segments were left out.
- Umbilical artery: In the thesis model two umbilical arteries run parallel, but Luria et al. [31] uses only one umbilical artery. The resistance for the two umbilical arteries was calculated, to be equivalent to the single resistance.
- Placenta: The placenta in the model of Luria et al. [31] has no resistance. The placenta is known to be a low resistance environment and the model requires a resistance, so it is set to 1, based on the range of the other values.

Comparison between Pennati et al. [45] and the fetal cardiovascular model.

Adjustments to make the model compatible with the fetal cardiovascular model:

- The parameters were for a fetus of 3 kg, so to be able to compare them with the fetus of 1500 g from Luria et al. [31], the values are scaled with (4.8) and (4.9) to a fetus of 1500 g. The model of Pennati et al. [45] is highly complex in comparison to the fetal cardiovascular model, but the values were adjusted to fit into the fetal cardiovascular model as closely as possible.
- Pulmonary artery: The pulmonary artery is a combination of two parts of the pulmonary artery lumped together.

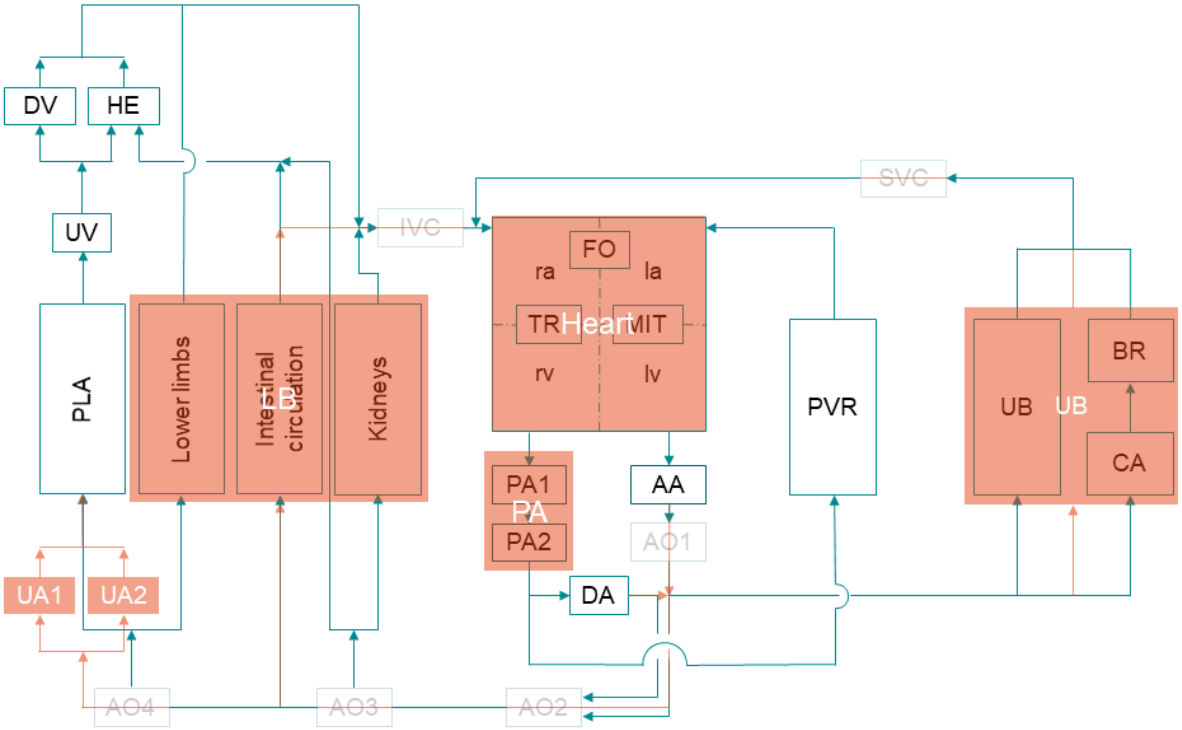

Figure 4.12: In green the segments available in the model of Pennati et al. [45] and in orange the adjustments that were made to fit the model to the fetal cardiovascular model. The biggest differences are again the heart and the lumped upper body. Further, the lower body parts were lumped together, umbilical arteries were added and the pulmonary parts lumped together. Lastly, the vena cava and lower parts of the aorta are left out.

- Aorta: The ascending aorta is used for resistance and compliance of the aorta in the fetal cardiovascular model. The aortic arch (AO1), thoracic descending aorta (AO2), abdominal descending aorta (AO3) and femoral bifurcation (AO4) are left out.
- Upper body: The brain, upper body, and cerebral arteries were lumped together.
- Lower body: The legs, kidneys, and intestines were lumped together into a lower body segment.
- Umbilical artery: An equivalent resistance is calculated for the two arteries, based on one resistance. Pennati et al. [45] give also resistance to some of the connections between segments. For instance between AO4 and the placenta, representing the umbilical artery resistance.
- Inferior and superior vena cava: The vena cava are left out of the analysis.

Comparison between Couto [11] and the fetal cardiovascular model.

Adjustments to make the model compatible with the fetal cardiovascular model:

- The parameters were for a fetus of 3 kg, so to be able to compare them with the fetus of 1500 grams from Luria et al. [31], the values were scaled with (4.8) and (4.9) to a fetus of 1500 g.
- Lungs: The lungs are a combination of the pulmonary peripheral vessels and pulmonary veins.
- Aorta: Assumed to be the intrathoracic arteries.
- Upper and lower body: They are given as the extrathoracic arteries and veins, and peripheral vessels. The distribution of flow rate over the upper and lower body is 23% and 19% of the cardiac output, as given in Table 4.4. They run parallel in the fetal cardiovascular model, so at 40 weeks of gestation, the resistance of the upper body is 0.83 times the resistance of the lower

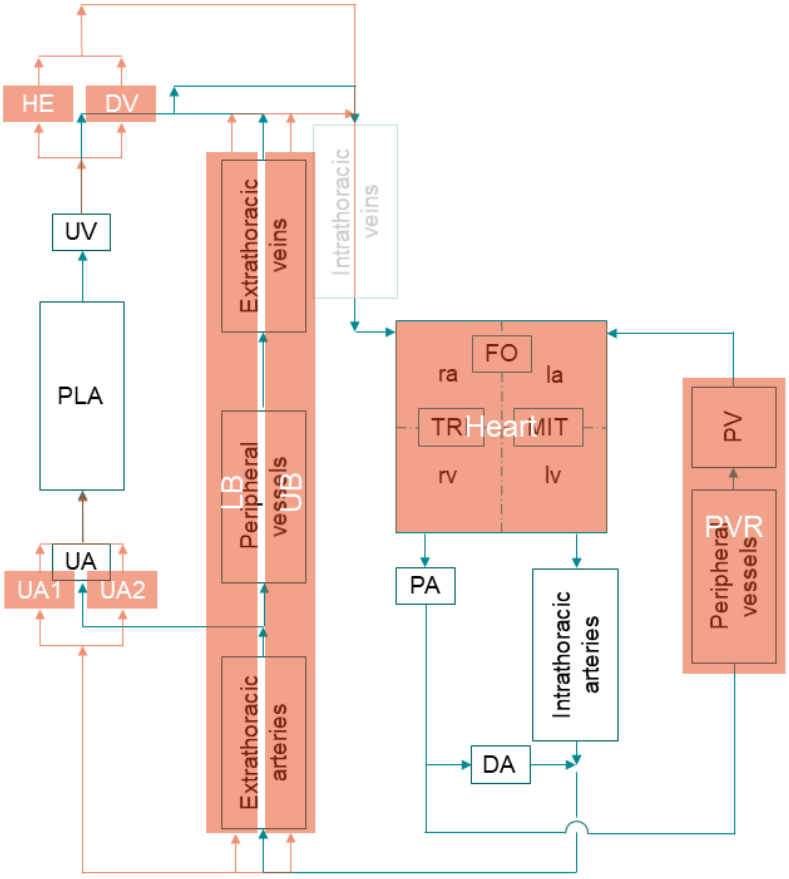

Figure 4.13: In green the segments available in the model of Couto [11] and in orange the adjustments that were made to fit the model to the fetal cardiovascular model. The heart was again not taken into account. The peripheral vessels and pulmonary veins were lumped together as the lungs. The umbilical artery was split into two segments and the hepatic system and ductus venosus were added. The intrathoracic arteries resemble the aorta and the intrathoracic veins are left out. The extrathoracic arteries and veins, and peripheral vessels were lumped together and split into a lower and upper body part.

body. This is used to calculate the resistance of both, equivalent to the total resistance of the extrathoracic arteries and veins, and the peripheral vessels.

- Umbilical artery: An equivalent resistance is calculated for the two arteries, based on one resistance.
- The placenta, hepatic system, and ductus venosus do not have a separate resistance. So they are set to 1 and 0.1, based on the range of the other values.

The fetal cardiovascular model needs values for compliance to be able to run the Simulink model. The compliance is of little influence because of the constant flow rate provided by the heart. So the missing values for compliance in all three models were set to 0.1.

Comparison of the variables

Table 4.6 and Table 4.7 give the results of the resistance and compliance for each segment in the fetal cardiovascular model for the three different studies.
Regarding resistance, the variables of Luria et al. [31] are smaller than Pennati et al. [45] and Couto [11] for the body and placenta, but bigger for the pulmonary artery, aorta and ductus arteriosus. The values from Pennati et al. [45] and Couto [11] are around 8.5 and 8 times as big as the ones from the study of Luria et al. [31], but this is mainly because of the upper body resistance being 25 times as big and

the umbilical vein is around 50 times as big. The rest of the segments differ less, they are on average around 1.5 to 3 times bigger. The variables for resistance from Pennati et al. [45] and Couto [11] are more comparable with each other. The variables from the study of Couto [11] are around 25% smaller than Pennati et al. [45], except for the ductus arteriosus and lower body which are 12 and 2.5 times bigger. However, the resistance of the placenta, hepatic system, and ductus venosus are assumed for Couto [11] and cannot be compared with Pennati et al. [45].
The compliance of the three articles is harder to compare. More assumptions are made because of missing values. However, the values that were given are more equivalent than the resistance of all the segments. Except for the lower body, upper body and placenta from Luria et al. [31], which are significantly bigger.

Table 4.6: The resistance of the segments in mmHg s mL^{-1} gathered from Luria et al. [31], Pennati et al. [45] and Couto [11]. The fifth column is the final choice for R in the fetal cardiovascular model.

Segment	R Luria et al. [31]	R Pennati et al. [45]	R Couto [11]	R
Pulmonary artery	1.00	0.14	0.04	0.04
Lungs	8.05	31.01	26.24	18
Aorta	1.00	0.24	0.04	0.2
Ductus arteriosus	5.07	0.02	0.24	0.2
Upper body	0.54	13.20	13.53	18
Lower body	8.05	5.92	15.28	22
Umbilical artery 1	4.00	15.60	12.72	13
Umbilical artery 2	4.00	15.60	12.72	13
Placenta	1.00	6.80	1.00	1
Umbilical vein	0.02	1.00	1.09	1
Hepatic system	0.05	0.32	0.1	0.5
Ductus venosus	1.05	2.60	0.1	0.5

Table 4.7: The compliance of the segments in mL mmHg^{-1} gathered from Luria et al. [31], Pennati et al. [45] and Couto [11]. The fifth column is the final choice for C in the fetal cardiovascular model.

Segment	C Luria et al. [31]	C Pennati et al. [45]	C Couto [11]	C
Pulmonary artery	0.01	0.06	0.06	0.06
Lungs	0.58	0.13	0.10	0.1
Aorta	0.35	0.02	0.05	0.05
Ductus arteriosus	0.1	0.1	0.1	0.1
Upper body	3.73	0.31	0.1	0.1
Lower body	2.73	1.70	0.1	0.1
Umbilical artery 1	0.1	0.1	0.1	0.1
Umbilical artery 2	0.1	0.1	0.1	0.1
Placenta	4.10	0.60	0.60	0.60
Umbilical vein	0.1	0.12	0.1	0.1
Hepatic system	0.93	0.12	0.80	0.80
Ductus venosus	0.1	0.1	0.1	0.1

The fifth columns of Table 4.6 and Table 4.7 give the choice for R and C that were used in the fetal cardiovascular model. The values from the study of Couto [11] were used as a start point. The data set of Couto [11] represents an average of the three data sets. The values for the pulmonary artery, ductus arteriosus, umbilical arteries, and umbilical vein are copied and rounded.
The aorta was given a bit bigger resistance, because of the distribution difference of flow between the aorta and the pulmonary artery as given in Table 4.4. The hepatic system and ductus venosus have the same flow rate passing through them [32]. They are also running parallel, so they need to have the same resistance. They are set a bit higher than the assumed values for Couto [11] after comparison with the values of Luria et al. [31] and Pennati et al. [45].
In the fetal cardiovascular model, the lower body runs parallel to the placental stream and the upper body parallel to these two. First, an equivalent resistance can be calculated for UA1, UA2, PLA, UV,

HE and DV. The equivalent resistance for the parallel segments is calculated with:

$$\frac{1}{R_{tot}} = \sum \frac{1}{R_i} \tag{4.14}$$

Next, the total resistance of the total placental stream is calculated with:

$$R_{tot} = R_1 + R_2 + +R_3 + ... + R_n \tag{4.15}$$

Then the following relations can be used to calculate the resistance of the upper body and lower body. PLAT resembles the equivalent resistance of the umbilical cord, placenta, hepatic system and ductus venosus.

$$\Delta P_{PLAT} = \Delta P_{LB} \tag{4.16}$$
$$R_{PLAT} Q_{PLAT} = R_{LB} Q_{LB} \tag{4.17}$$
$$R_{LB} = \frac{Q_{PLAT}}{Q_{LB}} R_{PLAT} \tag{4.18}$$

The same is applicable for the upper body: $R_{UB} = (R_{PLAT} Q_{PLAT})/Q_{UB}$. The distribution of flow for a fetus of 30 weeks was taken from Table 4.4. With this information an assumption was made for the resistance of the upper body and lower body.

$$R_{LB} = (42/17) R_{PLAT} \tag{4.19}$$
$$R_{UB} = (42/20) R_{PLAT} \tag{4.20}$$

4.3. Chapter conclusion

In this chapter, the method is explained of how the fetal cardiovascular model was designed in Simulink. For the elements, the equation of Poiseuille was combined with the equation to estimate compliance. These equations were used in all the blocks of the model, except for the heart. The heart is working as a pump with a constant output of flow and gives the pressure for the atria.
The segments are organised in such a way that the flow is distributed in the correct way via all the segments. The goal of this study is to see if an assist devices can be placed on an umbilical artery, so the placental circulation of the fetal cardiovascular system was modelled extensively.
Literature was consulted to find values for the parameters of the model. Unfortunately, the information is scarce because it is difficult to gather information about the fetus inside the womb. However, some useful equations are found to estimate values at a specific gestational age. By comparing three simulation studies, a data set was formed for the resistance and compliance to put in the fetal cardiovascular model.
The next step is to experiment with the fetal cardiovascular model and to observe the flow and pressure changes in the system under different conditions.

5 | Results

The goal is to improve conditions for the fetus at the distal side of the placenta. The experiments with the fetal cardiovascular model were to see how the flow is distributed across the body and how this distribution changes due to adjustments to the umbilical artery. Also, pressure differences were examined to see if they increase because of the adjustments and if the heart will still be able to pump blood around in the fetal body. The results give information about the reactions of the body on intervention and when to intervene.

5.1. Analysis of three different data sets in the fetal cardiovascular model

The variables from Luria et al. [31], Pennati et al. [45] and Couto [11], described in Table 4.6 and Table 4.7, were implemented in Simulink and the results of the simulation are shown in Figure 5.1, Figure 5.2 and Figure 5.3. Figure 5.1 gives the distribution of flow through the body and placenta as a percentage of CVO. For example, the sum of the flow rates through the aorta and the pulmonary artery is together 100%, because the flow is first distributed across those two vessels. The flow rate calculated with the data from the three studies was compared to the flow rates given in Table 4.4. Figure 5.2 gives the pressure drop across each segment in the system for all three data sets. Figure 5.3 shows two subplots giving information about heart function. The first subplot shows the total pressure building up in the system. This is the minimal pressure with which the heart needs to pump the blood into the aorta and pulmonary artery. The lower subplot of Figure 5.3 shows the distribution of blood across the pulmonary and systemic circuits and how it is returned to the left and right atrium. Next to the comparison of the three studies a sensitivity analysis was performed. The values of the study of Couto [11] were chosen as the basis because they are roughly in between the values of the other two studies. Whereupon one value at a time is changed into one of Luria et al. [31] or Pennati et al. [45] to evaluate the influence of changing one particular value on the total system. The twelve figures from this sensitivity analysis can be found in Appendix E.

5.1.1. Results of the sensitivity analysis

- In the study of Luria et al. [31], the average resistance is lower than the resistance of Pennati et al. [45] and Couto [11], so the overall pressure in the system is lower for the same cardiac output. This is clearly visible in Figure 5.2.
- The resistance of the ductus arteriosus from Luria et al. [31] and Couto [11] is high in comparison to Pennati et al. [45]. The flow rate is therefore very low through the ductus arteriosus for both studies in comparison to Pennati et al. [45] and the average values of Table 4.4.
- The lung resistance in the study from Luria et al. [31] is 3 to 4 times lower than those from Pennati et al. [45] and Couto [11]. However, the flow rate for the three studies is almost the same through the lungs. Resulting in a smaller pressure drop over the lungs for the variables from Luria et al. [31].
- The small differences in flow rate through the lungs between Luria et al. [31] and the other two studies are because of the very low resistance of the upper body. The upper body is one of the main streams in the model and therefore highly influencing the flow distribution. Because of the high resistance of the ductus arteriosus and the low resistance of the upper body for the data from Luria et al. [31], flow is mainly directed from the heart through the aorta towards the upper body. Which can be seen in Figure 5.1.
- Another value which is very small in the set from Luria et al. [31] in comparison to the values from Pennati et al. [45] and Couto [11] is the umbilical vein resistance. This low resistance results in a small pressure drop over the umbilical vein as can be seen in Figure 5.2. In Figure E.10 can be seen that the lower resistance for the umbilical vein from Luria et al. [31] does increase the flow through the umbilical cord. However, for a resistance that is 50 times as small, it does

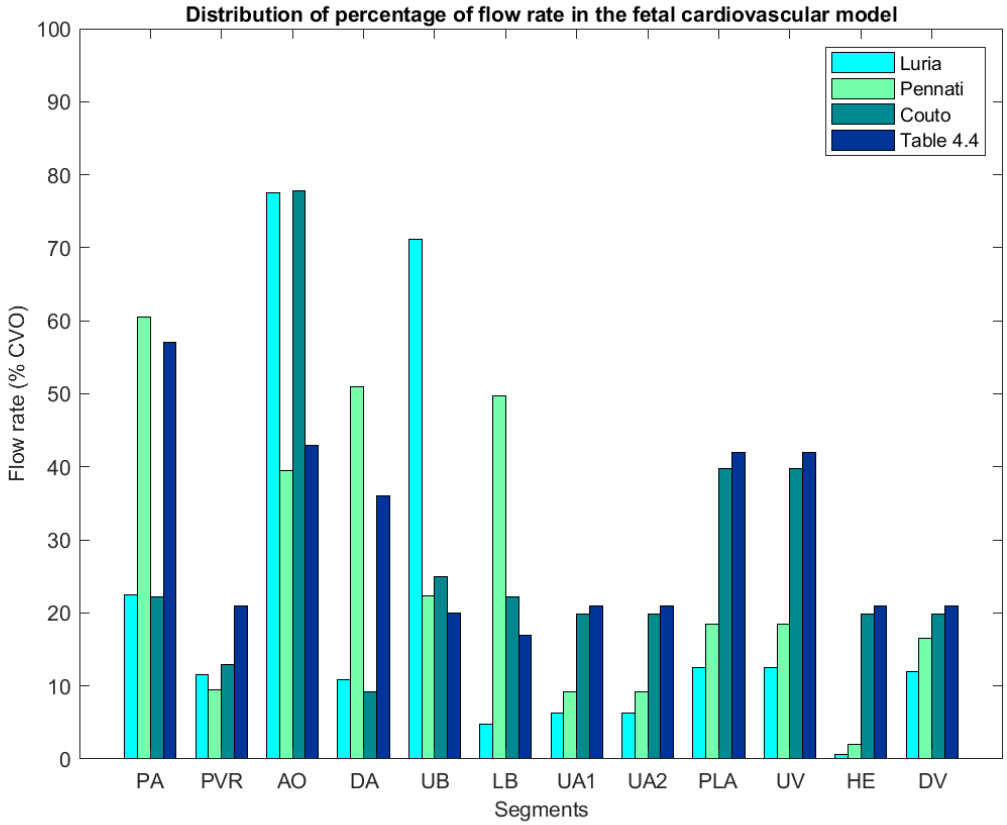

Figure 5.1: The percentage of combined ventricular output going through an segment. The percentages of flow rate for the studies of Luria et al. [31], Pennati et al. [45] and Couto [11] were calculated with the fetal cardiovascular model and compared with the flow distribution given in Table 4.4.

not influence the flow much, because the resistance of the umbilical arteries and placenta are determining the total resistance of the placental stream.

- The resistance for the lower body from the study of Pennati et al. [45] is 2.5 times as low as the one from Couto [11]. This is visible in Figure 5.1, where the percentage of flow through the lower body is relatively high for Pennati et al. [45]. The resistance from Luria et al. [31] for the lower body is also relatively small, but the resistance of the upper body is much smaller, so it confiscates all the flow. This is because the lower body is parallel to the upper body, as can be seen for the pressure drops over the upper and lower bodies, which are the same.

- In literature was found that the flow is distributed equally through the ductus venosus and hepatic system [32]. In the fetal cardiovascular system, both parts were modelled parallel. An equal flow distribution through a parallel system would mean that the resistance of both parts is the same. This is the case for the variables of Couto [11], but not for the other two sets which give different flow distributions across the hepatic system and ductus venosus. This is also visible in Figure E.11 and Figure E.12. They influence each other because they are running parallel. Also, they are situated at the end of the placental stream and their resistance is relatively low, so they mainly influence each other, but not the rest of the system.
  This principle is almost the same for the umbilical arteries. When one is changed, it influences mostly the flow going towards the other. However, the resistance of the umbilical arteries is bigger, so changes in its resistance are of greater influence on the blood flow going towards the placenta. As can be seen in Figure E.7 and Figure E.8. In Figure E.7 only one resistance is changed and influencing the flow rate travelling through the other umbilical artery. In Figure E.8 the resistance

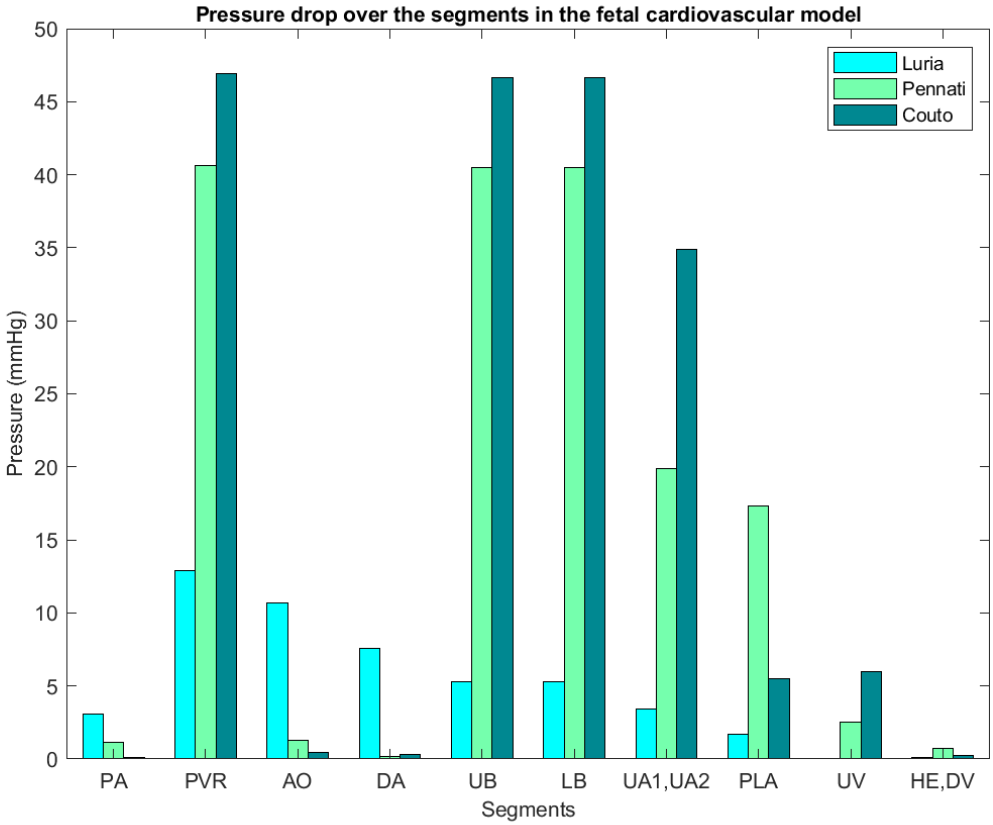

Figure 5.2: The pressure drop over an segment calculated by the fetal cardiovascular model for the data sets from Luria et al. [31], Pennati et al. [45] and Couto [11].

of both arteries is changed. Here they show the increase of flow through the placenta.

- The study of Pennati et al. [45] was the only one that gave a resistance for the placenta and creates therefore also a higher pressure drop over the placenta as is visible in Figure 5.2.

5.1.2. Consequences of different data sets

The input of the system is the flow rate without a pulse. This means that the system will stabilise to a point at which the total flow rate is returned back to the heart. So, the resistance of the total system influences the pressure building up in the system, as can be seen in Figure 5.3. The flow rate travelling through the 3 different simulations is the same, but the total resistance from Luria et al. [31] is lower and so is the pressure building up in the system.

Furthermore, it is clear that the system is built up into two parts which influence each other very little. The pulmonary artery, ductus arteriosus, and aorta are forming a loop and the second part is the rest of the body and the placenta. This can be seen in Figure 5.1 when looking at the outcomes with the data from Couto [11] and the values of Table 4.4. The flow in the body and placenta is very comparable, but the higher resistance of the ductus arteriosus in the set of variables from Couto [11] makes the flow travel directly through the aorta. Pennati et al. [45] give a lower resistance for the ductus arteriosus, and here it is clear that the flow rate is than distributed more evenly across the aorta and pulmonary artery.

The reason that the loop of the pulmonary artery, ductus arteriosus and aorta is reacting in this way is because of how the Simulink model was built. The heart is built as a simple current source. The division of flow rate through the pulmonary artery and aorta is calculated with Kirchhoff's voltage law.

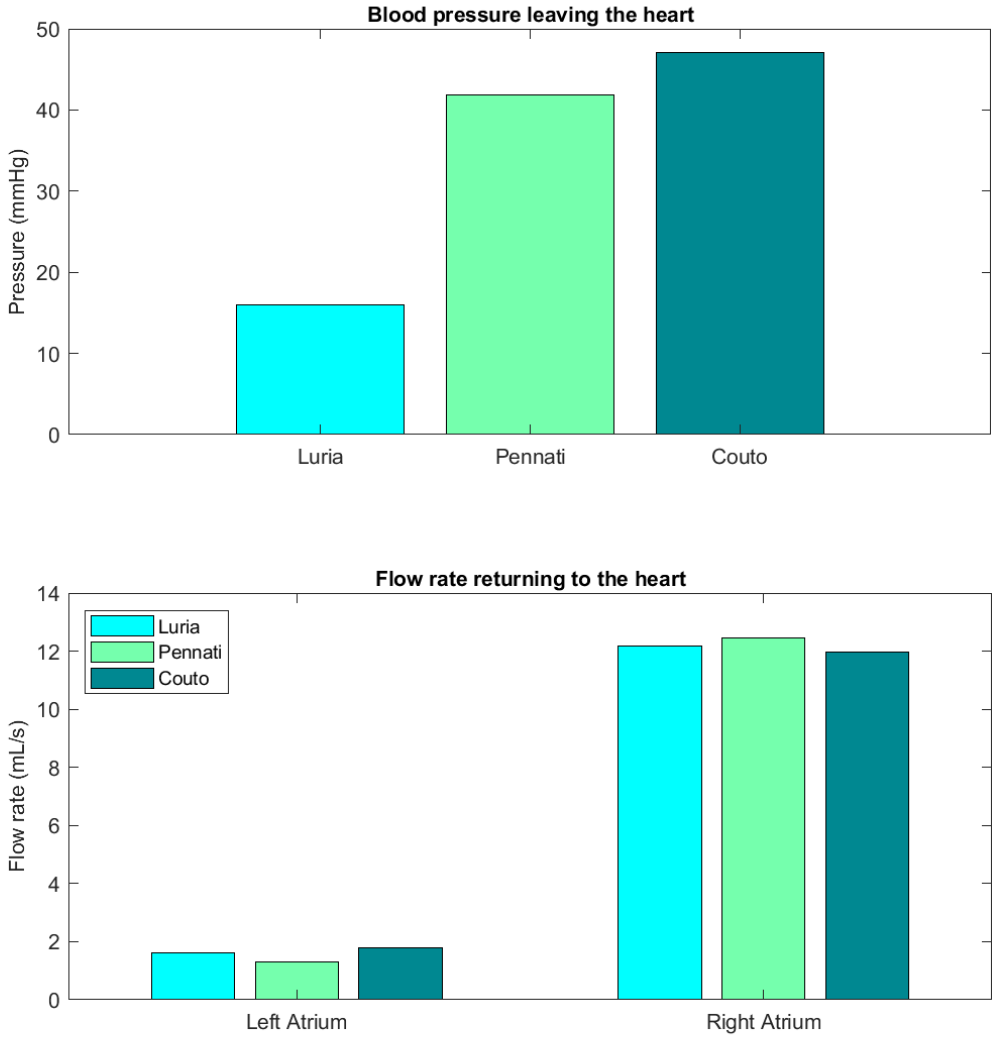

Figure 5.3: Two subplots showing the heart function for different input variables. The upper plot shows the total pressure building up in the system. The lower plot gives the flow rate returning to the heart after travelling through the body and placenta

Also, the pressure drop over the ductus arteriosus is dependent on the outgoing pressure of the pulmonary artery and aorta, and so is its flow rate. In this way, the three segments divide the flow across them to supply the rest of the body is. But changing one of the three resistances does not alter the flow distribution to the rest of the system. If the aorta has a high resistance, flow is directed via the pulmonary artery and ductus arteriosus to provide the systemic circuit with enough flow and vice versa for the pulmonary circuit. This is visible in Figure E.1, where the resistance of the pulmonary artery is increased and the ductus arteriosus flow becomes negative. This means that flow is going into the other direction, from the aorta towards the pulmonary circuit. When the resistance of the ductus arteriosus is increased, flow is divided across the pulmonary artery and aorta and the ductus arteriosus is excluded. This distribution of flow is mainly because of how the model was built in Simulink, but it is not entirely impossible in real-life. In the fetal body, flow can travel from left to right, from the aorta towards the pulmonary artery. This happens for example directly after birth, when the pulmonary resistance drops because the lungs inflate and the pulmonary blood flow increases. Shunting of blood can then

go in both directions in the foramen ovale shunt and ductus arteriosus [67].

The body and placenta, below the pulmonary artery, aorta and ductus arteriosus, consist of many somewhat parallel streams. If one resistance is much lower than the others, this stream will confiscate all the flow, as can be seen in Figure 5.1 for the upper body of Luria et al. [31] and the lower body of Pennati et al. [45]. If the resistance of the lungs becomes very small the flow through the ductus arteriosus will go from the aorta to the pulmonary circuit. This is something to keep in mind, to check if the resistance of one of the bigger streams is an outlier and primarily influencing the distribution of the flow.

The focus of this analysis of different data sources lays on resistance because the compliance is not of great influence on the model outcomes. The compliance is needed to calculate the flow rate and pressure drop, because of the equations used and the way the series and parallel blocks were implemented in Simulink. However, the input in the system is a constant flow rate, so the output grows towards an equilibrium state. This equilibrium state is the same as for a system without compliance. In the current system, compliance is of influence on the slope at the start of the simulation. A higher compliance results in a gradual slope towards the equilibrium state and small compliance in a steeper slope. No compliance would give a straight line from the start, because the pressure drop would only be dependent on a constant flow rate and the resistance of a segment.

To summarise, the consequence of different data sets is different for the two parts of the system. The pulmonary artery, ductus arteriosus and aorta function partially separate from the body and the placenta. If the heart is kept a constant current source, then especially the relative resistance of the lungs, body, and placental circulation are of importance for the results. Further, the height of the overall resistance of the system influences the total pressure building up in the system. Realistic values for the pressure in the fetal body could be checked in literature, and in this way, the resistance could be evaluated.

5.2. Simulation results for the period of 20 to 30 weeks of gestation

The data from the fifth columns of Table 4.6 and Table 4.7 was used to simulate the development of the fetal cardiovascular system. This data is for a fetus of 30 weeks. The scaling equations (4.7), (4.8) and (4.9) were used to calculate the values for 20 to 29 weeks of gestation.

The resistance of most of the segments at 30 weeks of gestation is fitted to the flow distribution given in Table 4.4. So, the results of the distribution of flow through the system are almost the same for the fetal cardiovascular model and Table 4.4 at 30 weeks. A comparison between the model and Table 4.4 of the flow rate in percentage of CVO for 20 and 30 weeks is given in Table 5.1.

Table 5.1: Flow rate in percentage of CVO in every segment at 20 and 30 weeks. A comparison between the values found in literature and the values calculated by the fetal cardiovascular model.

Segment	Literature, 20 GA	Model, 20 GA	Literature, 30 GA	Model, 30 GA
Pulmonary artery	53	53	57	55
Lungs	13	17	21	21
Aorta	47	47	43	45
Ductus arteriosus	40	36	36	34
Upper body	20	19	20	20
Lower body	17	18	17	17
Umbilical artery 1	25	23	21	21
Umbilical artery 2	25	23	21	22
Placenta	50	46	42	42
Umbilical vein	50	46	42	42
Hepatic system	25	23	21	21
Ductus venosus	25	23	21	21

The flow towards the lungs and upper body increases over the weeks. The upper body and lungs grow faster in the second trimester than other organs [44]. Their resistance decreases faster and the compliance increases more. This results in a change of the flow distribution across the different segments in the body. A bigger percentage goes towards the upper body and lungs, less through the ductus arteriosus and towards the lower body and placenta. This corresponds with the information found in literature and summarised in Table 4.4. Except for the upper body and lower body, but there was less information available about the flow distribution through those two segments and a small deviation of the flow distribution is possible. Figure 5.4 shows the flow rate for the whole period from 20 to 30 weeks and how its distribution changes through the weeks.

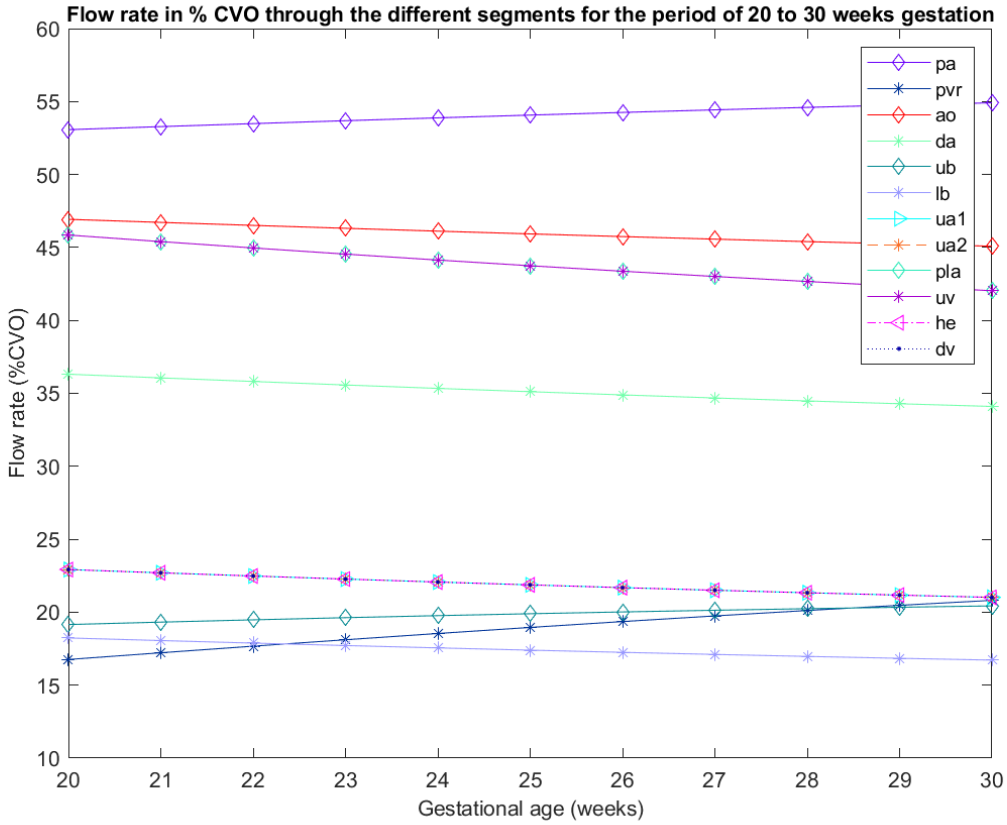

Figure 5.4: Flow rate flowing into all the segments of the fetal cardiovascular model over the period of 20 to 30 weeks of gestation. The flow rate is given in percentage of the total combined ventricular output. The lines of the placenta and umbilical cord overlap and start at 46% at 20 weeks. The lines of the umbilical arteries, hepatic system, and ductus venosus also overlap and start at 23% at 20 weeks.

The combined ventricular output grows over the weeks from 4 to 14 mL s^{-1}. The change in CVO per weight of the fetus is minimal. This was explained in Section 4.2.2 and the growth of CVO over the weeks can be found in Table 4.2. The flow rate distribution in the system is visualised in Figure 5.5. The flow rate is highest in the pulmonary artery and the aorta and after is distributed through the rest of the system.

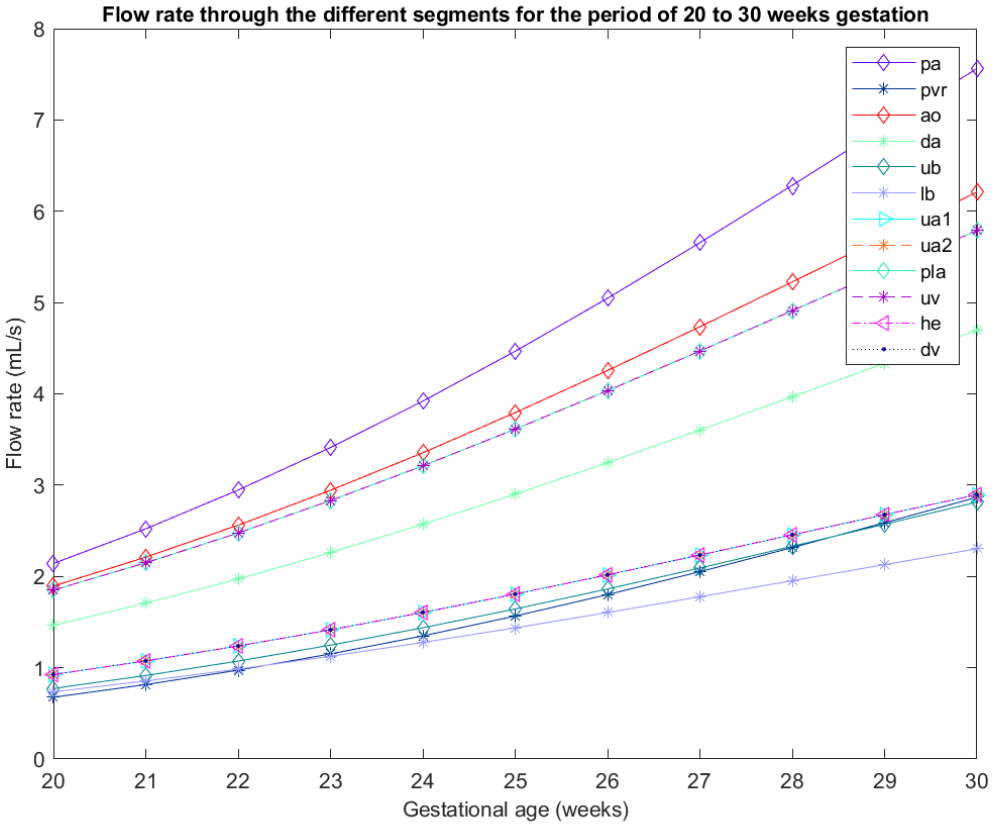

Figure 5.5: The flow rate distribution through the different segments in mL s^{-1} for the period of 20 to 30 weeks of gestation. The flow rate through the placenta and umbilical cord overlap and start at 1.9 mL s^{-1} at 20 weeks. The flow rate through the umbilical arteries, hepatic system and ductus venosus also overlap and start at 0.95 mL s^{-1} at 20 weeks.

The blood pressure at the start of every segment is calculated with the fetal cardiovascular model and given in Table 5.2. The values from the simulation are very comparable to the values found in the literature for a fetus of 30 weeks. Only the pressure at the start of the umbilical arteries is higher than in literature. An explanation could be that this is because of how the model was built. The inflow of the umbilical arteries comes from the same node as the flow going towards the upper body and lower body and therefore has the same pressure. In real life, flow has to travel a bit further before reaching the umbilical arteries and this could explain the decrease in pressure for the values found in literature. The pressure drop over each segment is also calculated in the fetal cardiovascular model and visible in Figure 5.6. The resistance of the segments lowers during growth and so does the pressure difference. The pressure drop over the upper and lower body is the same, because those two parts run in parallel. Lastly, the pressure drop over the placenta and the umbilical vein is also the same, but this is because they are assigned the same resistance.

Table 5.2: The blood pressure in the segments according to literature, taken from Table 4.5, and pressure values calculated by the fetal cardiovascular model.

Segment	Literature, 30 GA	Model, 30 GA
Pulmonary artery	53.88	52
Lungs		52
Aorta	53.90	52
Ductus arteriosus	53.72	52
Upper body		51
Lower body		51
Uumbilical arteries	35.36	51
Placenta		13
Umbilical vein	5.5	7
Hepatic system and ductus venosus		1.5

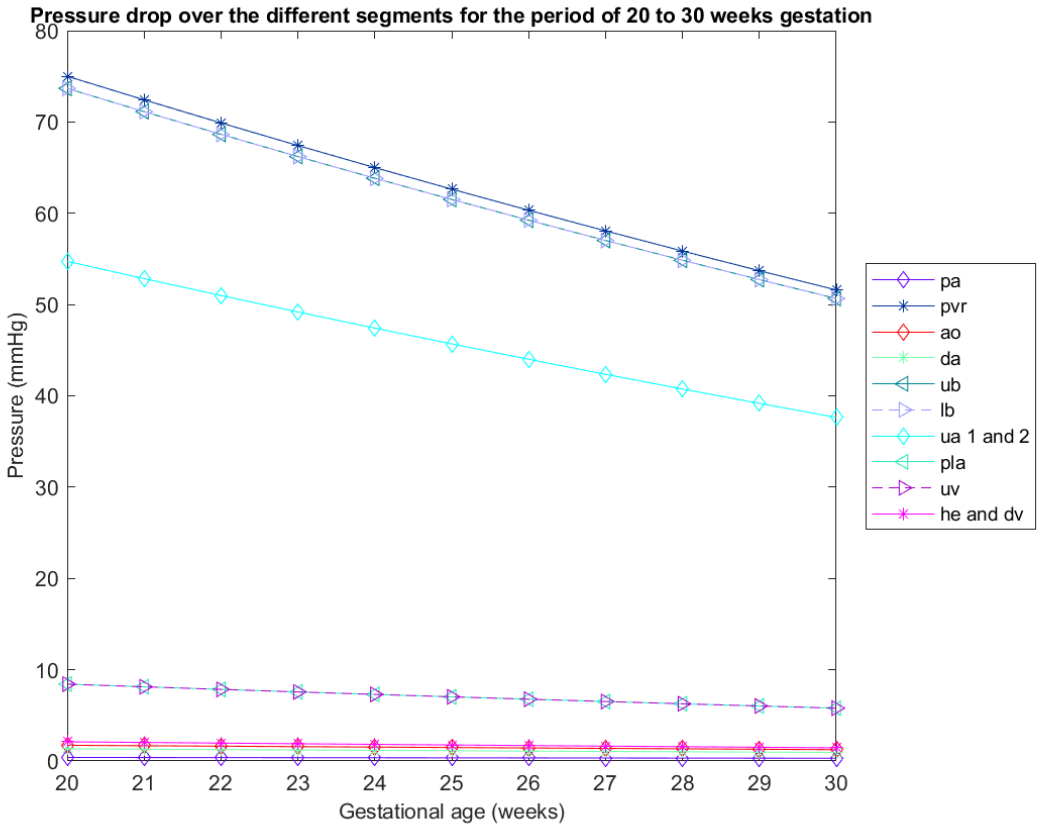

Figure 5.6: Pressure drop over each segment for 20 to 30 weeks of gestation. The upper and lower body overlap. Their pressure drop is a bit smaller than the pressure drop over the lungs (PVR). The placenta and umbilical vein have a similar pressure drop because they were modelled with the same resistance.

5.3. Implementation of an ECMO cannula

At this step, a cannula was added to the model to simulate the connection with an ECMO support system. One of the uterine arteries was combined with a resistance resembling a french cannula inside the artery. The goal was to check if blood would still be flowing through the umbilical artery with a decreased radius because of the attached cannula.

In table Table 4.3 the size of the umbilical artery is compared with possible sizes of french cannulae. The length of the umbilical artery is assumed to be 50 cm and kept constant [7, 20]. When the cannula is placed inside the umbilical artery, it needs to be anchored really well, so it was assumed that the cannula is placed in the umbilical artery over a length of 20 cm, so two-fifth of the total length. The new resistance for umbilical artery 1 was then estimated. This resistance is a combination of 3/5 of the original resistance and resistance formed by 20 cm of cannula. The resistance of the cannula is calculated with (3.4). The viscosity of fetal blood is set at 3 mPa s [49]. At 30 weeks the resistance of 20 cm cannula would give a resistance of 2.98 mmHg s mL^{-1}. The remaining 30 cm artery would have a resistance of 7.8 mmHg s mL^{-1}. Which brings the total resistance of the umbilical artery with the french cannula to 10.78 mmHg s mL^{-1}. However, this is lower than the resistance of the other umbilical artery, which has a resistance of 13 mmHg s mL^{-1}, as given in Table 4.6. This is not what to expect, because the radius of the umbilical artery is decreased, because of the cannula. The resistance for the umbilical arteries from the studies of Pennati et al. [45] and Couto [11] are probably based on other theory than (3.4). If the umbilical artery resistance is calculated with (3.4), with an assumed viscosity of 3 mPa s, a length of 0.5 m and a radius of 1.66 mm as in Table 4.3, then the resistance becomes 3.77 mmHg s mL^{-1}. This resistance is comparable with the resistance from the study of Luria et al. [31]. To evaluate the addition of a cannula to the umbilical artery, the resistance of both arteries needs to be estimated with (3.4). This is important to evaluate the response of the system on increasing the resistance of one of the umbilical arteries in comparison to the other one.

The effect of the lower resistance for the umbilical arteries can be compared with the results from the values of Luria et al. [31] in the fetal cardiovascular model. The overall resistance becomes lower because the equivalent resistance of the placental stream decreases by half. So, the pressure building up in the total system will be a bit smaller than the pressure shown in Figure 5.6. The results of this are shown in Figure 5.7. The lower resistance of the umbilical arteries increases flow towards the placenta and the flow to the upper and lower body and lungs decreases a bit. Also the flow through the aorta increases in comparison to the pulmonary artery flow.

It needs to be determined if the fetal heart is able to push flow through the cannula towards the ECMO system. The pressure implemented by the heart on the pulmonary artery and aorta is set to the values of the simulation without a cannula. In this way, it is possible to check if the blood flow can be pushed through the cannula without changing the blood pressure delivered by the heart.
The final assumption is that the pressure at the start of element UA1 can all be used to push blood through the cannula. This is because after the cannula, the radius of the rest of the tubes can be increased in size and a pump could increase the blood pressure again to keep the blood flowing to return it to the fetus eventually.

To summarise, the resistance of the umbilical arteries is calculated with (3.4). The resistance of umbilical artery 1 is changed to 3/5 of its resistance plus the resistance of a cannula of 20 cm. The pressure drop over umbilical artery 1 is the incoming pressure in the umbilical artery. The blood pressure at the start of the pulmonary artery and aorta is set to the values calculated for a system without a cannula, to keep the cardiac function constant.

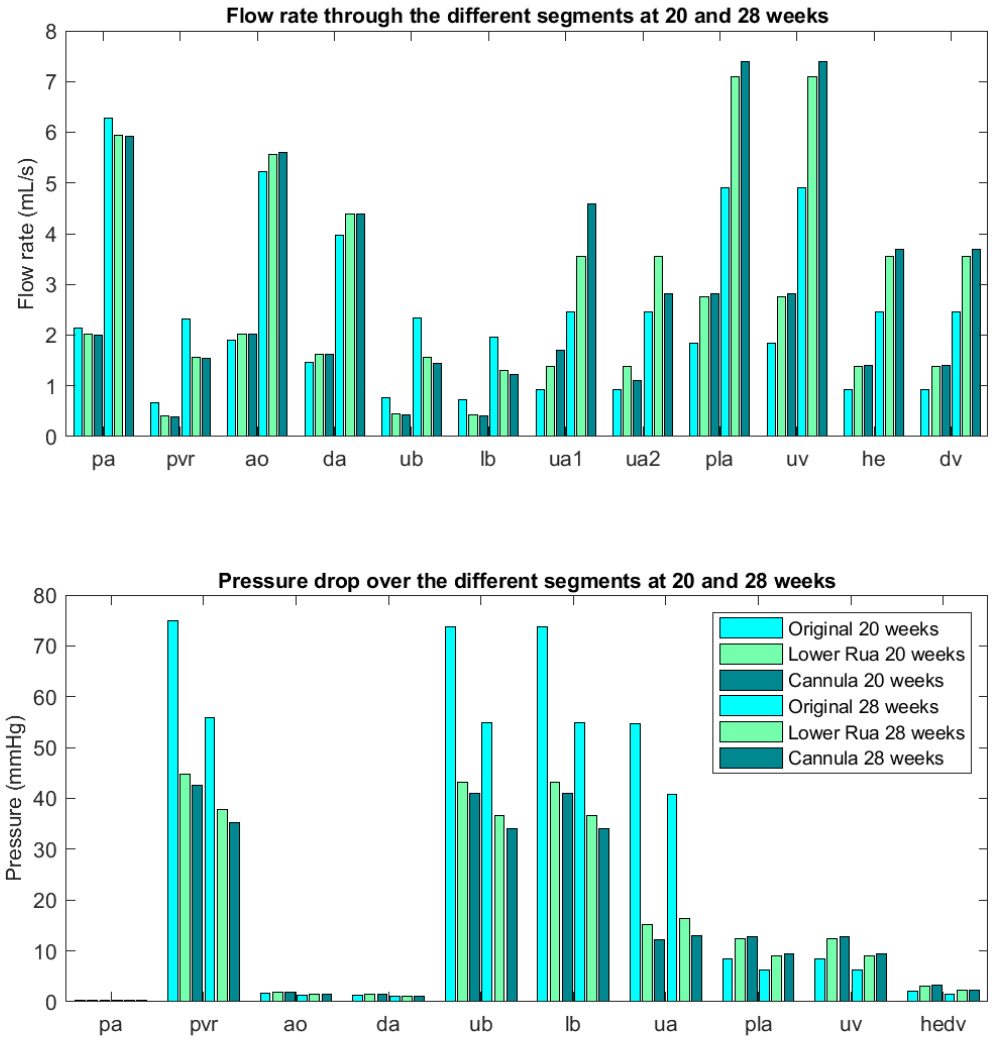

Figure 5.7: Two plots of the flow and pressure distribution at 20 and 28 weeks of gestation. The legend applies for both subplots. The bar plots give the flow and pressure for the original values as used in Section 5.2, the system with the resistance of the umbilical arteries calculated with (3.4), and when the cannula is added to umbilical artery 1.

Figure 5.8 shows the results from two simulations. The first simulation, with the diamond markers, is the simulation without cannula and with the resistance of the umbilical arteries calculated with (3.4). The second simulation, with the star markers, gives the results for the system with a cannula inserted. As in Figure 5.5, the placenta and umbilical vein overlap, as do the umbilical arteries, hepatic system, and ductus venosus. The flow through the two umbilical arteries shows the biggest changes. The cannula size changes in steps and this why the flow rate is not increasing gradually for the second simulation.

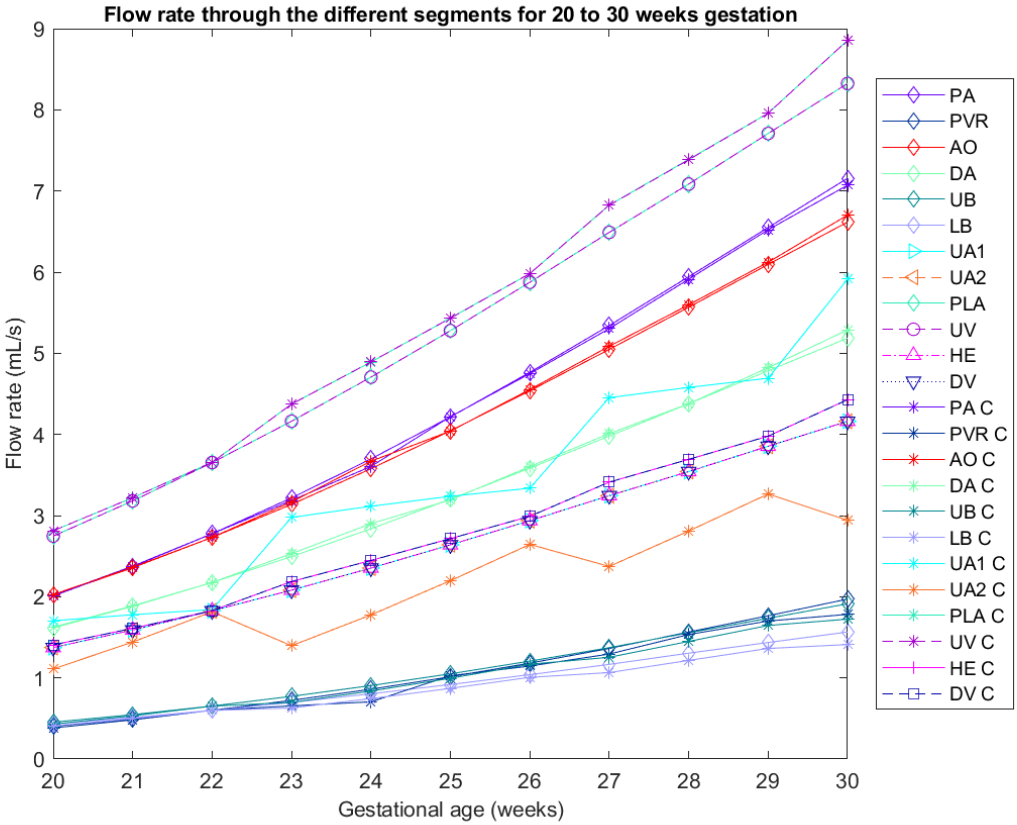

Figure 5.8: The flow distribution through the fetal system for the normal system and when a cannula is inserted into umbilical artery 1.

Figure 5.9 zooms in on the umbilical arteries and the placenta. The cannula was placed into umbilical artery 1. The flow through this artery increases above the level of the original flow rate. This simulation shows the possibility that with the available blood flow and pressure from the heart the blood flow could reach the ECMO system through the cannula. The flow through the placenta stays the same, which is wanted, but it stays mainly the same because of the two parallel modelled umbilical arteries.

5.4. Oxygen support

The oxygen saturation of fetal blood is lower than adults and around 45 to 65% [67]. Levels of oxygen in the blood are increased to an oxygen saturation of 85% when passing the placenta [27]. So, at 20 weeks around 50% of the CVO is saturated to a level of 85% and at 30 weeks this is around 42% of the CVO. By adding an external oxygenator to one of the umbilical arteries, flow through this artery could ideally be oxygenated to a level of 100%. If both vessels share the blood flow equally, this would result in an increase of oxygen saturation to 92.5% when blood is leaving the placenta. In Figure 5.9 can be seen that the flow through the umbilical artery with cannula is even increased. However, this is because of the higher pressure drop that is allowed over this artery. When the flow through the cannulated artery lowers in comparison to the other artery, then the effect of oxygenation will become smaller. During placental ischaemia, oxygen transfer is impaired and oxygen levels of blood are lower. For example, when blood flow through both umbilical arteries is parallel and increased to 65% in the placenta, but one of the umbilical arteries is cannulated and the oxygen saturation of blood in this artery is increased to an oxygen saturation of 100%, then the oxygen saturation of blood leaving the placenta would be increased to 85%. So, it is useful to oxygenate during placental ischaemia, even when there is less blood flowing through the cannulated artery in comparison to the second artery. Oxygenation is useful because of the high percentage of CVO travelling through the placenta.

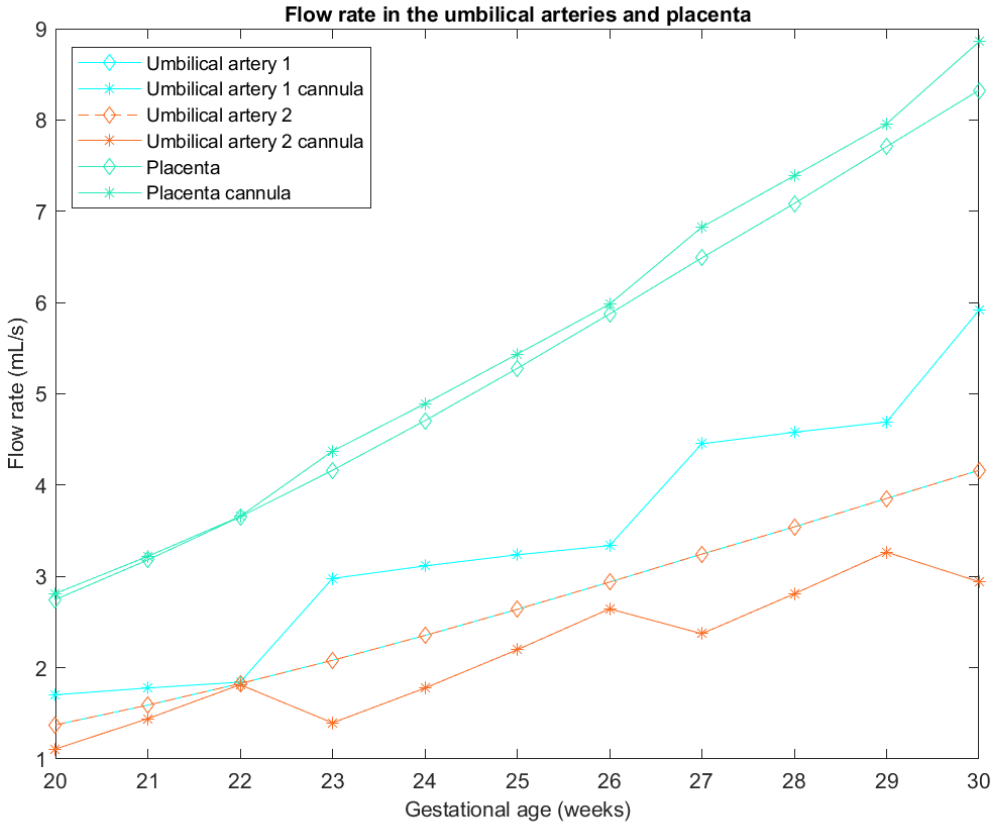

Figure 5.9: The flow rate for 20 to 30 weeks of gestation through the umbilical arteries and the placenta. The diamond markers show the normal system. The star markers give the result of the simulation with a cannula attached to umbilical artery 1.

5.5. Placental ischaemia

The simulations were all performed with values presenting a healthy fetus. This is because the information provided was data of healthy pregnancies. However, it is known that during adverse conditions as intrauterine growth restriction, which is related to non-branching angiogenesis and placental ischaemia, the placental flow is decreased [15, 31]. The placental resistance increases and the resistance of the brain decreases, because of the brain-sparing effect to provide the brain with enough oxygen during a shortage. A higher placental resistance would decrease the flow towards the placenta as shown in Figure E.9. The resistance of the placenta is higher in the study from Pennati et al. [45]. This results in flow relocating to the upper and lower body, and lungs, as is also the case for the original values shown in Figure 5.7. The pressure in the system increases because of higher total resistance, as can be seen in Figure 5.7. The original values were with a higher umbilical artery resistance and show that the overall pressure increases. So the flow through the placenta decreases, but there is a higher pressure available to push the flow through the cannula. This works until a certain value. At some point, the flow will bypass the placenta and flow towards other segments, as for instance for the study of Pennati et al. [45] shown in Figure 5.1, where the flow is relocated to the lower body. Secondly, the heart can also not increase pressure infinitely.

5.6. Chapter conclusion

In this chapter, an overview is given of how the fetal cardiovascular model reacts on different input values. First, a sensitivity analysis is performed to create a better understanding of the model. The height of the resistance of the elements in the fetal cardiovascular model influences the total pressure

building up in the system. Differences in resistance between the larger parallel segments in the model as the upper and lower body are very important for the flow distribution through the system. Data were fitted to mimic the flow distribution at 30 weeks as closely as possible. Subsequently, the cardiovascular system was simulated for the period of 20 to 30 weeks of gestation and the model outputs were very similar to data found in literature. The last simulations were to evaluate the implementation of an ECMO cannula. The results show a possibility for implementation of a cannula in the umbilical arteries, already at 20 weeks of gestation.

6 | Design recommendations for intrauterine ECMO

The simulations in Chapter 5 were performed to check if it is possible to cannulate an umbilical artery. The results of the simulations are promising. To extend this research, some first ideas and recommendations could be given for the design of the intrauterine ECMO device. In this chapter, there will be elaborated on the points of concern already mentioned in Section 1.2.

6.1. Design of the device and its placement

The idea is to support the fetus with gas transport during placental ischaemia. Further, a potential extension could be to also support it with nutrient transport. The device would possibly consist of conduit tubes, an artificial lung, and a pump. Probably also monitoring devices and a heating system are needed. The conduit tubes collect blood from the umbilical vessels via a cannula.

There are multiple sites at which the cannula can be placed. It could be placed near the placenta or near the abdomen of the fetus. The cannula can probably be anchored better at these sides than when attached to the middle of the umbilical cord. Attachment on the placenta could be more stable than on the fetal side of the umbilical cord because the fetus moves around inside the abdomen.
How to place these conduit tubes into the umbilical artery is also still a question. One option is minimally invasive surgery. The other is normal surgery, by which the fetus is approached with a laparotomy and hysterotomy, which are a large incision in the abdomen wall of the mother an incision in the uterus like with a Cesarean section. The chance on infections is lower for minimally invasive surgery, but the accessibility of the umbilical cord more complex.

The idea to place the cannula inside the umbilical artery instead of a vein is that there are two arteries. So, the flow towards the placenta remains intact during the procedure and there will still be a bit of oxygen exchange in the placenta. It is amongst other things very important for the brain to keep receiving oxygen [43].

The next point about placement is the anchoring of the device. The fetus moves inside the womb and could accidentally pull on the tubes. There are two anchoring sites, the cannulation site and the point where the tube pierces through the amniotic sac. An option to keep the amniotic sac attached to the uterine wall and prevent it from rupturing could be to use a small balloon, which is inflated after perforation to push the amniotic sac to the uterine wall.

One of the next steps is to estimate if a pump is needed to maintain fetal blood pressure. Studies into the design of artificial wombs are carrying out research to use pumpless circuits which only run on fetal cardiac output. In the study of Miura et al. [37] a parallel circuit of two oxygenators is used to decrease the resistance of the extracorporeal device. Pumpless systems are preferred because of their simplicity, fewer chances on haemolysis and inflammation [56]. The device will be primed with a primer fluid. this needs to be compatible with the fetal fluids. It also increases the fluid volume of the system. In the studies of Miura et al. [37] and Partridge et al. [43], who both designed artificial wombs to support premature lambs, the prime is maternal blood. The extra fluid volume inside the extracorporeal system increases the total blood volume. This extra volume does not influence the venous return or the haemodynamics of the fetal system. The ECMO system can be seen as a rigid system, so flow rate going in, comes out of the system at the same flow rate [12]. With a pump, the extra pressure difference in the umbilical artery can be compensated to maintain flow rates through the umbilical arteries and the placenta. If this is not managed well and umbilical vein flow and venous return do change, then shunting through the ductus venosus shunt and foramen ovale shunt will compensate for the changes in venous return [27]. The fetal heart can hardly increase its stroke volume because it is already oper-

ating at its peak performance. So, fetal heart rate is used to change cardiac output and to compensate for changes in the cardiovascular system in cooperation with the fetal shunts [23, 27].

6.2. Possible complications

Complications that could occur using ECMO are generally well-known. These possible complications and points of concern could be kept in mind while designing the intrauterine ECMO model. A common complication of ECMO is bleeding, which often happens at the cannulation site [12]. Other problems could be infections, haemolysis, and blood clotting. Anticoagulation therapy is needed to prevent blood clotting. A second concern is the compatibility of the device with the fetal system, and its blood and haemoglobin. Fetal blood has a higher haematocrit level than adult blood and fetal haemoglobin also differs from adult blood. The higher affinity for oxygen from fetal haemoglobin and a higher level of haematocrit could also be seen as an advantage to simplify gas exchange [56]. The third concern is the changing oxygen gradient between the fetal and maternal sides of the placenta because of the intrauterine support in the umbilical artery. It is not apparent if this will provoke a reaction in the maternal blood supply. Lastly, the mother is suffering from high blood pressure during pre-eclampsia. It is therefore important to maintain the blood pressure inside the placenta to protect the fetal chorionic trees.

6.3. Chapter conclusion

The first ideas for the intrauterine ECMO support system are to support the fetus with gas transport. The base parts for the system will be conduit tubes and cannulae, an artificial lung and if necessary a pump. The cannulation site is not established, but placement near the placenta or in the chorionic arteries seems a stable option. Installing the device via minimally invasive surgery would be less demanding for the mother and the chance on infections is smaller. Some critical issues to keep in mind while designing the system will be preventing complications, the anchoring of the cannulae in the arteries and of the tube on the uterine wall, and if a pump is needed to support the fetal heart.

7 | Conclusion

In this study, the feasibility of using intrauterine ECMO to support during placental ischaemia was investigated. This chapter will discuss the results and findings of this study and give some recommendations for future research on fetal support.

7.1. Discussion

Simulating the fetal cardiovascular system is useful to retrieve information about the cardiovascular response to the implementation of an assist device on an umbilical artery. The reason to look into the option to support the fetus during placental ischaemia is the high incidence of the condition under pregnant women and the systemic impact of placental ischaemia. The umbilical cord could be used to extract fetal blood and improve its oxygen levels, without having to cross the placental barrier first.

A fetal cardiovascular model was made in Simulink. Parts of the fetal cardiovascular system were lumped together into segments and combined in a lumped parameter model. Segments represent bigger parts of the body, such as the upper body or lungs. Unique segments of the fetal cardiovascular system were implemented as separate elements in the system. In particular, the ductus venosus and ductus arteriosus, which protect the immature liver and inflated lungs.

A sensitivity analysis was performed to increase understanding in the fetal cardiovascular model and the consequences of model choices. An important finding is that the fetal cardiovascular model can be divided into two parts, which influence each other minimally. Especially changes in the loop of the ductus arteriosus, pulmonary artery, and aorta evoke minimal reaction on the peripheral system. This is because the heart is modelled as a constant current source, dividing the flow rate over the pulmonary artery and aorta according to the needs of the peripheral system. Another finding is that the compliance is of little influence on the system, because of the constant combined ventricular output of the heart. However, when pulsatile flow would be implemented into the system, the compliance becomes of higher influence on the output. Compliance creates a buffer of blood inside some parts of the system. It also creates a phase shift for the output and dampens the pressure drop. In reality, compliance would influence the resistance of an element. For example; a highly compliant vessel would increase in radius because of applied blood pressure and thus decrease its resistance to blood flow. With the available information, no variable resistance could be implemented into the fetal cardiovascular model. A study into the possibilities for a variable resistance can be found in Appendix F. This option is examined, because it would give the opportunity to change the resistance of blood vessels in the system, by changing the radius. However, finding the values to implement a variable resistance into the fetal cardiovascular model was beyond the scope of this study.

The data about the heart, and resistance and compliance of the segments, used to simulate the fetal cardiovascular system, was chosen because the flow rate and pressure in the simulations were close to the flow rate and pressure found in literature. The umbilical artery with inserted cannula was allowed to use all the pressure provided as input in the segment. Simulations in the fetal cardiovascular model showed that the flow rate through that artery would increase. This simulation shows the opportunity that a cannula could be inserted into the umbilical artery and that the fetal system would be able to push blood through it. The resistance of the umbilical arteries was lowered to add the cannula resistance. This changes the flow distribution in the system. However, the resistance of both arteries is still compatible with the values from Luria et al. [31].

There is not much available information to use for the model. This is because during pregnancy, the fetus sits inside the womb, and it is unethical to enter the womb to measure blood pressure and blood flow. The information found, was of a fetus of 30 weeks of gestation and 1500 g. The data was extrapolated over a period of 20 to 28 weeks of gestation by using scaling factors. Parameters as flow

rate and blood pressure were collected from literature to be able to evaluate the simulations of the fetal cardiovascular model. For the flow rate, mainly data from the study of Kiserud and Acharya [27] was used. However, their values for the flow rate through the ductus arteriosus at 30 and 38 weeks seemed incorrect. The flow rate for the ductus arteriosus at 30 and 38 weeks was corrected and can be found in Table C.1. Values from literature were mostly rounded because such precision was not needed in the fetal cardiovascular model. Apart from an attempt to create a variable resistance, also research was done into the resistance of the placental vasculature. The placenta takes a prominent place in the fetal cardiovascular model and research was performed to understand its architecture, how its resistance is built up, and if this could be added to the model. The estimation of the resistance in this way would become to complex and is not implemented, but a summary is given in Appendix G.

The research objective focused on placental ischaemia. However, the simulations performed where with data based on information of healthy fetuses. Still, the simulations give information about how a fetal system would react with placental ischaemia. The resistance of the placenta would increase, so the flow rate through the placenta would decrease and relocate to other parts of the system, probably mostly to the brain. Examples of these scenarios were given in the sensitivity analysis. It was shown that for a higher total resistance also the pressure in the system would increase. So, the flow towards the placenta would be a bit lower and the resistance higher. The available pressure in the system would also increase, helping to push blood through the cannula. Further, with a lower flow rate to the placenta, oxygenation of blood in the umbilical artery still influences the average oxygen saturation of the blood. This is because of the high percentage of fetal cardiac output flowing towards the placenta.

7.2. Conclusion

In this study, a fetal cardiovascular model is created to simulate the fetal cardiovascular system. The model is able to simulate the haemodynamics of the fetal system during gestation. The model can be extended to create more realistic haemodynamics, such as pulsatile blood flow. Further steps in the design could be to add the whole intrauterine ECMO system including an oxygenator and pump. The simulations over a period of 20 to 30 weeks of gestation show an opportunity to insert a cannula inside one of the umbilical arteries while maintaining blood flow. This is a promising first step in determining the feasibility of intrauterine ECMO to support the fetus during placental ischaemia.

7.3. Recommendations for further research

During this study, a first step was made into the design of an intrauterine ECMO device. Here are some recommendations for further research to improve the fetal cardiovascular model and to create a fetal support system.

- A first useful step would be to model the fetal heart with the two ventricles and pulsatile blood flow. The behaviour of the loop of the pulmonary artery, ductus arteriosus and aorta would then become more realistic. Also, under pulsatile flow, compliance would get more influence on the flow rate in the elements.
- It would be preferable to find information about the fetal cardiovascular system during placental ischaemia. In this way, simulations with the ECMO cannula would become more realistic and research into the feasibility would improve.
- The next step to improve the fetal cardiovascular model is to expand the Simulink model with an oxygenator and pump. The oxygenator can be modelled as a resistance. The pump could be implemented as a pressure step to increase blood pressure before its entering the placenta. It needs to be determined if a pump is really needed, or if the fetal heart is strong enough to provide a pumpless circuit with blood flow. The tubes after the cannula can become larger in size, resulting in lower resistance to blood flow towards the oxygenator.
- It would be very helpful for future research if a database would be created in which information of the fetal cardiovascular system is gathered. Useful data would be data about blood flow and pressure in different parts of the fetal body and placental circulation. Also, information about the resistance, compliance, and inductance of different organs or segments would be very useful.

Lastly, vascular dimensions as length, radius, wall thickness, and volume are very useful. There is information available about children and adults, but information about the fetus is scarce, while research into the design of the artificial womb is already performed for a few decades.

Bibliography

[1] Alma Aurioles-Garibay, Edgar Hernandez-Andrade, Roberto Romero, Faisal Qureshi, Hyunyoung Ahn, Suzanne M. Jacques, Maynor Garcia, Lami Yeo, and Sonia S. Hassan. Prenatal diagnosis of a placental infarction hematoma associated with fetal growth restriction, preeclampsia and fetal death: Clinicopathological correlation. *Fetal Diagnosis and Therapy*, 36(2):154–161, 2014. ISSN 14219964. doi: 10.1159/000357841.

[2] Ofer Barnea. Open-Source Programming of Cardiovascular Pressure-Flow Dynamics Using SimPower Toolbox in Matlab and Simulink. *The Open Pacing, Electrophysiology & Therapy Journal*, 3(1):55–59, 2010. ISSN 1876536X. doi: 10.2174/1876536x01003010055.

[3] J. Gordon Betts, Peter Desaix, Eddie Johson, Jody E. Johson, Oksana Korol, Dean Kruse, Brandon Poe, James A. Wise, Mark Womble, and Kelly A. Young. *OpenStax Anatomy & Physiology*. OpenStax, Houston, 2013. ISBN 9781938168130. URL https://openstax.org/details/anatomy-and-physiology.

[4] G Bol Raap, K Caliskan, D W Donker, N de Jonge, J R Lahpor, R J M Klautz, H van Swieten, W Suyker, H F Verwey, and A A Voors. Consensus Werkgroep LVAD van de Nederlandse Vereniging voor Thoraxchirurgie en de Nederlandse Vereniging Voor Cardiologie. pages 1–25, 2014.

[5] G. J. Burton, A. W. Woods, E. Jauniaux, and J. C.P. Kingdom. Rheological and Physiological Consequences of Conversion of the Maternal Spiral Arteries for Uteroplacental Blood Flow during Human Pregnancy. *Placenta*, 30(6):473–482, 2009. ISSN 01434004. doi: 10.1016/j.placenta.2009.02.009.

[6] Graham J. Burton and Eric Jauniaux. What is the placenta? *American Journal of Obstetrics and Gynecology*, 213(4):S6.e1–S6.e4, 2015. ISSN 10976868. doi: 10.1016/j.ajog.2015.07.050. URL http://www.ncbi.nlm.nih.gov/pubmed/26428504.

[7] W. L. Capper, J. G. Cowper, and L. J. Myers. A transfer function-based mathematical model of the fetal-placental circulation. *Ultrasound in Medicine and Biology*, 28(11-12):1421–1431, 11 2002. ISSN 03015629. doi: 10.1016/S0301-5629(02)00658-0. URL https://www.sciencedirect.com/science/article/pii/S0301562902006580.

[8] Terri A. Cavaliere. From Fetus to Neonate: A Sensational Journey. *Newborn and Infant Nursing Reviews*, 16(2):43–47, 6 2016. ISSN 15273369. doi: 10.1053/j.nainr.2016.03.004. URL https://www.sciencedirect.com/science/article/pii/S1527336916000313.

[9] I L Chernyavsky, O E Jensen, and L Leach. A Mathematical Model of Intervillous Blood Flow in the Human Placentone. *Placenta*, 31(1):44–52, 2010. ISSN 0143-4004. doi: https://doi.org/10.1016/j.placenta.2009.11.003. URL http://www.sciencedirect.com/science/article/pii/S0143400409003476.

[10] A R Clark, M Lin, M Tawhai, R Saghian, and J L James. Multiscale modelling of the feto-placental vasculature. *Interface focus*, 5(2):20140078, 2015. ISSN 2042-8898. doi: 10.1098/rsfs.2014.0078. URL http://www.ncbi.nlm.nih.gov/pubmed/25844150https://www.ncbi.nlm.nih.gov/pubmed/25844150.

[11] Carla Sá Couto. Mathematical Models For Educational Simulation of Cardiovascular Pathophysiology. 2009.

[12] ELSO. ELSO Guidelines for Cardiopulmonary Extrcorporeal Life Support. Technical Report November, Extracorporeal Life Support Organization, Ann Arbor, MI, USA, 2013. URL www.elsonet.org.

[13] Y.C. Fung. *Biodynamics: circulation*. New York, 1984. ISBN 0387908676.

[14] Patricia Garcia-Canadilla, Paula A. Rudenick, Fatima Crispi, Monica Cruz-Lemini, Georgina Palau, Oscar Camara, Eduard Gratacos, and Bart H. Bijens. A Computational Model of the Fetal Circulation to Quantify Blood Redistribution in Intrauterine Growth Restriction. *PLoS Computational Biology*, 10(6):1–14, 6 2014. ISSN 15537358. doi: 10.1371/journal.pcbi.1003667. URL http://dx.plos.org/10.1371/journal.pcbi.1003667.

[15] Patricia Garcia-Canadilla, Fatima Crispi, Monica Cruz-Lemini, Stefania Triunfo, Alfons Nadal, Brenda Valenzuela-Alcaraz, Paula A. Rudenick, Eduard Gratacos, and Bart H. Bijnens. Patient-specific estimates of vascular and placental properties in growth-restricted fetuses based on a model of the fetal circulation. *Placenta*, 36(9):981–989, 9 2015. ISSN 01434004. doi: 10.1016/j.placenta.2015.07.130. URL https://www.sciencedirect.com/science/article/pii/S0143400415300242?via%3Dihub.

[16] J S Gill, C M Salafia, D Grebenkov, and D D Vvedensky. Modeling oxygen transport in human placental terminal villi. *Journal of Theoretical Biology*, 291:33–41, 2011. ISSN 0022-5193. doi: https://doi.org/10.1016/j.jtbi.2011.09.008. URL http://www.sciencedirect.com/science/article/pii/S0022519311004644.

[17] Zoya Gordon, D. Elad, R. Almog, Y. Hazan, A. J. Jaffa, and O. Eytan. Anthropometry of fetal vasculature in the chorionic plate. *Journal of Anatomy*, 211(6):698–706, 2007. ISSN 00218782. doi: 10.1111/j.1469-7580.2007.00819.x.

[18] Denise Grady. The mysterious tree of a newborn's life, the push to understand the placenta, 2014. URL https://www.nytimes.com/2014/07/15/health/the-push-to-understand-the-placenta.html. Date accessed: 2018-03-20.

[19] F Greiss. Uterine and Placental Blood Flow. 2008. doi: DOI10.3843/GLOWM.10197. URL http://www.glowm.com/section_view/heading/Uterine%20and%20Placental%20Blood%20Flow/item/197#sectionView. Date accessed: 2019-02-11.

[20] A. Guettouche, J. C. Challier, Y. Ito, C. Papapanayotou, Y. Cherruault, and A. Azancot-Benisty. Mathematical modeling of the human fetal arterial blood circulation. *International Journal of Bio-Medical Computing*, 31(2):127–139, 8 1992. ISSN 00207101. doi: 10.1016/0020-7101(92)90068-4. URL https://www.sciencedirect.com/science/article/pii/0020710192900684.

[21] Giovanna Guidoboni, Alon Harris, Simone Cassani, Julia Arciero, Brent Siesky, Annahita Amireskandari, Leslie Tobe, Patrick Egan, Ingrida Januleviciene, and Joshua Park. Intraocular pressure, blood pressure, and retinal blood flow autoregulation: A mathematical model to clarify their relationship and clinical relevance. *Investigative Ophthalmology and Visual Science*, 55(7):4105–4118, 5 2014. ISSN 15525783. doi: 10.1167/iovs.13-13611. URL http://www.ncbi.nlm.nih.gov/pubmed/24876284http://www.pubmedcentral.nih.gov/articlerender.fcgi?artid=PMC4083771.

[22] Alan E. Guttmacher and Catherine Y. Spong. The human placenta project: It's time for real time. *American Journal of Obstetrics and Gynecology*, 213(4):S3–S5, 2015. ISSN 10976868. doi: 10.1016/j.ajog.2015.08.037. URL http://dx.doi.org/10.1016/j.ajog.2015.08.037https://www.ncbi.nlm.nih.gov/pubmed/26428502.

[23] Frank L Hanley. Fetal responses to extracorporeal circulatory support. *Cardiology in the Young*, 3(3):263–272, 1993. ISSN 1467-1107.

[24] Martin Hlaváč. Windkessel model analysis in matlab. *Proceedings of 10th conference STUDENT EEICT*, (3):5, 2004. URL http://www.feec.vutbr.cz/EEICT/2004/sbornik/03-Doktorske_projekty/01-Elektronika/09-lahvo.pdf.

[25] J. Huynh, D. Dawson, D. Roberts, and R. Bentley-Lewis. Systemic review of placental pathology in maternal diabetes mellitus. *Placenta*, 36(2):101–114, 2015. doi: 10.1016/j.placenta.2014.11.021.A.

[26] A. L. Karimu and G. J. Burton. The effects of maternal vascular pressure on the dimensions of the placental capillaries. *BJOG: An International Journal of Obstetrics & Gynaecology*, 101(1): 57–63, 1994. ISSN 14710528. doi: 10.1111/j.1471-0528.1994.tb13011.x. URL https://www.ncbi.nlm.nih.gov/pubmed/8297870.

[27] Torvid Kiserud and Ganesh Acharya. The fetal circulation. *Prenatal diagnosis*, 24:1049–1059, 2004. doi: 10.1002/pd.1062.

[28] William D. Lakin, Scott A. Stevens, Bruce I. Tranmer, and Paul L. Penar. A whole-body mathematical model for intracranial pressure dynamics. *Journal of Mathematical Biology*, 46(4):347–383, 2003. ISSN 03036812. doi: 10.1007/s00285-002-0177-3.

[29] C Lees, G Albaiges, C Deane, M Parra, and K H Nicolaides. Assessment of umbilical arterial and venous flow using color Doppler. *Ultrasound Obstet Gynecol*, 14:250–255, 1999.

[30] Mabelle Lin, Benjamin Mauroy, Joanna L. James, Merryn H. Tawhai, and Alys R. Clark. A multiscale model of placental oxygen exchange: The effect of villous tree structure on exchange efficiency. *Journal of Theoretical Biology*, 408:1–12, 11 2016. ISSN 00225193. doi: 10.1016/j.jtbi.2016.06.037. URL https://www.sciencedirect.com/science/article/pii/S0022519316301710.

[31] Oded Luria, Jacob Bar, Josef Shalev, Michal Kovo, Abraham Golan, and Ofer Barnea. Inverse Solution of the Fetal-Circulation Model Based on Ultrasound Doppler Measurements. *Cardiovascular Engineering and Technology*, 5(2):202–216, 2014. ISSN 18694098. doi: 10.1007/s13239-013-0153-7.

[32] Mhairi G MacDonald and Mary M K Seshia. *Avery's Neonatology: Pathophysiology and Management of the Newborn 7th, Ch 16*. 7 edition, 2015. ISBN 1451192681.

[33] Elaine Nicpon Marieb and Katja N. Hoehn. *Human Anatomy and Physiology*. Pearson Education Limited, 10 edition, 2015. ISBN 9781292096971.

[34] Roger G. Mark. Cardiovascular mechanics I,II,III, 2004. URL https://ocw.mit.edu/courses/health-sciences-and-technology/hst-542j-quantitative-physiology-organ-transport-systems-spring-2004/readings/cardio_mech.pdf.

[35] E Ménigault, M Berson, P Vieyres, B Lepoivre, D. Pourcelot, and L Pourcelot. Feto-maternal circulation: Mathematical model and comparison with Doppler measurements. *European Journal of Ultrasound*, 7(2):129–143, 4 1998. ISSN 09298266. doi: 10.1016/S0929-8266(98)00018-4. URL https://www.sciencedirect.com/science/article/pii/S0929826698000184?via%3Dihub#BIB26.

[36] Dan Mihu, Ciortea Razvan, Andrei Malutan, and Carmen Mihaela. Evaluation of maternal systemic inflammatory response in preeclampsia. *Taiwanese Journal of Obstetrics and Gynecology*, 54(2): 160–166, 2015. ISSN 18756263. doi: 10.1016/j.tjog.2014.03.006. URL http://dx.doi.org/10.1016/j.tjog.2014.03.006.

[37] Yuichiro Miura, Tadashi Matsuda, Haruo Usuda, Shimpei Watanabe, Ryuta Kitanishi, Masatoshi Saito, Takushi Hanita, and Yoshiyasu Kobayashi. A Parallelized Pumpless Artificial Placenta System Significantly Prolonged Survival Time in a Preterm Lamb Model. *Artificial Organs*, 40(5): E61–E68, 2016. ISSN 15251594. doi: 10.1111/aor.12656.

[38] Leslie Myatt and James M. Roberts. Preeclampsia: Syndrome or Disease? *Current Hypertension Reports*, 17(11), 2015. ISSN 15343111. doi: 10.1007/s11906-015-0595-4.

[39] Dariusz Nowak, Hanna Kozłowska, Anna Zurada, and Jerzy Gielecki. The development of the pulmonary trunk and the pulmonary arteries in the human fetus. *Polish Annals of Medicine*, 18 (1):31–41, 1 2011. ISSN 12308013. doi: 10.1016/S1230-8013(11)70021-2. URL https://www.sciencedirect.com/science/article/pii/S1230801311700212.

[40] Gabriela Ortiz-Leon, Marta Vilchez-Monge, and Juan J. Montero-Rodriguez. An updated Cardiovascular Simulation Toolbox. *Proceedings - IEEE International Symposium on Circuits and Systems*, pages 1901–1904, 2013. ISSN 02714310. doi: 10.1109/ISCAS.2013.6572238.

[41] Gabriela Ortiz-león, Marta Vílchez-monge, Juan J Montero-rodríguez, Escuela De Ingeniería Electrónica, Instituto Tecnológico, De Costa Rica, Costa Rica, and Escuela De Física. Simulations of the Cardiovascular System Using the Cardiovascular Simulation Toolbox. *Medical Cyber Physical Systems – Medical Device Interoperability, Safety, and Security Assurance (MCPS'14)*, 1(August 2015):28–37, 2014. ISSN 21906807. doi: 10.4230/OASIcs.MCPS.2014.28.

[42] J T Parer. Fetal circulation, 2008. URL http://www.glowm.com/section_view/heading/FetalCirculation/item/194. Date accessed: 2019-01-23.

[43] Emily A. Partridge, Marcus G. Davey, Matthew A. Hornick, Patrick E. McGovern, Ali Y. Mejaddam, Jesse D. Vrecenak, Carmen Mesas-Burgos, Aliza Olive, Robert C. Caskey, Theodore R. Weiland, Jiancheng Han, Alexander J. Schupper, James T. Connelly, Kevin C. Dysart, Jack Rychik, Holly L. Hedrick, William H. Peranteau, and Alan W. Flake. An extra-uterine system to physiologically support the extreme premature lamb. *Nature Communications*, 8:1–15, 2017. ISSN 20411723. doi: 10.1038/ncomms15112. URL http://dx.doi.org/10.1038/ncomms15112.

[44] Giancarlo Pennati and Roberto Fumero. Scaling approach to study the changes through the gestation of human fetal cardiac and circulatory behaviors. *Annals of Biomedical Engineering*, 28 (4):442–452, 4 2000. ISSN 00906964. doi: 10.1114/1.282. URL http://link.springer.com/10.1114/1.282.

[45] Giancarlo Pennati, M. Bellotti, and R. Fumero. Mathematical modelling of the human foetal cardiovascular system based on Doppler ultrasound data. *Medical Engineering and Physics*, 19(4):327–335, 6 1997. ISSN 13504533. doi: 10.1016/S1350-4533(97)84634-6. URL http://linkinghub.elsevier.com/retrieve/pii/S1350453397846346.

[46] S Perazzolo, R M Lewis, and B G Sengers. Modelling the effect of intervillous flow on solute transfer based on 3D imaging of the human placental microstructure. *Placenta*, 60:21–27, 2017. ISSN 0143-4004. doi: https://doi.org/10.1016/j.placenta.2017.10.003. URL http://www.sciencedirect.com/science/article/pii/S014340041731144X.

[47] Tomas Prior, Edward Mullins, Phillip Bennett, and Sailesh Kumar. Umbilical venous flow rate in term fetuses: Can variations in flow predict intrapartum compromise? *American Journal of Obstetrics and Gynecology*, 210(1):1–61, 1 2014. ISSN 00029378. doi: 10.1016/j.ajog.2013.08.042. URL https://www.sciencedirect.com/science/article/pii/S0002937813009307?via%3Dihub.

[48] L K Proctor, B Fitzgerald, W L Whittle, N Mokhtari, E Lee, G. MacHin, J. C.P. Kingdom, and S J Keating. Umbilical cord diameter percentile curves and their correlation to birth weight and placental pathology. *Placenta*, 34(1):62–66, 2013. ISSN 01434004. doi: 10.1016/j.placenta.2012.10.015. URL https://www.placentajournal.org/article/S0143-4004(12)00408-0/pdf.

[49] M W Rampling and M A Anwar. Haemorheology in the Foetus and the Neonate. *Series on Biomechanics*, 27(1):76–83, 2012.

[50] Christopher W.G. Redman and Anne Cathrine Staff. Preeclampsia, biomarkers, syncytiotrophoblast stress, and placental capacity. *American Journal of Obstetrics and Gynecology*, 213 (4):S9.e1–S9.e4, 2015. ISSN 10976868. doi: 10.1016/j.ajog.2015.08.003. URL http://dx.doi.org/10.1016/j.ajog.2015.08.003.

[51] Rijksoverheid. Tot hoeveel weken kan ik een abortus laten uitvoeren? URL https://www.rijksoverheid.nl/onderwerpen/abortus/vraag-en-antwoord/abortus-hoeveel-weken. Date accessed: 2019-05-17.

[52] Michael F. Robbins. *Ultimate Electronics: Practical Circuit Design and Analysis*. 2017. URL https://www.circuitlab.com/textbook/lumped-element-model/. Date accessed: 2019-01-07.

[53] James M Roberts. Pathophysiology of ischemic placental disease. *Seminars in Perinatology*, 38(3):139–145, 2014. ISSN 0146-0005. doi: 10.1053/j.semperi.2014.03.005. URL http://dx.doi.org/10.1053/j.semperi.2014.03.005.

[54] Christian J. Roth, Eva Haeussner, Tanja Ruebelmann, Franz V. Koch, Christoph Schmitz, Hans Georg Frank, and Wolfgang A. Wall. Dynamic modeling of uteroplacental blood flow in IUGR indicates vortices and elevated pressure in the intervillous space-a pilot study. *Scientific Reports*, 7, 2017. ISSN 20452322. doi: 10.1038/srep40771.

[55] Shier Nee Saw, Chia Dawn, Arijit Biswas, Citra Nurfarah Zaini Mattar, and Choon Hwai Yap. Characterization of the in vivo wall shear stress environment of human fetus umbilical arteries and veins. *Biomechanics and Modeling in Mechanobiology*, 16(1):197–211, 2 2017. ISSN 16177940. doi: 10.1007/s10237-016-0810-5. URL http://link.springer.com/10.1007/s10237-016-0810-5.

[56] Mark Schoberer, Jutta Arens, Anne Lohr, Matthias Seehase, Reint K. Jellema, Jennifer J. Collins, Boris W. Kramer, Thomas Schmitz-Rode, Ulrich Steinseifer, and Thorsten Orlikowsky. Fifty Years of Work on the Artificial Placenta: Milestones in the History of Extracorporeal Support of the Premature Newborn. *Artificial Organs*, 36(6):512–516, 2012. ISSN 0160564X. doi: 10.1111/j.1525-1594.2011.01404.x.

[57] Dick Schoot and Wim Daniëls. *De baarmoeder*. Prometheus Amsterdam, 2017. ISBN 9789044632866.

[58] Mirthe H. Schoots, Sanne J. Gordijn, Sicco A. Scherjon, Harry van Goor, and Jan Luuk Hillebrands. Oxidative stress in placental pathology. *Placenta*, pages 1–9, 2018. ISSN 15323102. doi: 10.1016/j.placenta.2018.03.003. URL https://doi.org/10.1016/j.placenta.2018.03.003.

[59] N Schwartz, H S Quant, M D Sammel, and S Parry. Macrosomia has its roots in early placental development. *Placenta*, 35(9):684–690, 2014. ISSN 15323102. doi: 10.1016/j.placenta.2014.06.373. URL http://dx.doi.org/10.1016/j.placenta.2014.06.373.

[60] Alexander S Serov, Carolyn Salafia, Denis S Grebenkov, and Marcel Filoche. The role of morphology in mathematical models of placental gas exchange. *Journal of Applied Physiology*, 120(1):17–28, 2016. ISSN 8750-7587. doi: 10.1152/japplphysiol.00543.2015. URL http://jap.physiology.org/lookup/doi/10.1152/japplphysiol.00543.2015https://www.ncbi.nlm.nih.gov/pubmed/26494446http://www.physiology.org/doi/abs/10.1152/japplphysiol.00543.2015.

[61] Liron Sheffer, William P. Santamore, and Ofer Barnea. Cardiovascular simulation toolbox. *Cardiovascular Engineering*, 7(2):81–88, 2007. ISSN 15678822. doi: 10.1007/s10558-007-9030-z.

[62] Robert M. Silver. Examining the link between placental pathology, growth restriction, and stillbirth. *Best Practice & Research Clinical Obstetrics & Gynaecology*, 49:89–102, 2018. ISSN 15216934. doi: 10.1016/j.bpobgyn.2018.03.004. URL http://linkinghub.elsevier.com/retrieve/pii/S1521693418300701.

[63] Pieter C. Struijk. *Assessment of hemodynamic parameters in the fetal and utero-placental circulation using doppler ultrasound*. Rotterdam, 2006. ISBN 9085592399.

[64] M. Beatrijs van der Hout-van der Jagt, S. Guid Oei, and Peter H.M. Bovendeerd. A mathematical model for simulation of early decelerations in the cardiotocogram during labor. *Medical Engineering and Physics*, 34(5):579–589, 6 2012. ISSN 13504533. doi: 10.1016/j.medengphy.2011.09.004. URL https://www.sciencedirect.com/science/article/pii/S1350453311002293.

[65] M. Beatrijs Van der Hout-van der Jagt, Germaine J.L.M. Jongen, Peter H.M. Bovendeerd, and S. Guid Oei. Insight into variable fetal heart rate decelerations from a mathematical model. *Early Human Development*, 89(6):361–369, 6 2013. ISSN 03783782. doi: 10.1016/j.earlhumdev.2012.12.001. URL https://www.sciencedirect.com/science/article/pii/S0378378212002769?via%3Dihub.

[66] M C van Patot, G Ebensperger, M Gassmann, and A J Llanos. The hypoxic placenta. *High Alt Med Biol*, 13(3):176–184, 2012. ISSN 1557-8682 (Electronic) 1527-0297 (Linking). doi: 10.1089/ham.2012.1046. URL https://www.ncbi.nlm.nih.gov/pubmed/22994517.

[67] Jeroen J. Van Vonderen, Arno A.W. Roest, Melissa L. Siew, Frans J. Walther, Stuart B. Hooper, and Arjan B. Te Pas. Measuring physiological changes during the transition to life after birth. *Neonatology*, 105(3):230–242, 2014. ISSN 16617819. doi: 10.1159/000356704.

[68] Lee Waite and Jerry Fine. *Applied biofluid mechanics*. The McGraw-Hill companies, 2007. ISBN 0071509518. doi: 10.1036/0071472177.

[69] Yuping Wang and S. Zhao. *Vascular biology of the placenta*. Morgan & Claypool Life Sciences, San Rafael (CA), 2010. URL https://www.ncbi.nlm.nih.gov/books/NBK53254/.

[70] Frank M. White. *Fluid mechanics*. The McGraw-Hill companies, New York, seventh edition, 2011. ISBN 9780071311212.

A | Placental Ischaemia

Following is a short explanation of all the placental pathologies involved with placental ischaemia shown in Figure 1.2. The ordering of the data is based on the articles of Gill et al. [16], Roberts [53], Silver [62].

- Local effect
  - Oxidative stress
    Due to less antioxidants and excessive generation of reactive oxygen species, levels of reactive oxygen species become too high and cause oxidative stress [66].
  - Endoplasmic reticulum stress
    During endoplasmic reticulum stress, the unfolded protein response is activated and protein synthesis is disturbed [53].
- Systemic effect
  - PE (non-branching angiogenesis)
    Through PE the mother becomes hypertensive, oedematous and gets proteinuria. It is a systemic syndrome because multiple organs of the mother could be affected like liver and brain.
  - Non-branching angiogenesis
    Non-branching angiogenesis means that only longer capillaries are formed [16].
    - Eclampsia
      In severe cases, pre-eclampsia can lead to eclampsia, which is the onset of seizures during pregnancy.
    - HELLP
      HELLP-syndrome has many similarities with PE. It stands for Haemolysis, Elevated Liver enzymes, and Low Platelets. Damaged blood cells constipate the mothers liver, which is going to swell and its function is deteriorating [57].
    - Gestational hypertension
      Gestational hypertension occurs after 20 weeks of gestation and manifests, other than PE, without proteinuria, but only with a high blood pressure of > 140/90 mmHg.
- Other placental diseases
  - Extensive branching angiogenesis
    During branching angiogenesis, looped capillaries are formed from existing capillaries.
    - Diabetes
      Maternal diabetes can come in three variants. Pregestational type 1 diabetes mellitus, type 2 and gestational diabetes mellitus. Huynh et al. [25] reviewed the topic and found increased villous immaturity and increased angiogenesis for pre-gestational and gestational diabetes as the most common abnormalities and specifically for gestational diabetes enlarged placenta thickness.
    - Anaemia
      By anaemia there is a shortage of red blood cells or haemoglobin. During pregnancy, there is a higher maternal blood production, when the proportion plasma is too high in comparison to haematocrit it can result in anaemia [16].
    - High altitude exposure
      At high altitude, there is less oxygen in the atmosphere leading to hypoxic stress and thus high altitude exposure. Firstly, the placenta acts with lower trophoblast invasion into the uterine wall and spiral arteries and thus lowering uteroplacental blood flow. This

first response also applies on anaemic placentas [66]. Secondly, two responses follow; a compensatory one of increased angiogenesis and an adaptive one of down-regulation of fetal growth and less nutritional transport.

- fetal growth problems
  Impaired function of the placenta can lead to alterations in fetal growth.
  - IUGR
    Growth of the placenta in the first trimester is limited for intrauterine growth restriction (IUGR), also called fetal growth restriction (FGR). IUGR is often defined as not reaching its genetic growth potential. IUGR affects around 15% of all pregnancies and is a risk factor for stillbirth [58].
  - SGA
    A child could be small for gestational age (SGA) and this is also a risk factor for stillbirth, like IUGR. Again probably caused by uteroplacental insufficiency and ischaemia. If the estimated fetal weight is below the 10^{th}- or 5^{th}-percentile of the population one speaks of SGA [62].
  - LGA
    LGA is defined as a birth weight of $\geq 90^{th}$-percentile for gestational age.
  - Macrosomia
    Infants with macrosomia have a birth weight of ≥ 4000 g, [59].
- Other
  - Placental infarction and haematoma
    Placental infarction may occur when the maternal intervillous flow is interrupted, because of blood clotting in the spiral arteries or decidual veins. There is also a form of placental infarction haematoma, where there is the first occlusion of spiral arteries and infarction of placental cells, followed by re-perfusion causing haematoma [1].
  - Preterm delivery
  - Recurrent pregnancy loss
  - Multiple gestation
    Multiple gestation causes higher risks for mother and fetus. Perinatal mortality is 4-fold higher than for singletons and associated with placental or umbilical cord disorders.

- Placental disorders
  Placenta ischaemia and uteroplacental insufficiency are closely related. fetal genetic abnormalities or birth defects can also decrease fetal growth and vascular abnormalities and developmental disorders can lead up to ischaemia. Silver [62] gives in his paper about placental pathology, growth restriction and stillbirth a neat structure of placental pathologies. Three distinctions are made: developmental, inflammatory and circulatory disorders.
  - Development disorders
    - Umbilical cord
      Umbilical cord disorders are cases by which there are missing arteries in the umbilical cord or the umbilical cord is inserted wrongly in the placenta through which the cord is not enough protected by Wharton's jelly.
    - Placental membranes
      The placental membranes could be circummarginate or circumvallate inserted, which means that the membranes are inserted away from the peripheral edge of the placenta, but this is mostly occurring by multiple gestation.
    - Circulatory
      The fetal terminal villi could be immature or are very small with wide-open intervillous spaces. This makes diffusion more difficult. All development disorders are closely linked to IUGR.
  - Inflammatory
    - Maternal
      The maternal inflammatory response is inflammation of the membranes through bacterial infection.

- ◊ fetal
  During a fetal inflammatory response, the umbilical vein, arteries or cord could be infected or the villi in the chorionic plate.
- ◊ Villitis
  Villitis is a placental injury by which maternal lymphocytes are transferred across the placenta. Inflammation of villi happens to the terminal and branched villi, but not to stem villi.

– Circulatory disorders
  - ◊ Maternal
    Maternal circulatory disorders are vascular obstructions, haematoma, parenchymal infarction, thrombus and fibrin depositions, all interrupting or complicating perfusion of the IVS.
  - ◊ fetal
    fetal circulatory disorders are blood clots in the chorionic plate or villi. Lastly, there is the fetal circulatory disorder called oedema or placental hydrops which is a prenatal form of heart failure.

B | Literature research into cardiovascular models

Firstly, an exploratory search was performed on DuckDuckGo[1] with combinations of the following search terms: MATLAB, Simulink, model, blood flow, maternal, fetal, neonatal, cardiovascular. One of the first hits was the Cardiovascular simulation toolbox from Sheffer et al. [61] and articles about the Windkessel model [24].

Next, after scanning the articles of Sheffer et al. [61] and Hlaváč [24], to get familiar with the subjects, a detailed search was performed in Pubmed[2], Google Scholar[3] and Scopus[4].
In Pubmed the following search terms were used in different arrangements: MATLAB, Simulink, model, blood flow, cardiovascular, uterine, placenta, fetus, vascular system, perfusion system, simulation. These searches resulted in a total of 118 hits and 6 useful articles.
In Google Scholar searches were performed with the following terms: Simulink, model, blood flow, fetal, uterine, placenta, maternal, circulation. Which resulted in 178 hits and 4 saved articles, with many similar hits compared to Pubmed. Except for the model of Sheffer et al. [61], no other specific models were found.
In Scopus combinations of words used were: Simulink, model, blood flow, uterine, placenta, simulation. A total of 161 hits were given, again with the model of Sheffer et al. [61] as a result and many hits similar to the ones found in Pubmed.

To filter the results a requirement was free full text to be available and the titles were scanned and if necessary the abstracts for confirmation that the articles indeed included models and preferable in Simulink and MATLAB. Differences between the search terms resulted after several iterations of searches, some combinations just gave excessive amounts of hits and others zero hits. The reason for the small number of saved articles is that many articles did not include any computer model. Mostly mathematical models were found or information about imaging techniques for measuring blood flow, which is not useful for this study.

[1] www.duckduckgo.com
[2] www.ncbi.nlm.nih.gov/pubmed
[3] scholar.google.nl
[4] www.scopus.com

C | Flow rate

At the next page, Table C.1 gives an overview of the found variables in literature for the blood flow in different body parts.

Table C.1: Values found in literature for the percentage of CVO distributed through the different segments.

Study	GA (weeks)	Left CO	Right CO	PVR	DA	UB	Brain	LB	LB and PLA	PLA	HE	DV
Garcia-Canadilla et al. [14]	33	40 to 47	53 to 60	13 to 25		10 to 14	15 to 16		50 to 60			
MacDonald and Seshia [32]											50 of UV	50 of UV
Van Vonderen et al. [67]	40	66.67	33.33	3.33	30							30
Cavaliere [8]	40			9						40		50 to 60 of UV
Ménigault et al. [35]	40			8		20			67	40		
Kiserud and Acharya [27]	20	47	53	13	40					50		
”	30	43	57	21	36					41,5		
”	38	40	60	25	35					33		
Couto [11]	40	40	60	18	42					34		
Guettouche et al. [20]	27,5	45	55		39,3					23		
Capper et al. [7]	28			15		27		33		24		

D | Blood pressure

At the next page, Table D.1 gives an overview of the found variables in literature for the blood pressure in different body parts.

Table D.1: Values found in literature for the pressure in mmHg inside segments.

Study	GA (weeks)	Systolic	Diastolic	MAP	AO	PA	DA	PVR	UB	LB	UA	PLA	UV	Venous	LAP	RAP
Luria et al. [31]	30															
Garcia-Canadilla et al. [14]	33			40												
Ménigault et al. [35]	40			42	32 to 55											
Kiserud and Acharya [27]	20	15 to 20	< 5	15									4.5			
”	30	30 to 40	5 to 15										2 to 9			
”	38												6			
van der Hout-van der Jagt et al. [64]	40	58	26	45										1 to 14		
Struijk [63]		1.06* GA (wks) +15.91	0.67* GA(wks) +2.47	0.87* GA (wks) +10.33												
Parer [42]															2	3
Guettouche et al. [20]	25 to 30				53.9	53.88	53.72				35.36					
Couto [11]	40							47	46	46					5	6
Saw et al. [55]	32															
Clark et al. [10]	40										50	20				
Wang and Zhao [69]	40										50	30 (villi)	20			
Capper et al. [7]	28	77	55								52.67					

E | Sensitivity analysis

A sensitivity analysis is performed on the fetal cardiovascular model with as input the values from the study of Couto [11]. One factor at a time is changed with a variable from Luria et al. [31] or Pennati et al. [45]. In this way, the influence of that segment on the rest of the system could be identified.

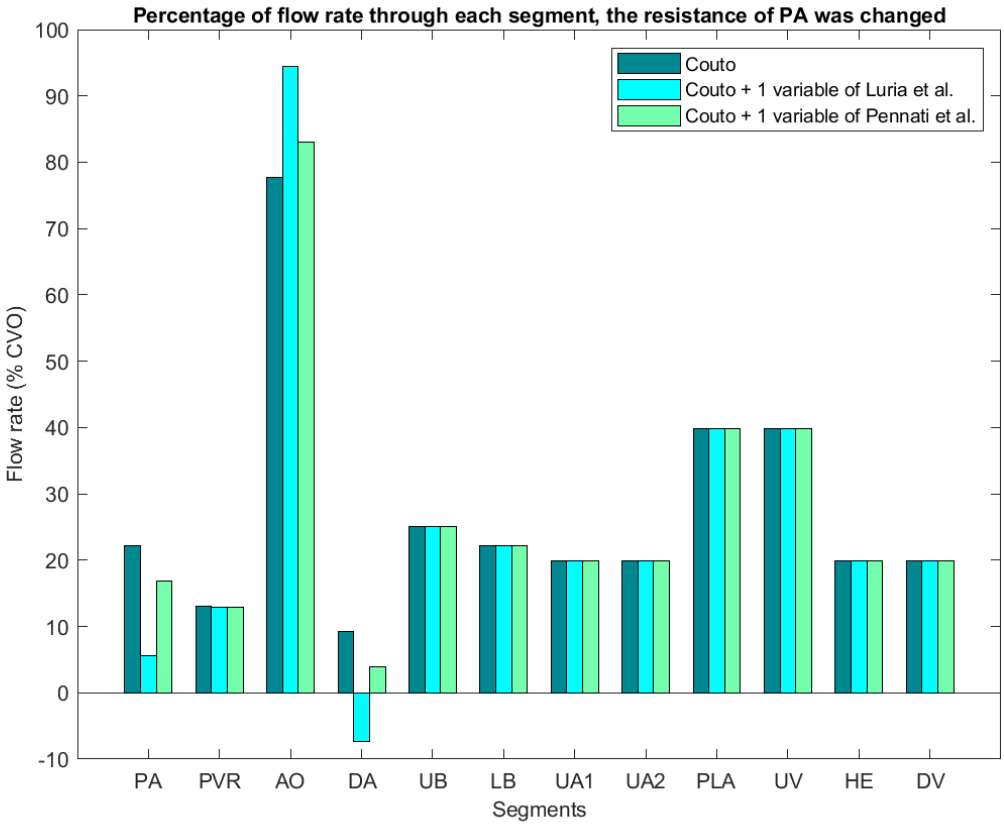

Figure E.1: Variables of Couto [11] were implemented into the fetal cardiovascular model and the value for PA was changed two times into a value from Luria et al. [31] or Pennati et al. [45] to evaluate its influence on the system.

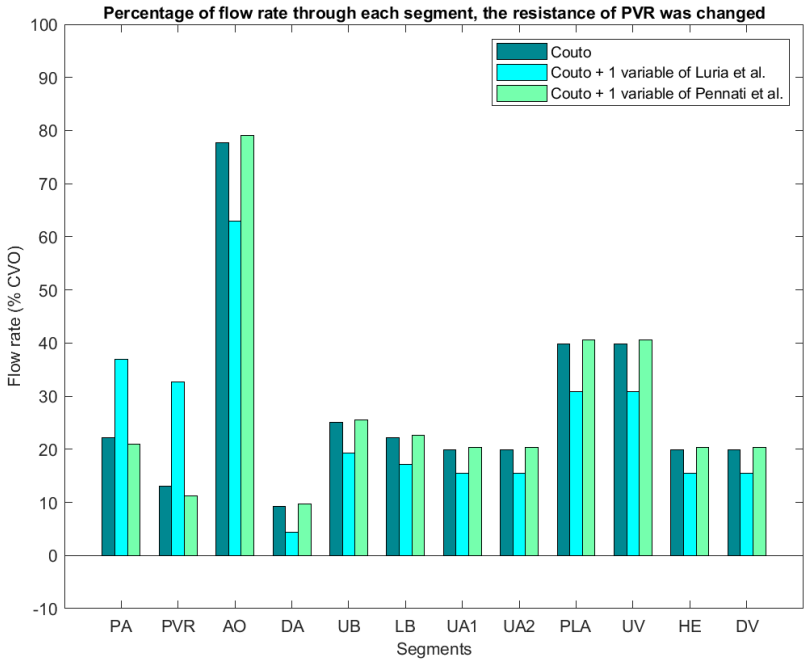

Figure E.2: Variables of Couto [11] were implemented into the fetal cardiovascular model and the value for PVR was changed two times into a value from Luria et al. [31] or Pennati et al. [45] to evaluate its influence on the system.

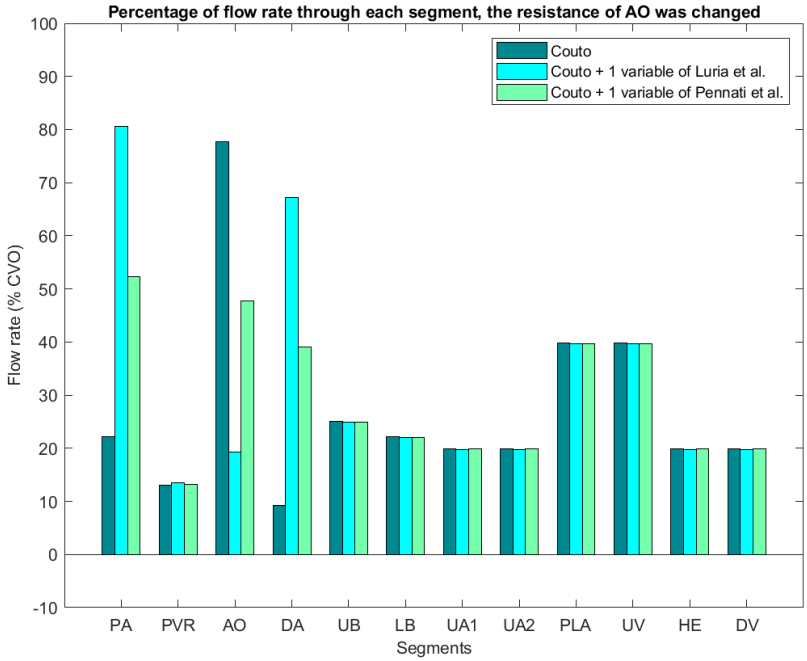

Figure E.3: Variables of Couto [11] were implemented into the fetal cardiovascular model and the value for AO was changed two times into a value from Luria et al. [31] or Pennati et al. [45] to evaluate its influence on the system.

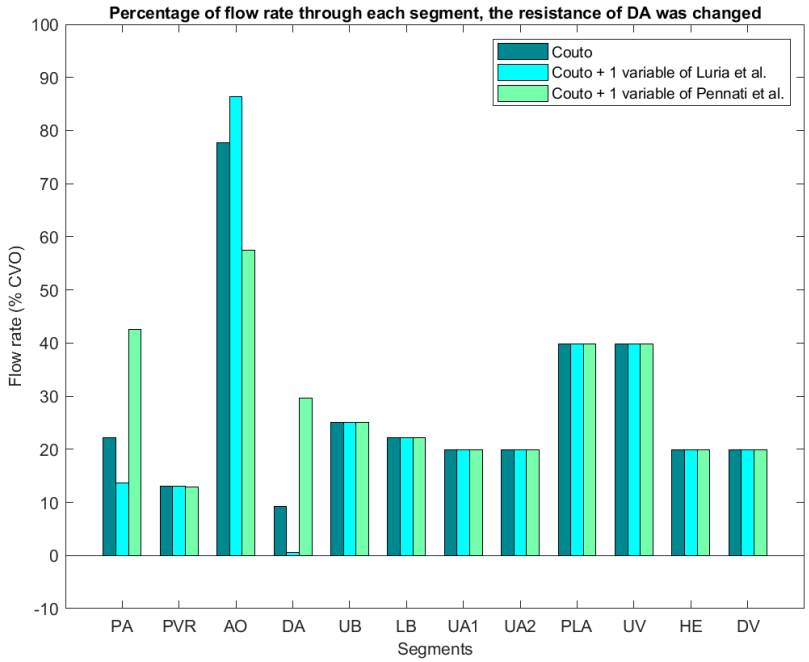

Figure E.4: Variables of Couto [11] were implemented into the fetal cardiovascular model and the value for DA was changed two times into a value from Luria et al. [31] or Pennati et al. [45] to evaluate its influence on the system.

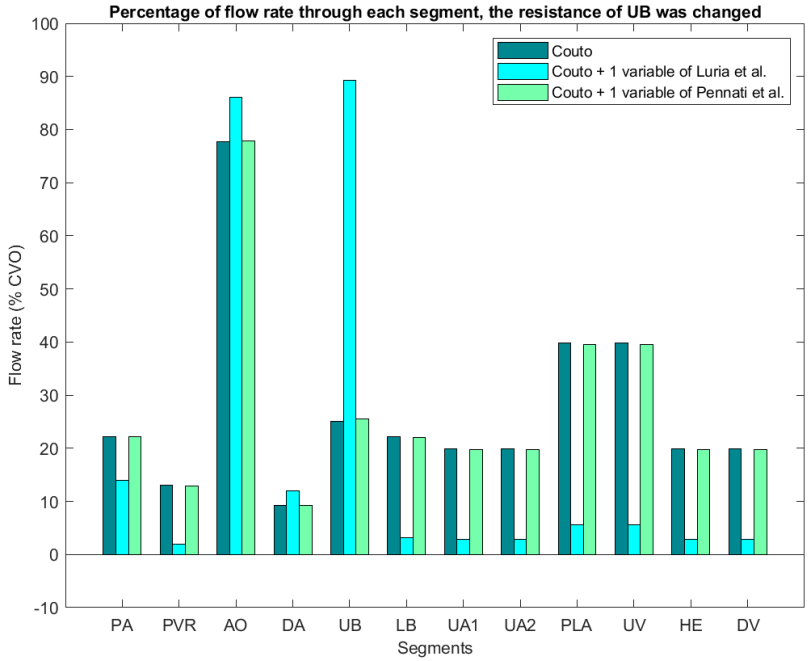

Figure E.5: Variables of Couto [11] were implemented into the fetal cardiovascular model and the value for UB was changed two times into a value from Luria et al. [31] or Pennati et al. [45] to evaluate its influence on the system.

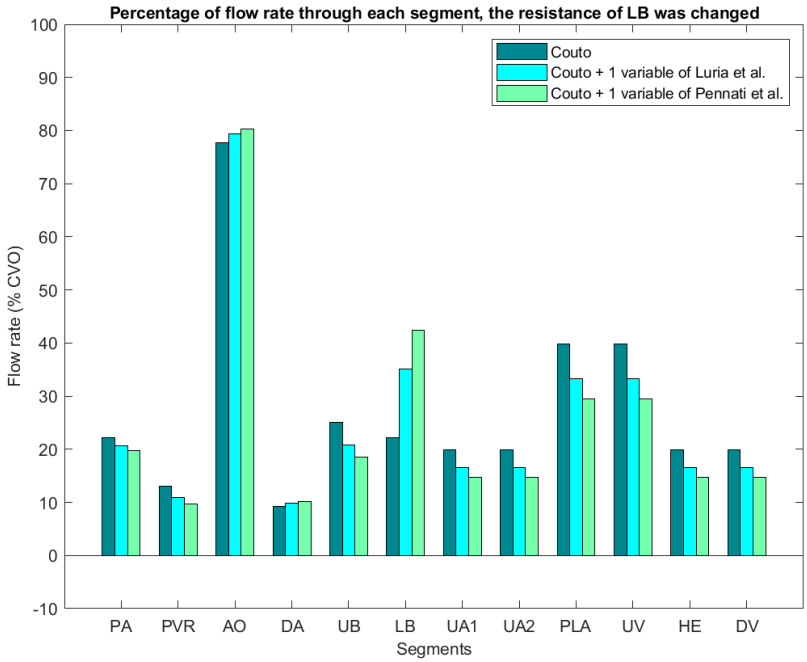

Figure E.6: Variables of Couto [11] were implemented into the fetal cardiovascular model and the value for LB was changed two times into a value from Luria et al. [31] or Pennati et al. [45] to evaluate its influence on the system.

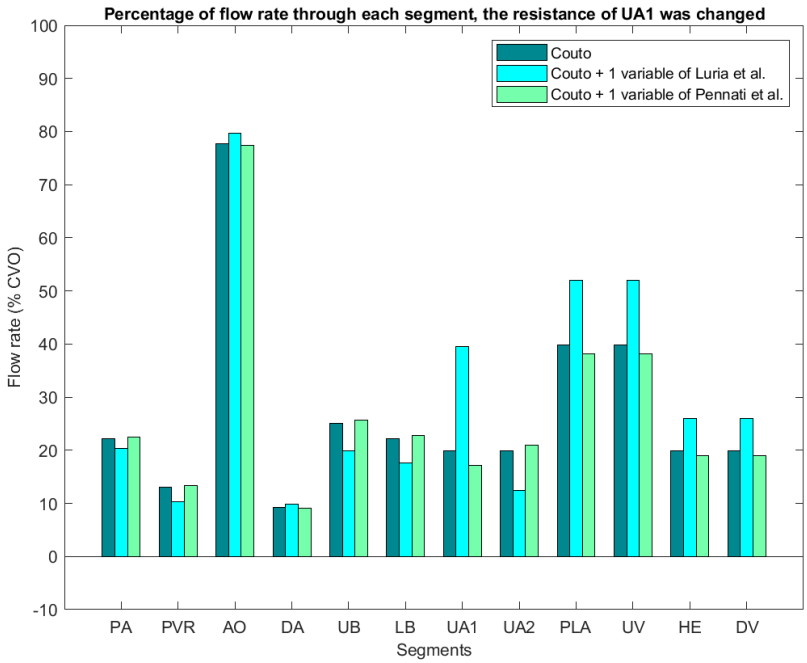

Figure E.7: Variables of Couto [11] were implemented into the fetal cardiovascular model and the value for UA1 was changed two times into a value from Luria et al. [31] or Pennati et al. [45] to evaluate its influence on the system.

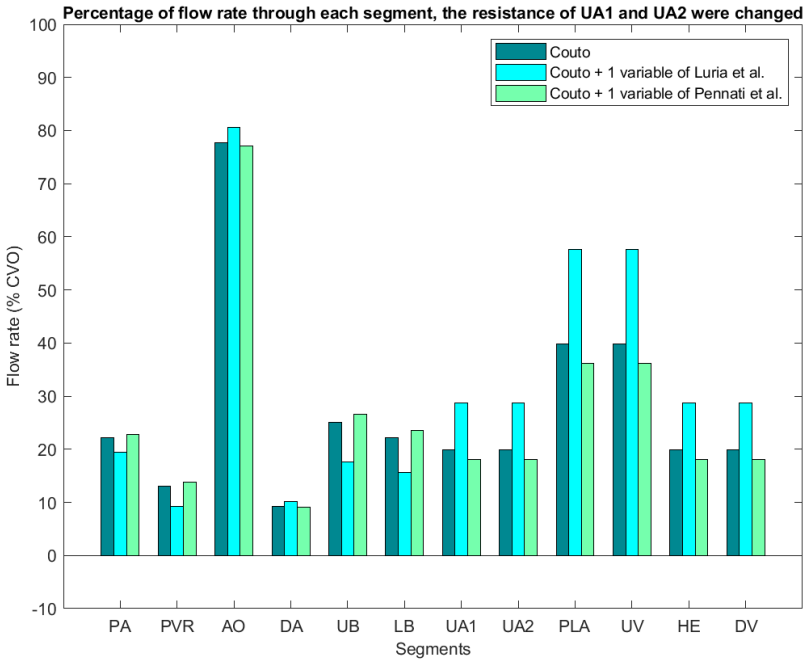

Figure E.8: Variables of Couto [11] were implemented into the fetal cardiovascular model and the value for UA1 and UA2 were changed two times into a value from Luria et al. [31] or Pennati et al. [45] to evaluate its influence on the system.

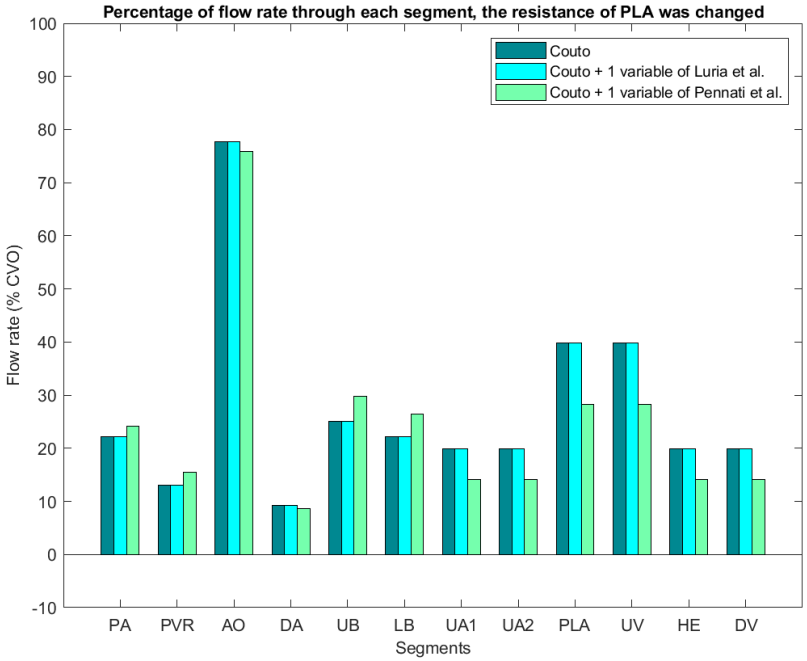

Figure E.9: Variables of Couto [11] were implemented into the fetal cardiovascular model and the value for PLA was changed two times into a value from Luria et al. [31] or Pennati et al. [45] to evaluate its influence on the system.

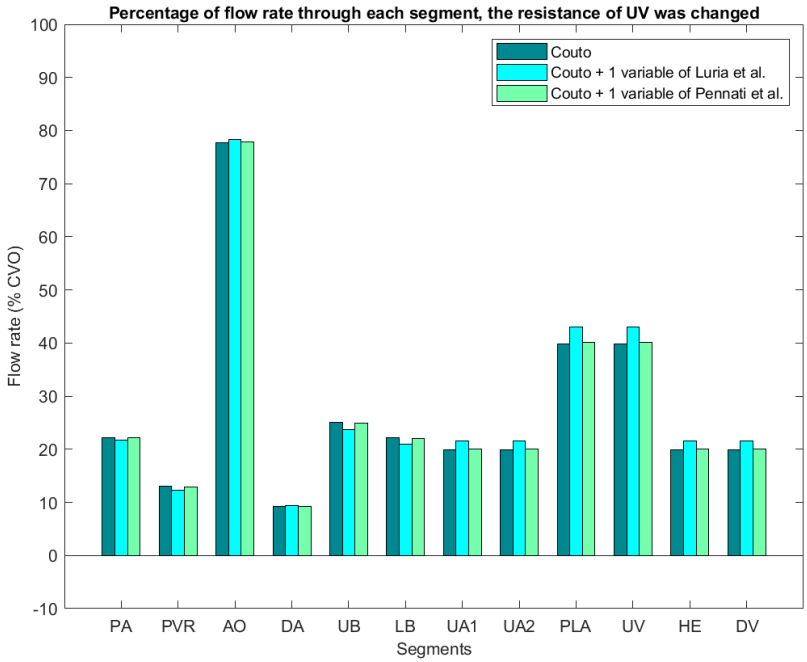

Figure E.10: Variables of Couto [11] were implemented into the fetal cardiovascular model and the value for UV was changed two times into a value from Luria et al. [31] or Pennati et al. [45] to evaluate its influence on the system.

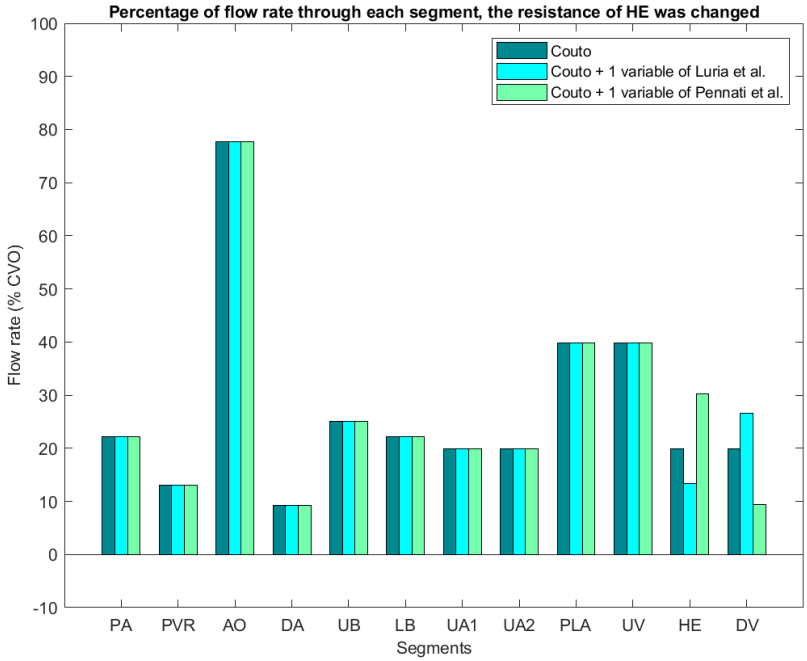

Figure E.11: Variables of Couto [11] were implemented into the fetal cardiovascular model and the value for HE was changed two times into a value from Luria et al. [31] or Pennati et al. [45] to evaluate its influence on the system.

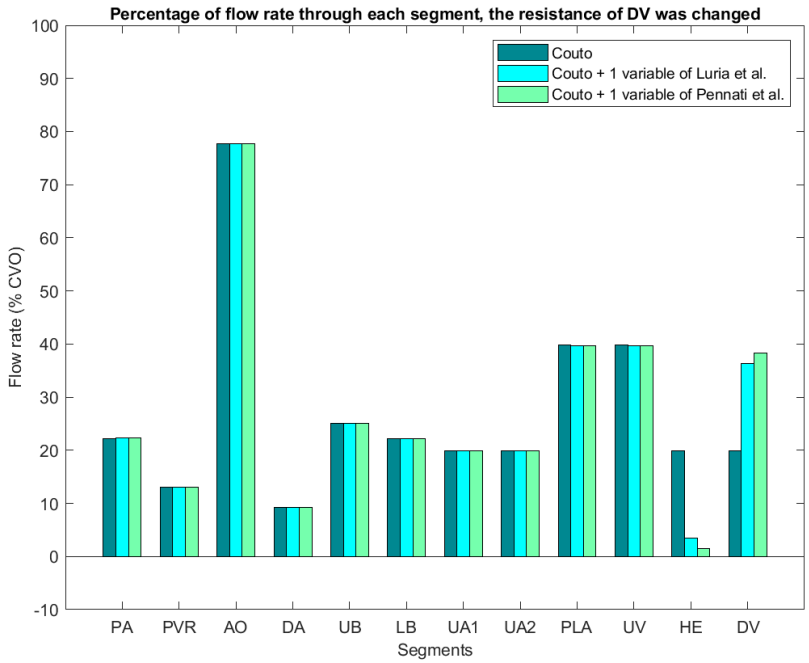

Figure E.12: Variables of Couto [11] were implemented into the fetal cardiovascular model and the value for DV was changed two times into a value from Luria et al. [31] or Pennati et al. [45] to evaluate its influence on the system.

F | Variable resistance

By adding compliance, in real life the diameter of vessels would change and so would the resistance. So the question is how resistance changes through volume changes by compliance and applied pressure and how this could be applied into the model. For instance, when compliance is added into the system and a vessel increases in size, the resistance would decrease. However, studies as Luria et al. [31], Pennati et al. [45] and Couto [11] only give R and C and no information about the radius or length of vessels. For organs, this would be even more complicated, because an approximation of radius and length is needed. Vessels and organs with compliance distend through applied blood pressure. The diameter-pressure relationship is called distensibility and distensibility times volume gives compliance [28]. Distensibility differs for different organs and through the body. Volume adjustments differ, for example, extracranial and intracranial, because of the scull adding more outside pressure to the brain. Also, local metabolic needs can evoke local vessel size adjustments. Using compliance, elastance or distensibility for pressure-volume calculations, does not take auto-regulation of vessel sizes and collapsing of vessels into account. The question is if it is useful to make a variable resistance depending on compliance and pressure changes while neglecting other regulatory systems.
There are examples in the literature of variable compliance and resistance. For these equations, however, many extra variables are needed such as the radius, wall thickness, and Young's modulus [14, 21, 28, 29, 34]. The foretalas and variables now planned to use are very simplistic and the input variables are simply resistance and compliance. For now, information is lacking to solve the variable resistance equations. An option could be to calculate a variable resistance with only available information.

Let's assume a vessel of length L_v, with a radius r and with resistance R and compliance C. There is a input flow Q_{in} and pressure P_{in} and output flow Q_{out} and pressure P_{out}. Length L_v is unknown and assumed to be constant and radius $r(t)$ is also unknown and changes over time. The result is that the resistance only depends on the radius.

$$R(r) = \frac{8\eta L_v}{\pi r^4} \tag{F.1}$$

The volume change of the vessel can be calculated with the compliance and pressure drop.

$$\Delta V = C\Delta P = C(P_{in} - P_{out}) \tag{F.2}$$

Looking at one time step, the variables that change through blood flow and pressure are the volume and radius of the vessel.

$$\begin{aligned} t_0 : V_0, r_0 \quad & V_0 = \pi r_0^2 L_v \\ t_1 : V_1, r_1 \quad & V_1 = \pi r_1^2 L_v \end{aligned}$$

The first step is estimating the new radius, r_1.

$$V_1 - V_0 = \pi r_1^2 L_v - \pi r_0^2 L_v \tag{F.3}$$

$$r_1 = \sqrt{\frac{V_1 - V_0 + (\pi r_0^2 L_v)}{\pi L_v}} \tag{F.4}$$

It is not possible to calculate the change in radius with just using $\Delta r = (\Delta V/(\pi L))^{\frac{1}{2}}$. This is because two vessels with a different radius, but with the same Δr, will not have the same ΔV. The added area through Δr is different of size for both vessels.

The resistance at t_0 is given by

$$R_0 = \frac{8\eta L_v}{\pi r_0^4} \tag{F.5}$$

At t_1 the new resistance can be estimated by rewriting (F.4) into (F.1).

$$R_1 = \frac{8\eta L_v}{\pi r_1^4} \tag{F.6}$$

$$= \frac{8\eta L_v (\pi L_v)^2}{\pi (V_1 - V_0 + (\pi r_0^2 L_v))^2} \tag{F.7}$$

$$= \frac{8\eta \pi L_v^3}{(V_1 - V_0 + (\pi r_0^2 L_v))^2} \tag{F.8}$$

$$= \frac{8\eta \pi L_v^3}{(V_1 - V_0)^2 + (2(V_1 - V_0)\pi r_0^2 L_v) + (\pi^2 r_0^4 L_v^2)} \tag{F.9}$$

Known variables in the model are the volumetric flow rate, resistance and compliance of organs and vessels and the output pressure in the heart. The exact dimensions of vessels and organs are unknown. After evaluating the options to calculate a variable resistance, it can be concluded that the model comes one known variable short. For the vessel (F.9) would be an option if the length of the vessels is known. With the length and (F.1), r_0 could be calculated and eventually R_1. This part could be implemented in a model easily when more information is known. For this project it is not useful, because it would add another estimated variable and more uncertainty to the outcome.

G | Bifurcation of the placental vasculature

A big portion of the cardiac output of the fetus flows towards the placenta, making it a very important component of the fetal cardiovascular system. The placental vasculature could be divided into three parts after entering the placenta from the umbilical cord. First, there are the chorionic arteries covering the surface of the placenta like an umbrella as can be seen in Figure G.1. From this umbrella grow the villi trees towards the basal plate. Starting with the stem part consisting of stem villi, secondly the intermediate villi, and third the canopy of leaves formed by the capillary convolutes. In the placenta, the capillaries dictate the overall the resistance, as mentioned before in Section 2.1.2.

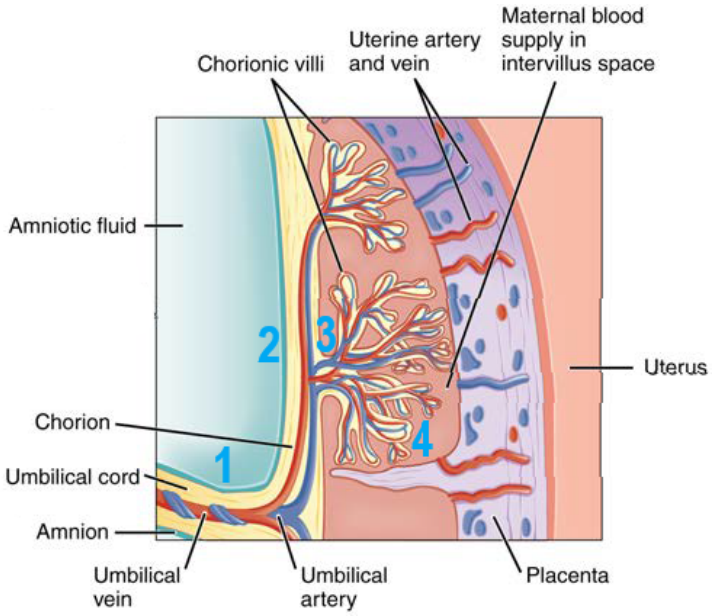

Figure G.1: The placental tree. 1: The umbilical cord. 2: The chorionic arteries. 3: The villous stem. 4: The villous capillaries. This is part of Figure 1.1 [3, pg.1333].

After entering the placenta, the umbilical vessels will bifurcate to cover the surface of the placenta. At 5 mm after insertion into the placenta, the two umbilical arteries merge together into the Hyrtl anastomosis [17]. The merged artery bifurcates into chorionic vessels covering the chorionic plate. Bifurcation of the blood vessels can have a monopodial or dichotomous branching pattern. Monopodial branching means that small daughter branches sprout from a long parent vessel. The parent vessel keeps a fairly constant diameter and can cover a long distance. A dichotomous tube branches into two daughter vessels of roughly the same size. The ratio between the parent vessel and its child is 0.6 to 0.8 for dichotomous vessels and 0.1 to 0.3 for monopodial vessels [17].
Efficient blood supply to all cotyledons of the placenta is needed for sufficient exchange of oxygen and nutrients between mother and fetus. To cover the area optimally, a combination of the patterns is the ideal option. The place of insertion of the umbilical cord on the placenta can differ from being at the centre, the periphery or somewhere in between. A central cord insertion has a primarily dichotomous pattern to cover the whole placenta, with some monopodial branches to cover spaces in between. However, by peripheral insertion, a long distance across the placenta needs to be covered. Also, the perpendicular areas need to be covered, so in the case of peripheral insertion, the first one to three bifurcations are dichotomous, followed by a monopodial pattern. To cover the whole placenta with

chorionic vessels around 6 to 8 generations of bifurcation are needed. When covering a placenta of around 200 mm in diameter it would mean that the chorionic arteries terminate in 60 to 100 villi trees [10]. Centre insertion is the most optimal for good blood supply. Peripheral insertion is linked to cases of pregnancy-induced hypertension as described in Section 1.1.1. Peripheral cord insertion could originate from an abnormal intrauterine oxygen gradient or nutrient shortage.

The villous trees, following the chorionic arteries, run through approximately 15 generations of asymmetric bifurcation and cover together approximately 20 mm. The villous trees contain arterioles and venules and they branch along with the villous tree. From the venules in the capillary convolutes, veins flow back to the umbilical vein. The veins in the placenta are assumed to be twice the size of arteries. The tree bifurcates asymmetrically because it needs to fill the whole hemispherical cotyledon in such a way that blood flow of the mother in the intervillous space is not obstructed but that it still ensures optimal oxygen exchange. Secondly, the central cavity is kept empty at the place where the spiral artery of mothers side is placed. So, growth is asymmetric and a combination of dichotomous and monopodial growth. Villous trees do not only start at the last bifurcations of the chorionic arteries but also from earlier generations. The average diameter of the vessels entering the villous space is 0.77 mm. The diameter of vessels entering the capillary convolutes is 0.03 mm after 15 generations of bifurcations. Lin et al. [30] use a parent to daughter ratio of 0.975 for the length and 0.8 for the diameter of bifurcating vessels in the villous tree.

The last part is the terminal convolutes following on the intermediate villi. A stem villous tree goes through at least 4 generations before terminal convolutes protrude [10]. After 4 generations the diameter of the vessels becomes smaller than 0.03 mm. Which is when the Fahraeuss-Lindqvist effect will occur and viscous forces become dominant. Estimating the flow with Pouiseuille will become more difficult.

These three parts give an idea of how the placental vasculature is built up. The third part of the placental vasculature, the villi ‘canopies’, are covering the biggest area of blood vessels and influencing the resistance of the placenta very much. Unfortunately, the information about this part is minimal. Lin et al. [30] and Clark et al. [10] tried to make computer models of these parts. However, the study of Lin et al. [30] is not clear about how they calculated the terminal part. Secondly, based on the information given in the article of Clark et al. [10], their results can not be reproduced. Clark et al. [10] finds a resistance for a single terminal villi unit which is very high and uses a viscosity of $\eta = 3.36 * 10^{-}6$ Pa s, which is very low in comparison to commonly used blood viscosity.
Estimating the resistance of the placenta will involve many assumptions. Calculating the resistance based on the found information is not possible, because the part influencing the resistance primarily is not clarified enough. To estimate the placental resistance an average resistance will be based on the pressure drop over the placenta and the flow passing through.